DUDLEY KNOX LIBRARY
NAVAL POSTGRADUATE SCHOOL
MONTEREY, CALIFORNIA 93943

NAVAL POSTGRADUATE SCHOOL

Monterey, California

THESIS

TRAILING VORTEX ATTENUATION DEVICES

by

Kenneth G. Heffernan

June 1985

Thesis Advisor: T. Sarpkaya

Approved for public release; distribution is unlimited.

T223063

REPORT DOCUMENTATION PAGE		READ INSTRUCTIONS BEFORE COMPLETING FORM
1. REPORT NUMBER	2. GOVT ACCESSION NO.	3. RECIPIENT'S CATALOG NUMBER
4. TITLE *(and Subtitle)* Trailing Vortex Attenuation Devices		5. TYPE OF REPORT & PERIOD COVERED Dual Master's Thesis; June 1985
		6. PERFORMING ORG. REPORT NUMBER
7. AUTHOR(s) Kenneth G. Heffernan		8. CONTRACT OR GRANT NUMBER(s)
9. PERFORMING ORGANIZATION NAME AND ADDRESS Naval Postgraduate School Monterey, California 93943		10. PROGRAM ELEMENT, PROJECT, TASK AREA & WORK UNIT NUMBERS
11. CONTROLLING OFFICE NAME AND ADDRESS Naval Postgraduate School Monterey, California 93943		12. REPORT DATE June 1985
		13. NUMBER OF PAGES 109
14. MONITORING AGENCY NAME & ADDRESS *(if different from Controlling Office)*		15. SECURITY CLASS. *(of this report)* Unclassified
		15a. DECLASSIFICATION/DOWNGRADING SCHEDULE

16. DISTRIBUTION STATEMENT *(of this Report)*

Approved for public release; distribution is unlimited.

17. DISTRIBUTION STATEMENT *(of the abstract entered in Block 20, if different from Report)*

18. SUPPLEMENTARY NOTES

19. KEY WORDS *(Continue on reverse side if necessary and identify by block number)*

Trailing Vortices

20. ABSTRACT *(Continue on reverse side if necessary and identify by block number)*

Trailing vortices generated by large aircraft pose a serious hazard to other planes. Numerous studies have been carried out to destroy them either before and/or after their formation. The present investigation is a survey and critical assessment of all the known active/passive devices and wingtip modifications proposed to achieve vortex attenuation. It is concluded that some devices, such as the wing tip sails, have promise in affecting the vortex roll-up in the vicinity of the aircraft. However

more data and analysis on this and other devices are needed before they can be incorporated into existing aircraft or future designs.

Approved for public release; distribution is unlimited.

Trailing Vortex Attenuation Devices

by

Kenneth G. Heffernan
Lieutenant, United States Navy
B.S., United States Naval Academy, 1978

Submitted in partial fulfillment of the
requirements for the degree of

MASTER OF SCIENCE IN MECHANICAL ENGINEERING

and the degree of

MASTER OF SCIENCE IN AERONAUTICAL ENGINEERING

FROM THE

NAVAL POSTGRADUATE SCHOOL
June 1985

Thesis
H42145
c.1

ABSTRACT

Trailing vortices generated by large aircraft pose a serious hazard to other planes. Numerous studies have been carried out to destroy them either before and/or after their formation. The present investigation is a survey and critical assessment of all the known active/passive devices and wingtip modifications proposed to achieve vortex attenuation. It is concluded that some devices, such as the wing tip sails, have promise in affecting the vortex roll-up in the vicinity of the aircraft. However, more data and analysis on this and other devices are needed before they can be incorporated into existing aircraft or future designs.

TABLE OF CONTENTS

I. INTRODUCTION 12

II. BRIEF REVIEW OF THE FUNDAMENTAL ASPECTS OF WINGTIP VORTICES 13

III. EXPERIMENTAL EVALUATION OF THE VORTEX MINIMIZATION DEVICES 22
  A. INTRODUCTION 22
  B. ACTIVE DEVICES 24
  C. PASSIVE DEVICES 29

IV. SUMMARY 39

V. CONCLUSIONS 46

APPENDIX A: FIGURES 47

LIST OF REFERENCES 104

INITIAL DISTRIBUTION LIST 109

LIST OF TABLES

I Horizontal Separation Requirements 22
II Categorical Listing of Vortex Attenuating Devices 24
III Induced Rolling Moment Coefficients for Various Devices 28
IV Biplane Winglet Addition Efficiency Factors . . . 37
V Recapitulation of the Advantages and Disadvantages of Active Devices 40
VI Recapitulation of the Advantages and Disadvantages of Passive Devices 41

LIST OF FIGURES

1 Formation of Wake Vortex Showing Induced Velocities 47

2 Sketch of Trailing Vortex System 47

3 Trailing Vortex Hazard Potentials 48

4 Sketch of the Induced Flow 48

5 Test Arrangement in NASA Facilities 49

6 Arrangement of the Langley Vortex Research Facility 50

7 Effects of Central Jet on the Measured Tangential and Axial Mean Velocity Profiles 51

8 Effects of Central Jet on the Rolling Moment Coefficient 52

9 Sketch and Close-Up Views of a Forward Blowing Jet 53

10 Sketch and Close-Up Views of a Rearward Blowing Jet 54

11 Sketch and Close-Up Views of a Downward Blowing Jet 55

12 Sketch and Close-Up Views of a Deflected Jet . . . 56

13 Basic Model of a Boeing 747 Aircraft 57

14 Effect of Engine Reverse Thrust on the Vortex Induced Rolling Moment Coefficient on a Learjet Probe Model 58

15 Sketch of a Spanwise Extended Blowing Tube 59

16 Effect on Lift-to-Drag Ratio from Spanwise Extended Tube Blowing 59

17 Effect on Lift-to-Drag Ratio from Spanwise Extended Tube Blowing at Transport Model Wingtip 60

18 Rolling Moments Measured by a Small-Wing Model at 7.5 Spans Downstream a Transport Model with a Blowing Tube 60
19 Sketch of Individually Controlled Discrete Wingtip Jets 61
20 Two Typical Wingtip Jet Configurations 62
21 Sketch and Close-Up Views of a Blown Flap 63
22 Effect of a Blown Flap on the Vortex Velocity Distribution 64
23 Wingtip-Mounted Engines on a Transport Model: Front and Side Views 65
24 B-747 Wake Vortex Disturbance on a T-37B Probe Aircraft--Oscillating Ailerons and Spoilers 66
25 Sketch of Fixed Crossed Blades (Four Inch) 67
25a Sketch of Fixed Crossed Blades (Eight Inch) 67
26 Sketch and Close-Up Views of Wingtip Mounted Splines 68
27 Sketch of Spline Assembly at Wingtip 69
28 Photograph of the Spline Assembly on the Wingtip 70
29 Sketch of Cabled Drogue Cone and Cabled Chute . . . 71
30 Sketch and Close-Up Views of a Vortex Generator . . 72
31 Sketch of Wingfins on a Transport Aircraft Model 73
32 Summary of Reductions in Rolling Moment Coefficient for Various Wingfin Configurations (7.8 Spans Downstream) 74
33 Parabolic Wingfins 75
34 Vortex Strength Term vs. Fin Angle of Attack . . . 76
35 Maximum Vortex Strength Term vs. Fin Aspect Ratio 77
36 Wingtip Mounted Spoiler 78
37 Variation of Rolling Moment Coefficient with Distance behind a Basic Model: No Device, Spoiler, Spline 79

38 Variation of Rolling Moment Coefficient with Distance behind a Flapped Model: No Device, Spoiler, Spline 80
39 Sketch of Flight Spoilers on a B-747 Aircraft Model 81
40 Photograph of Flight Spoilers on a B-747 Aircraft Model: Segments 1 and 2 Deflected 45 Degrees 82
41 Variation of Rolling Moment Coefficient with Distance behind the B-747 Aircraft Model (Spoiler Deflection) 83
42 Three View Sketch of DC-10 Model with Flaps Retracted 84
43 Sketch of Flight Spoilers on a DC-10 Model 85
44 Variation of Rolling Moment Coefficient with Distance behind the DC-10 Aircraft Model (Spoiler Deflection) 86
45 Three View Sketch of B-747 Model with Flaps Retracted 87
46 Photograph of Porous Wingtip 88
47 Nondimensional Maximum Tangential Velocity vs. Lift Coefficient 88
48 Maximum Tangential Velocity vs. Downstream Distance 89
49 Lift Distribution on O-1A Wing with and without Porous Tip 89
50 Wingtip Edge Shape Configurations 90
51 Changeover Position from Axial Velocity Excess to Axial Velocity Deficit behind NACA 6412 Wing Section 91
52 Comparison of Axial Velocity Profile for Various Wingtip Edge Shapes (20 Chordlengths Downstream) 92

53 Comparison of Tangential Velocity Profile for Various Wingtip Edge Shapes (20 Chordlengths Downstream) 93
54 Sketch of End Plate and Wingtip Extension 94
55 Photograph of Whitcomb Winglet 94
56 Geometric Drawing of the Whitcomb Winglet 95
57 Incremental Lift Coefficient Variation for Constant Drag Coefficient (M=0.78) 96
58 Tangential Velocity Profile Downstream Whitcomb Winglet (5 Chordlengths) 97
58a Tangential Velocity Profile Downstream Whitcomb Winglet (20 Chordlengths) 97
59 Axial Velocity Profile Downstream Whitcomb Winglet (5 Chordlengths) 98
59a Axial Velocity Profile Downstream Whitcomb Winglet (20 Chordlengths) 98
60 Spanwise Pressure Distribution for Various Wingtip Edge Shapes and Whitcomb Winglet 99
61 Spanwise Load Distribution of Whitcomb Winglet (M=0.78) 100
62 Forces on an Auxiliary Surface Mounted on the Tip of a Wing 101
63 View of Paris Aircraft Fitted with Wingtip Sails 101
64 Wingtip Sail Geometry 102
65 Effect of Wingtip Sails on Lift-Induced Drag . . 103
66 Sketch of Biplane Winglet 103

ACKNOWLEDGEMENTS

The author wishes to express his sincere appreciation to Distinguished Professor T. Sarpkaya for his invaluable guidance, advice and encouragement during this research. His wealth of knowledge and dedication to the advancement of science are truely inspirational.

I. INTRODUCTION

Vortex motion has long been a subject of great interest to Hydro and Aero-dynamicists. Only in the last decade has it received renewed emphasis, based mainly on the persistance of trailing vortices created by jumbo jets. These vortices pose a hazard to following aircraft. Additionally, the elimination or the reduction of the intensity of these vortices has the advantages of reducing drag and increasing the aerodynamic efficiency of the wing.

The purpose of this review is to make a critical assessment of the efforts that have been made in the study of trailing vortices and their implication on the understanding and/or control of wingtip vortices. Two possible avenues exist in the alleviation of the wake vortex hazard. The first is their avoidance, where systems are installed at terminal areas to warn aircraft of possible hazards. The second approach , and the one pursued herein, is the modification of vortex patterns in an effort to minimize their effects on the following aircraft and to improve the aerodynamic characteristics of the generating aircraft.

First, a brief review of wingtip vortices is presented. This includes the vortex formation by the roll-up of the vortex sheet and the vortex structure. Then , an investigation of the analytical models which have been devised to describe the structure of the vortices is undertaken. Followed by, wingtip modifications that have thus far been used or proposed in an attempt to attenuate the wingtip vortices.

II. BRIEF REVIEW OF THE FUNDAMENTAL ASPECTS OF WINGTIP VORTICES

The spanwise loading across a two-dimensional airfoil (i.e. of infinite span) is uniform. The lift produced by the camber and/or the increased angle of attack, with respect to the flow direction, is created by the pressure difference between the upper and lower surfaces of the airfoil.

However, when the span is finite, as in practice, the differential pressure between the surface allows air to spill over the wingtips and consequently change the flow field. This equalization of pressure over the wingtips alters the spanwise loading of the airfoil, creating a modified pressure or lift distribution which goes to zero at the wingtips. There are added spanwise velocity components that direct the overall flow outward towards the tips on the lower surface and inward towards the root on the upper surface. When these components meet at the trailing edge of the span, the air rolls up into a number of small vortices. The vorticity shed by the airfoil rolls up into two counter-rotating vortices and its spanwise location is dictated by the spanwise loading. The vorticity is concentrated in areas where the wing loading changes dramatically, therefore they appear more or less near the wingtips (see Figure 1). [Ref. 1]

The vortex system created by a lifting surface can best be described as a combination of three individual vortices. They are the bound vortex, the trailing vortex, and the starting vortex. The bound vortex is placed at the aerodynamic center of the wing, which is the quarter chord line for subsonic flight. This vortex has a circulation Γ whose strength varies along the span to match the change in spanwise loading of the airfoil. From Helmholtz theorems, that a vortex-filament has a constant circulation and cannot end in a fluid, it follows that as the spanwise loading changes the bound vortex must change. This is accomplished by truncating the vortex filaments along the span in increments of Δy which correspond to increments of circulation $\Delta \Gamma$. These filaments run downstream of the lifting surface to infinity (or the starting vortex) and are the trailing vortices. By summing all these filaments an accurate profile of the spanwise loading distribution can be made. This method of modeling has been termed "horseshoe vortex" and is shown in Figure 2. [Ref. 2]

A tangential flow pattern is created by the culmination of these horseshoe vortices. In addition to the effect on following aircraft as indicated on Figure 3, the trailing vortices have a detrimental effect on the generating aircraft. The resultant induced velocity is in a downward direction, particularly in between the vortex pair, and is called downwash. As shown in Figure 4, the downwash velocity, in conjunction with the free stream velocity, acts to tilt the flow seen by the airfoil. Since effective lift acts normal to the effective flow direction, there is a force component which is opposite to the undisturbed flow direction. This drag force is termed induced drag and is common to all finite wingspans.

Various attempts have been made to model the structure of trailing vortices mainly concerned with the far-field structure after the roll-up process has been completed. This is normally within a few spanlengths behind the wing. These studies simplify the roll-up with the assumptions that the process is fast enough to be inviscid (viscosity and turbulence discounted), yet slow enough that it can be modeled as two dimensional. Two methods have been prevalent, a step by step calculation from the initial wake structure or calculations based on preservation of certain invariant quantities.

The first method attempts to take the steady roll-up of the three dimensional vortex sheet and break it down into a two dimensional sheet which is stepped through the roll-up process at small time increments. Westwater [Ref. 3] represented the vortex sheet by a finite number of vortex filaments and examined their motion by numerical analysis. However, this method fails to accurately reproduce the inner portion of the spiral at the tips (vortex core), not due to numerical inaccuracies, but to interaction between vortex filaments that are adjacent to one another on the sheet. Kaden [Ref. 4] used the similarity solution of Prandtl for unsteady roll-up of an infinite sheet to approximate a solution for the finite sheet, but again this fails because of the ever increasing arc length between adjacent point vortices in the vortex core.

The direct calculation of the roll-up process is based on the conservation of certain quantities, namely

I) Conservation of circulation

$$\Gamma_0 = -\int_0^{b/2} d\Gamma(y)/dy \, dy = \int_0^{b/2} d\Gamma(r)/dr \, dr \qquad \text{(eqn 2.1)}$$

II) The Centroid of vorticity

$$\Gamma_0 \bar{y} = \int_0^{b/2} y \, d\Gamma(y)/dy \, dy \qquad \text{(eqn 2.2)}$$

where b/2 is the wing semi-span, $d\Gamma/dy$ is the strength of the vortex sheet, Γ_0 is the circulation at the centerline of the wing and $\bar{y}$ is the centroid of vorticity over the semi-span of the wing. The distribution of circulation $\Gamma(y)$ that is set by the wing loading determines the values of Γ_0 and $\bar{y}$.

A principal model that was used when the study of aircraft trailing vortices first came to the forefront was that of Spreiter and Sacks [Ref. 5]. The roll-up wake consists of two counter rotating Rankine vortices, with the circulation concentrated in the vortex core and distributed uniformly throughout. With the circulation Γ_0 and $\bar{y}$ set by the equations (2.1) and (2.2) above, the additional unknown of the vortex core radius was determined by requiring the conservation of kinetic energy to account for induced drag. While their assumption seemed natural, experimental data indicated that this model was not sufficient, for it overestimated the core size and underestimated the maximum tangential velocity.

Then, in 1971, the model of Betz (1932) **[Ref. 6]** was resurrected by Donaldson [Ref. 7] showing greater agreement with flight test data. Betz proposed that in addition to those quantities in equations (2.1) and (2.2) the second moment of vorticity, shed by each wing semi-span, should be conserved, taking the form

$$I = -\int_0^{b/2} (y-\bar{y})^2 \, d\Gamma(y)/dy \, dy = \int_0^R r^2 \, d\Gamma(r)/dr \, dr \qquad \text{(eqn 2.3)}$$

Donaldson et al. [Ref. 8] and Rossow [Ref. 9] have offered modifications to the original form of the Betz model which will handle spanwise loading which differ significantly from the elliptical loading. These models fail on two counts. The tangential velocity at the center of the vortex core does not go through zero, thus not truly modeling the vortex core, but allowing the tangential velocity to decay slowly from the center. Also, as pointed out by Moore and Saffman [Ref. 10], the rolled up vortex does not conserve kinetic energy.

Another method which has been used to model the tangential velocity profile of laminar line vortices has been the model of Lamb [Ref. 11]. His similarity solution has assumed a constant axial velocity, which is not truly the case, and has been applied to laminar trailing vortices by replacing the time variable with z/U_0 where z is the axial distance and U_0 is the free stream velocity. This solution is written as

$$\eta = r \,/(\Gamma_\infty z/U_0)^{\frac{1}{2}} \qquad \text{(eqn 2.4)}$$

$$\Gamma/\Gamma_\infty = 1 - \exp\,(-\eta^2 \,/\, 4\nu/\,\Gamma_\infty) \qquad \text{(eqn 2.5)}$$

where the circulation Γ is a function of the similarity variable η and Γ_∞ is the total circulation of the vortex. The Γ_∞ term presents a problem when comparing results of different origins. Some authors have taken Γ_∞ to be the wing root circulation while experimental evidence presented by Dosanjh, et al. [Ref. 12] has shown that the circulation in each of the trailing vortices is only about 60% of that at the wing root. This is due to the interaction between vortices shed off the wing-fuselage interface. On actual models these vortices are generated opposite to the trailing vortex and act to decrease the circulation.

The Lamb model has recently been preferred to others because it exhibits rigid body rotation for small radii with tangential velocity increasing linearly with radius, peaking and then decaying exponentially to zero. It has been extended to turbulent trailing vortices based on work by Squire [Ref. 13] who suggested that the kinematic viscosity term be replaced by an eddy viscosity ν_T , which is a function of the vortex Reynolds number Γ_∞/ν . As with the Lamb vortex, the circulation in the core region, where the tangential velocity reaches a maximum, should be 71.6% of the overall circulation, however experimental results indicate that only 37-60% actually exists in the core [Ref. 14].

Hoffmann and Joubert [Ref. 15] have approached the analysis of the turbulent trailing vortex in yet another manner. Their analysis is along lines similar to Prandtl's law of the wall used with turbulent boundary layers, and has modeled the circulation outside the core region and a small boundary layer buffer region by the logarithmic profile;

$$\Gamma/\Gamma_1 = 1/H \ln(r/r_1) + 1 \qquad \text{(eqn 2.6)}$$

where Γ_1 and r_1 are the core circulation and core radius and H is a constant. This also assumes that the flow in the core region is independent of the flow outside and is of a universal form where Γ/Γ_1 is a unique function of r_1 . These last two models for turbulent vortices still fail to accurately quantify the circulation and velocity profiles and require correlation with experimental results to obtain the necessary terms, such as the eddy viscosity ν_T and the universal constant H .

There also exists an axial velocity component associated with trailing vortex flow. This axial flow is associated with the rotational motion of the vortex itself and the profile/induced drag of the wing. A low pressure region is formed in the core by the centrifugal acceleration of the fluid, and as the vortex decays downstream, the tangential velocities decrease and the core pressure increases giving a positive axial pressure gradient. This, of course, occurs during the latter stages of vortex growth and has been investigated by Batchelor [Ref. 16] assuming small axial velocity as compared with the free stream velocity. As for the viscous airfoil drag terms, Brown [Ref. 17] has made a theoretical study which indicates that in the rolled up region before the vortex has spread and been dissipated by turbulent diffusion, the combination of induced and profile drag can either create an axial velocity excess or defect dependent on their magnitudes. Experimental tests [Ref. 18,19] have exhibited both velocity excess and deficit yet no method has been devised which can accurately predict what profile exists.

The axial as well as the tangential velocity distributions at any section behind the wing shows a varied dependence on certain critical parameters of wing section, wingtip shape, Reynolds number, angle of attack (AOA) and the distance of the station downstream from the wing [Ref. 20 : p. 911]. With this number of parameters, the difficulty in coming up with a single model which can accurately describe the motion of the vortex is understandable. Moreover, the experimental results which are used to compare the theoretical models are obtained mostly by intrusive means, (Hot wire anemometer, vorticity meter, bubbles, etc.) possibly disturbing the flow. Clearly the laser velocimeter, with the added high-speed spatial scanning feature, may offer a solution to this problem [Ref. 21]. It can minimize the effects of "vortex meandering" which would normally result in inaccurate velocity distributions due to spatial movement of the vortex filament. Additionally, relating wind tunnel/tow tank data to full-scale aircraft is difficult due to differences in Reynolds number (based on wing chord) which may differ by one to two orders of magnitude. Furthermore, the scale and intensity of the free-stream turbulence is easily measured/controlled in the wind tunnel but not in actual flight tests.

A new vortex model has recently been introduced by Staufenbiel [Ref. 22]. It is a modified form of the Lamb model where a reduced circulation $q\ \Gamma_\infty$ $(q<1)$, is assigned to the core region, and the remainder, i.e., $(1-q)\ \Gamma_\infty$,to the outer region. This model attempts to achieve better correlation with experimental data by mathematical means and seeks to conserve both the second moment of vorticity (vortical dispersion) and the rotational energy. This leads to much smaller core radii and to increased values of the maximum tangential velocity. Even though the resulting velocity profile contains an inflection point (leading to instabilities), Staufenbiel's model has clear advantages over those proposed previously. A comparison of the models cited reveals:

a) Betz model: Does not conserve kinetic energy and exhibits no viscous core region (solid body rotation) where the velocity goes to zero at the center;

b) Spreiter and Sacks model: Vortical dispersion is not satisfied by the Rankine vortex alone;

c) Lamb model: It is for a laminar vortex. Furthermore, it does not satisfy vortical dispersion. Though it may be modified to include turbulence effects by changing the kinematic viscosity to an eddy viscosity, there is no real measure of turbulence within the vortex and the choice of ν_T is somewhat arbitrary.

Progress in accurately modeling the structure of a turbulent vortex has been slow in developing, and is certainly attributable to the extreme complexity of the problem. Efforts continue in seeking improvements of older models through the use of additional conservation laws and better computational techniques in order to simulate the characteristics of real vortices. Hopefully, the modeling of the vortex structure can improve the understanding of the motion of vortices and the importance that the various parameters play in establishing and dictating the flow field. If the vortex can be accurately modeled, then the possibility exists that the vortex may be controlled or annihilated. This may be accomplished through the use of instabilities introduced into the flow or features added to the wing tips which control the size, velocities and the motion of the vortex. The ultimate goal is to modify the vortex in a manner which will improve the characteristics of the body that generates them and also to dissipate or to minimize the destructive effects of the vortices as quickly as possible following their formation.

III. EXPERIMENTAL EVALUATION OF THE VORTEX MINIMIZATION DEVICES

A. INTRODUCTION

In the United States, the primary impetus in the advancement of vortex alleviation methods has been the drive to reduce the separation distances between aircraft. This is of particular interest in terminal areas around busy airports, where these distances restrict their potential utilization due to delays in takeoff and landing. With this vortex hazard in mind, the Federal Aviation Administration (FAA) has set the following separation requirements.

TABLE I
Horizontal Separation Requirements

Generating Aircraft Following Aircraft	Heavy	Large	Small
Heavy	4 nm	3 nm	3 nm
Large	5 nm	3 nm	3 nm
Small	6 nm	4 nm	3 nm

nm - nautical mile

Heavy > 300,000 lbs.
300,000 lbs. > Large > 12,500 lbs.
12,500 lbs. > Small

The goal of continuing research is to reduce these separation distances without sacrificing safety. In conjunction, additional research has been targeted directly at improving the cruise capabilities of the aircraft.

A critique of the various methods investigated to attain these goals is difficult. Much of the experimental work has been done in wind tunnels and tow tanks or by actual flight evaluation. The Reynolds numbers, aircraft configuration (cruise, approach, landing, etc.) and airfoil data (shape, aspect ratio, camber, angle of attack, etc.) differ widely between various studies. The data presented in various reports are not in a form conducive to comparison. Additionally, the characteristics of the ambient turbulence are often unreported, making the duplication of the results at other facilities rather dubious.

Most of the research that will be referenced here has been sponsored by the National Aeronautics and Space Administration (NASA). NASA uses four different facilities: The 40x80 ft. wind tunnel at NASA Ames Research Center, the Langley Vortex Research Facility (a towing basin using air as the test medium), the Vertical/Short Takeoff and Landing (V/STOL) wind tunnel at Langley Research Center and the Hydronautics Ship Model Basin in Laurel, Md. (see Figures 5, 6). An effort has been made in their investigations to alleviate some of the problems cited above. Common models, standard measurement techniques, and consistent Reynolds numbers were used in these facilities. [Ref. 23]

There is no unique way to classify all the devices that have been tested. Though several logical means of classification do come to mind: (1) The nature of the device concerned with the overall effect on the aircraft or vortices (i.e., active or passive devices); (2) Model vs. prototype; (3) Subsonic vs. supersonic; (4) Civilian vs. military; and (5) Phase of flight or configuration (i.e. landing, cruise). Partly for reasons which will become clear later, it was decided to discuss these devices in two broad categories: Active devices and Passive devices.

Active devices dynamically interact with the vortex system. These devices attempt to alter the vortex by (a) emitting a jet or sheet of air at various stations along the span, or (b) oscillating the control surfaces which vary the spanwise loading with time. Passive devices involve static interaction with the vortices. Thus, they change the characteristics of the vortex by altering or controlling the flow over the wing. Both categories involve concepts of turbulence introduction, instability initiation and countersign circulation. Table II is a listing of devices by category.

TABLE II

Categorical Listing of Vortex Attenuating Devices

ACTIVE	PASSIVE
Blowing Jet Blown Flap Wingtip-Mounted Jet Wingtip Propeller Spoiler & Aileron Oscillation	Spline Cabled Drogue Cone or Chute Vortex Generator Spoiler Trailing-Edge Flap Porous Wingtip Wingtip Shaping Wingtip Extension

B. ACTIVE DEVICES

Apparently, the first proposal for vortex modification by mass injection was presented by Rinehart, et al. [Ref. 24]. The mass injection principle is intended to introduce turbulence into the flow field, accelerating the destruction of the vortex. Blowing jets, blown flaps and wingtip mounted jet engines exploit this idea.

Blowing jets have been the subject of exhaustive studies. Snedeker [Ref. 25] and Poppleton [Ref. 26] introduced axial flow directly into the vortex core and found that the tangential velocities were greatly reduced while the core radius increased (see Figure 7). However, as shown in Figure 8, the rolling moment created on an airfoil (25 chordlengths downstream) was relatively uneffected by the jet momentum. This is a point which will continuously become evident throughout this review. Reduction of tangential velocities within the vortex cannot be directly correlated with reduced rolling moments. These results were limited to very short downstream distances, indicating that the effects of axial blowing jets are not immediately manifested in vortex breakdown. Kirkman, et al. [Ref. 27 : pp. 8-13], using the Hydronautics ship model basin, tested four variations of the blowing jet: forward, rearward, downward and deflected (Figures 9-12). The investigation conducted on a 3/100 scale model of the B-747 transport aircraft (see Figure 13) emphasized far-field effects (up to 8 km full-scale) including velocity distributions and induced rolling moments on following aircraft. The model ran at Reynolds numbers of 7.5 x 10^5 and 9.3 x 10^5 in a cruise (the lift coefficient C_L = 0.4) and 30 degrees flapped (C_L = 1.2) conditions with jet momentum coefficients between 4.6 x 10^{-4} to 8.3 x 10^{-4}. With these low jet momentum coefficients, only the deflected jet produced any appreciable change in the tangential velocity distribution in comparison to the unmodified aircraft. The slight decrease, at a full-scale distance of 4.42 km downstream, may have been more a function of the protruding nozzle face, creating added turbulence, rather than that of the mass injection. At the same downstream distance, the rolling moments experienced by the following Learjet model exceeded the full aileron deflection capabilities to maintain level flight.

Investigation of the vortex attenuation attained by varying the thrust levels of the installed jet engines has also been conducted. Using the same model, Patterson and Brown **[Ref. 28]** found that maximum engine thrust could produce a 20% decrease in vortex-induced rolling moments (1.63 km downstream). They also found that engine positioning and reverse thrusting could reduce the rolling moment (see Figure 14), though at these distances, the probe aircraft still could not resist a sustained roll.

Yuan and Bloom **[Ref. 29]** demonstrated that a tube (.6 chordlength) extending from the trailing edge of a straight wing tip blowing a sheet of air downward (Figure 15) can significantly decrease the induced rolling moment (7.5 spanlengths downstream). Additionally, the jet momentum coefficient, ($C_\mu = .018$), improved the aircraft lift-to-drag ratio (L/D) at moderate angles of attack (Figure 16). The jet momentum coefficient is defined as,

$$C_\mu = \rho V_j^2 S_j / \tfrac{1}{2} \rho U_0^2 S \qquad \text{(eqn 3.1)}$$

in which, ρ is the medium density, V_j and U_0 are the jet and free stream velocities and S_j and S are the jet and wing areas. However, further investigation **[Ref. 30 : pp. 225-226]** found that for a transport aircraft model, the improvement of L/D was less pronounced in the cruise configuration. Also, the flapped configuration erased the effect of blowing altogether, and dramatically increased the induced rolling moment (Figures 17, 18).

Recent research conducted by Wu and Vakili **[Ref. 31]** at the University of Tennessee Space Institute has been directed towards specifically improving wing aerodynamic characteristics. Different configurations of blowing jets, directed spanwise off the wingtip, have been explored. Three discrete jets, as shown in Figures 19 and 20, with varying angles off the span axis have been most effective in altering the pressure distribution over the wing. Tests were made in the wind tunnel on a NACA 0012-64 airfoil (Re= 4 x 10^5) with C_μ varying from .001 to .01. The jet blowing alters the flow field, effectively increasing the wingspan. Flow visualization studies carried out in the water tunnel found that wingtip-jet blowing not only injected turbulence, but generated secondary vortices. All these secondary vortices drew some of their energy from the wingtip vortex and marked interaction was noted which could effectively alleviate the wake vortex hazard. More concentrated blowing in the forward jet produced greater vortex dispersion.

The upwardly-deflected blown flap, located near the wingtip (Figure 21), is another device which has reduced both tangential velocities and induced rolling moments [Ref. 27 : pp. 8,15,73]. Its effects are shown in Figure 22 and Table III . Again, this was for an extremely small momentum coefficient (4.94 x 10^{-4}) and was demonstrated only in a cruise configuration at 4.42 km downstream. Only one study on this type of device has been found, in spite of the fact that it yields half the rolling moment of the unattenuated case. More research should be conducted in this area.

The blowing concept has one obvious detractor. It requires bleed air from some source which is most logically the engine. This requires drawing power off the engine and an air transport system through the wing. Therefore, this method cannot easily be applied to existing aircraft due to the enormous propulsion/airframe modification requirements. This concept, if effective, must be incorporated into future aircraft design requirements.

Wingtip-mounted jet engines (Figure 23) have been explored [Ref. 30,32 : pp. 224-225, p. 746]. The data, for

TABLE III

Induced Rolling Moment Coefficients for Various Devices [Ref. 27]

Generating Aircraft (Boeing 747)	Following Aircraft (Gates Learjet)	
Configuration	Induced Rolling Moment Coefficient, C_l	Induced Rolling Velocity, p degrees/second
Cruise-Basic	0.402	1042
Cruise-Vortex Generators (Device I)	0.103	268
Cruise Blown Flap (Device F)	0.202	530
Cruise Spline (Device H-1)	0.304	800
Flaps 30 - Basic	0.845	2200

Note: Maximum rolling-angular velocity corresponding to full aileron deflection on Gates Learjet is 120 degrees per second at an aircraft speed of 120 knots. This corresponds to a rolling moment coefficient $C_l = 0.0463$.

a momentum coefficient of .02, gives results similar to the rearward blowing jet. It decreases the induced drag but is still ineffective in reducing the vortex hazard. Wingtip props are currently being explored by Loth [Ref. 33]. The propeller rotation, opposite to the vortex roll-up, would counter the tip vortex circulation. The wingtip prop produces a flow field where upwash is created inboard of the wingtip, rather than the customary downwash. This upwash can even result in additional thrust. The overall effectiveness is dependent not only on the propeller's diameter, but also on the amount of vorticity it can produce. Wing tip mounted jet engines and propellers have drawbacks, also. The increase in wing weight due to structural considerations may be prohibitive. Furthermore, consideration must be given to the effects of asymmetric thrust in the event of a single engine failure.

Control surface oscillation has produced interesting results with respect to vortex attenuation. Actual flight test investigation [Ref. 34] has examined transport aircraft. Initial results with a B-747 indicated that past 3 nautical miles (NM) the use of specific aileron/spoiler configuration produced wakes with no rotary motion (Figure 24). This was at a set frequency of 6 sec/cycle and required complex manipulation of the control surfaces by the pilot. Subsequent tests on the L-1011 could not reproduce the favorable results of the B-747. Attempts to recreate the 747 maneuvers required inputs from both the pilot and co-pilot. The attenuation levels were attained by landing-configured aircraft with landing gear extended. However, the oscillation surfaces produced generating aircraft rolling motion that would be unacceptable for final approach.

C. PASSIVE DEVICES

Numerous studies have involved the use of splines as an attenuation device. The earliest study by Uzel and Marchman [Ref. 35] used various crossed blades (Figure 25, 25a) at the wingtips. They showed their capability of reducing both the maximum tangential velocity and increasing core size. Kirkman, et al. [Ref. 27 : pp. 16-18,101] with towing tank results for a 3/100 scale model B-747 showed similar effects with his spline (Figure 26). But, at 4.42 km downstream, the rolling moment was still outside the controllable aileron limits of the Learjet. Additionally, the drag increase due to those devices was between 70-280% in cruise configuration. Croom [Ref. 36,37 : pp. 4-7, 6-10] showed that the spline was much less effective in reducing the rolling moment when the aircraft was in the flapped condition ($Re=5.74 \times 10^5$, $C_L = 1.25$). The effectiveness was dependent on the flap settings in conjunction with the location of the spline along the span. Flap settings drastically changed the vorticity pattern off the span, so that a spline located near the wingtip might be fine for cruise, but little help at lower speeds when flaps are extended. Actual flight testing by Hastings, et al. [Ref. 38] has also demonstrated the effectiveness of wingtip-mounted splines in reducing rolling moments. The spline diameter was 55% of the chordlength and mounted 50% of the chordlength aft the wing trailing edge. Aileron control could only be maintained beyond 2.5 NM downstream of the unattenuated vortex while the spline reduced this distance to .62 NM. These results were obtained with a Douglas C-54 as the generating aircraft and a Piper Cherokee as the probe aircraft. The spline appears quite effective, and its construction allows it to be deployed for takeoff and landing just as the spokes on an umbrella (Figures 27, 28). Placement of the spline is critical and multiple splines may be necessary on heavily flapped aircraft.

The cabled drogue cone and cabled chute, shown in Figure 29, have been mentioned just in passing. The drogue cone [Ref. 27 : p. 17] was towed approximately 1.5 spanlengths behind the model with little change in the velocity field farther downstream. It appears that this technique was unacceptable based on the difficulties in intercepting the vortex. Patterson [Ref. 32 : pp. 745-746], examining the cabled chute, found velocity profiles similar to those of the spline. Yet, the tremendous increase in drag produced by the chute made its use impractical.

The use of vortex generators or wingfins has been examined in a tow tank, but more extensively in a wind tunnel. Kirkman, et al. [Ref. 27 : p. 19], again using the .03 scale model B-747, mounted 18 wingfins along the 75% chordline of each semispan (Figure 30). These wingfins were

(3) Is the device going to create additional wing stress problems? (e.g. gust loading or other unsteady flow effects, higher wing root moments, wing fatigue (high frequency vibration), structural limits on the device and its attachment points, etc.);

(4) What are the effects on ground and terminal area operations? (Ground clearance for the device , mobility around the device (fueling, taxiing, loading, etc.), and the noise characteristics);

(5) Will the device still produce favorable results under varying conditions of flight? (cruise, flaps extended for takeoff/landing, gear extended or retracted);

(6) Can the loss of the device on a single wingtip be handled without producing catastrophic results?;

(7) What are the effects of the device on the trailing vortices further downstream?; and

(8) Is the device applicable to the military as well as civilian aircraft?

With these factors in mind, it appears that only three of the existing devices hold any promise. They are the discrete wingtip jets, the Whitcomb winglet, and the wingtip sails. While these devices have shown improvements in the aircraft lift-to-drag ratio, all the research has been limited to near-field effects alone. Therefore, no tangible evidence exists that these devices really do reduce the wake vortex hazard further downstream. However, based solely on the data reported, the existence of secondary vortices and the possible dissipation that their interaction can create, it is conjectured that these devices can achieve some degree of vortex attenuation. Both the wingtip jets and the Whitcomb winglet produced multiple vortices at short distances downstream. The wingtip sails are also expected to produce multiple vortices even though there is not yet any experimental data to confirm it. It is of course possible that further downstream these vortices could coalesce into a single vortex recreating the vortex hazard to the following aircraft. Only with continued research can one answer the question of whether these devices dissipate or reinforce the trailing vortex.

The employment of passive devices seems a much simpler approach. However, the benefits of active devices, such as the wingtip jets, cannot be ignored. The ability to vary flow rates and directions to changing flight conditions, the lack of additional wing stresses at moderate blowing angles off the spanwise axis, the lack of ground clearance problems, and the ON-OFF capability make the wingtip jets attractive for use on civilian as well as military aircraft provided that the bleed air requirements do not degrade the engine performance significantly.

The use of wingtip jets would entail considerable aircraft modification. This would rule out a retrofit capability. The details of a bleed air piping system ducted through the wings, engine tapping for high pressure air, and control/monitoring devices for air flow and jet orifice positioning are enormous. One must also consider that passive devices, like the winglet and wingtip sail, cannot simply be fabricated and attached to the wingtips. These devices, to be structurally sound when operated over a wide variety of airspeeds and maneuver forces, must be an integral part of the wing itself. This would require completely new wings on anything other than possibly light aircraft.

While further research on the above devices is recommended, there are certainly other possible avenues which could be explored. All proposed devices have tried to destroy the vortex core by imposing adverse pressure gradients on the flow, in hopes that this will lead to vortex breakdown. Another concept,which may prove to be fruitful, is the attempt to vary the vortex strength periodically.

The introduction of a pulsating jet or nozzle which would provide step input changes to the circulation of the wingtip vortex might very well lead to the early destruction of the trailing vortex system. Also, a method might be devised for slicing the wingtip vortex, with jets normal to the vortex.

V. CONCLUSIONS

A survey and critical assessment of the known active and passive devices for wake vortex minimization warranted the following conclusions:

(1) None of the devices has been sufficiently investigated under laboratory and environmental conditions for immediate use on new or existing aircraft;

(2) Among the devices which do not require energy input from the aircraft, the wingtip sails and winglets have certain advantages. However, there is no information regarding their effectiveness on the demise of the vortices far downstream;

(3) Among the devices which do require energy input by the aircraft, discrete wingtip jets appear to be most effective;

(4) All the devices examined in this investigation require extensive research if their full potential on various aircraft is to be realized. Such research should clearly identify the effectiveness of each device on the near wake as well as the far wake several miles downstream of the aircraft;

(5) It appears that there is room for the development of new concepts, means and/or devices, in addition to those considered herein , which will lead to an overall effective solution of the most important problem of modern aviation.

APPENDIX A

FIGURES

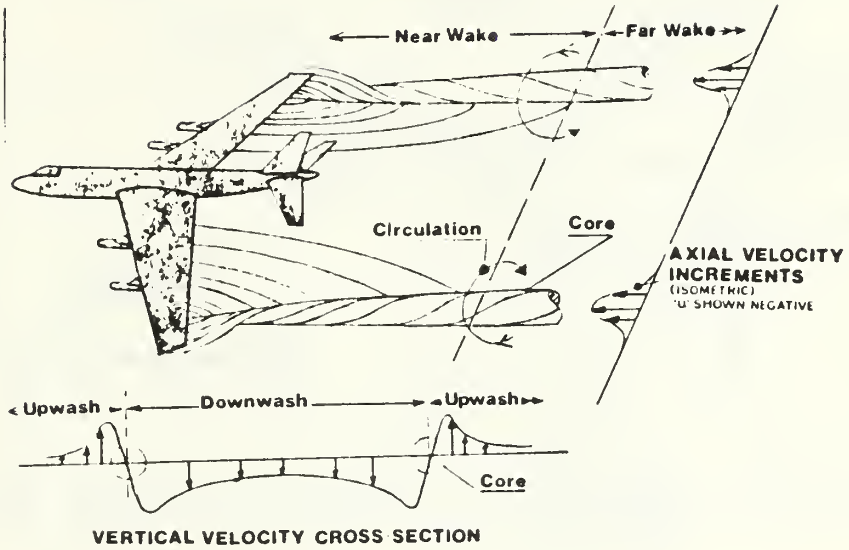
Near Wake
Far Wake
Circulation
Core
AXIAL VELOCITY INCREMENTS
(ISOMETRIC)
'U' SHOWN NEGATIVE
Upwash
Downwash
Upwash
Core
VERTICAL VELOCITY CROSS SECTION

Figure 1   Formation of Wake Vortex Showing Induced Velocities [Ref. 1].

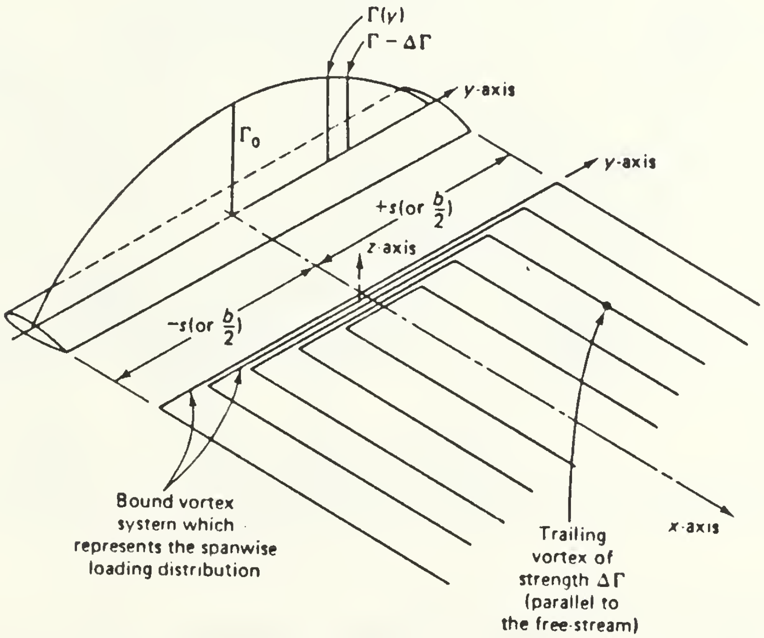
$\Gamma(y)$
$\Gamma - \Delta\Gamma$
y-axis
Γ_0
y-axis
$+s(\text{or } \frac{b}{2})$
z axis
$-s(\text{or } \frac{b}{2})$
Bound vortex system which represents the spanwise loading distribution
Trailing vortex of strength $\Delta\Gamma$ (parallel to the free-stream)
x-axis

Figure 2   Sketch of Trailing Vortex System [Ref. 2].

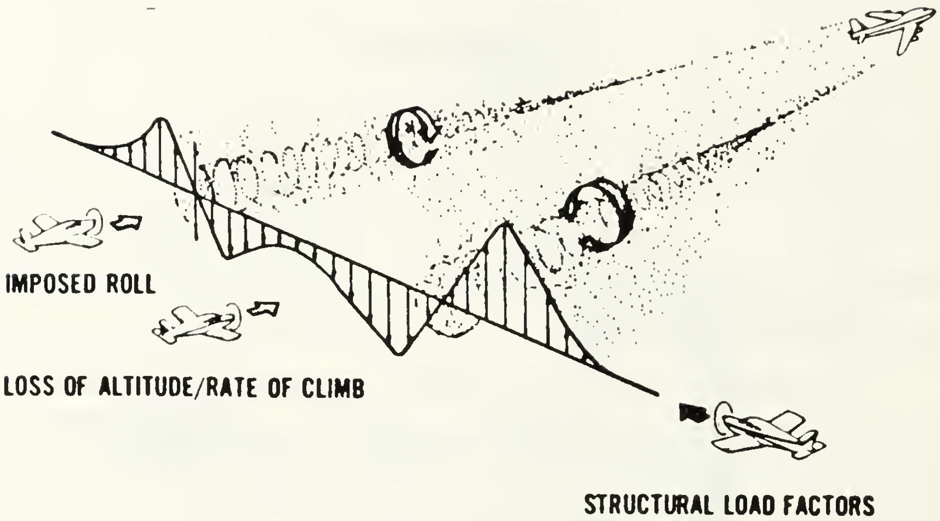
IMPOSED ROLL
LOSS OF ALTITUDE/RATE OF CLIMB
STRUCTURAL LOAD FACTORS

Figure 3 Trailing Vortex Hazard Potentials [Ref. 1].

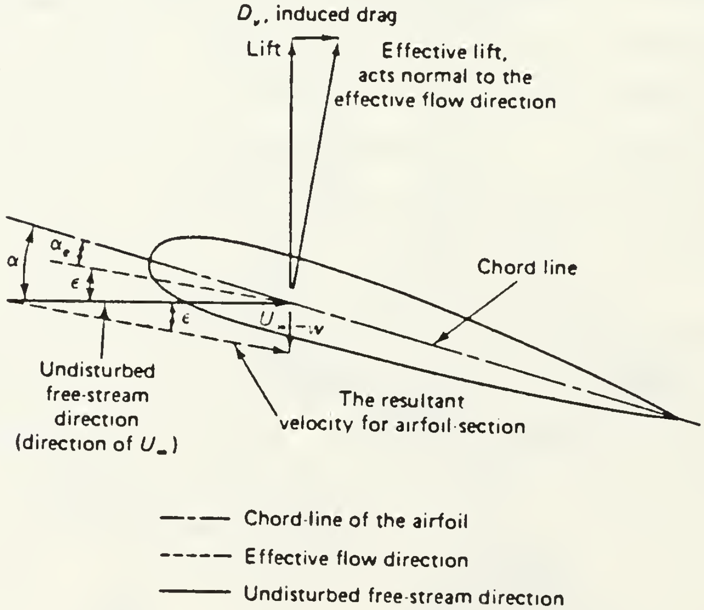
D_v, induced drag
Lift
Effective lift,
acts normal to the
effective flow direction
α
α_e
ϵ
ϵ
U_∞
$-w$
Chord line
Undisturbed
free-stream
direction
(direction of U_∞)
The resultant
velocity for airfoil-section
Chord-line of the airfoil
Effective flow direction
Undisturbed free-stream direction

Figure 4 Sketch of the Induced Flow [Ref. 2].

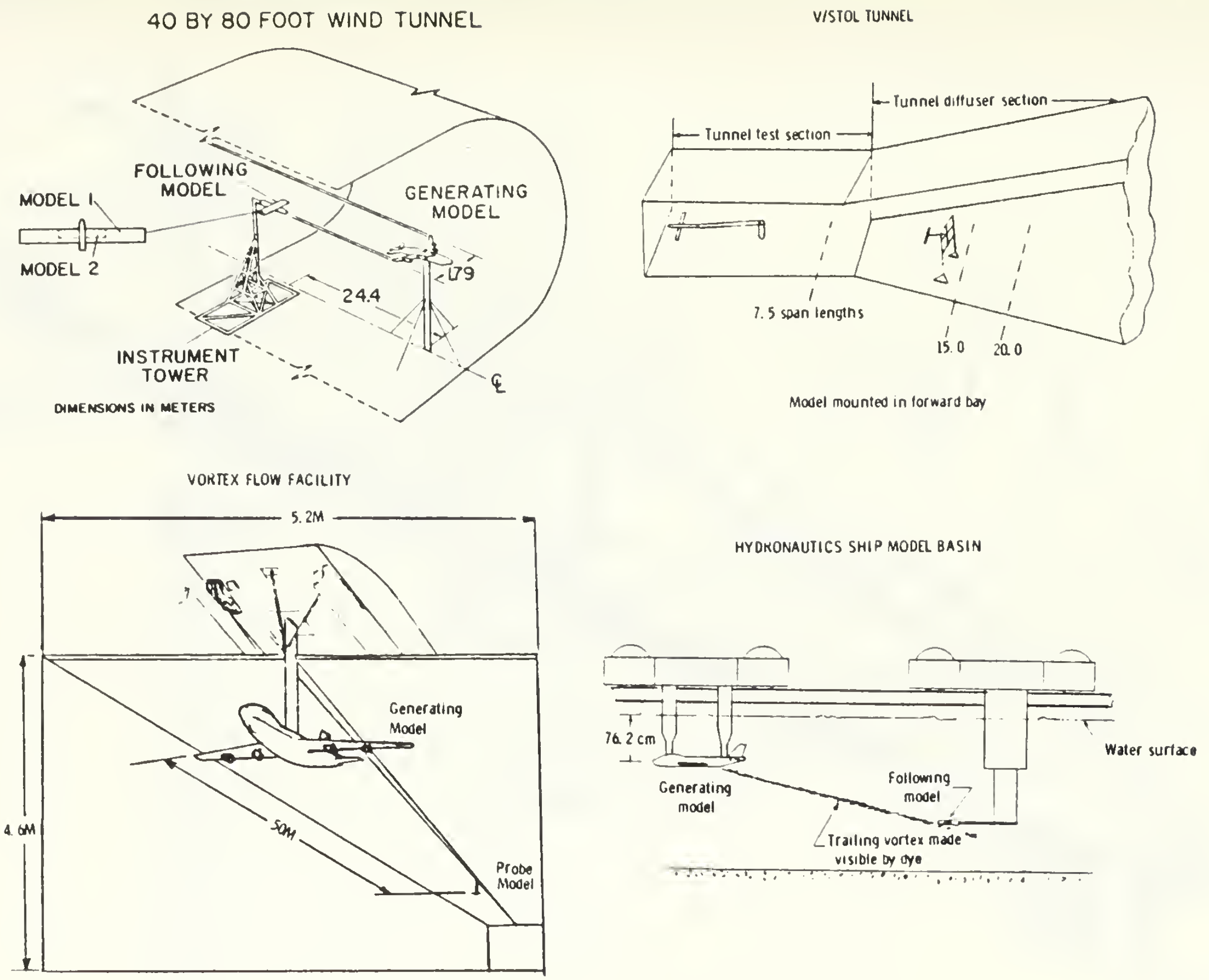
40 BY 80 FOOT WIND TUNNEL
FOLLOWING MODEL
MODEL 1
MODEL 2
GENERATING MODEL
24.4
.79
INSTRUMENT TOWER
℄
DIMENSIONS IN METERS
V/STOL TUNNEL
Tunnel diffuser section
Tunnel test section
7.5 span lengths
15.0
20.0
Model mounted in forward bay
VORTEX FLOW FACILITY
5.2M
Generating Model
4.6M
50M
Probe Model
HYDRONAUTICS SHIP MODEL BASIN
76.2 cm
Water surface
Generating model
Following model
Trailing vortex made visible by dye

Figure 5 Test Arrangement in NASA Facilities [Ref. 23].

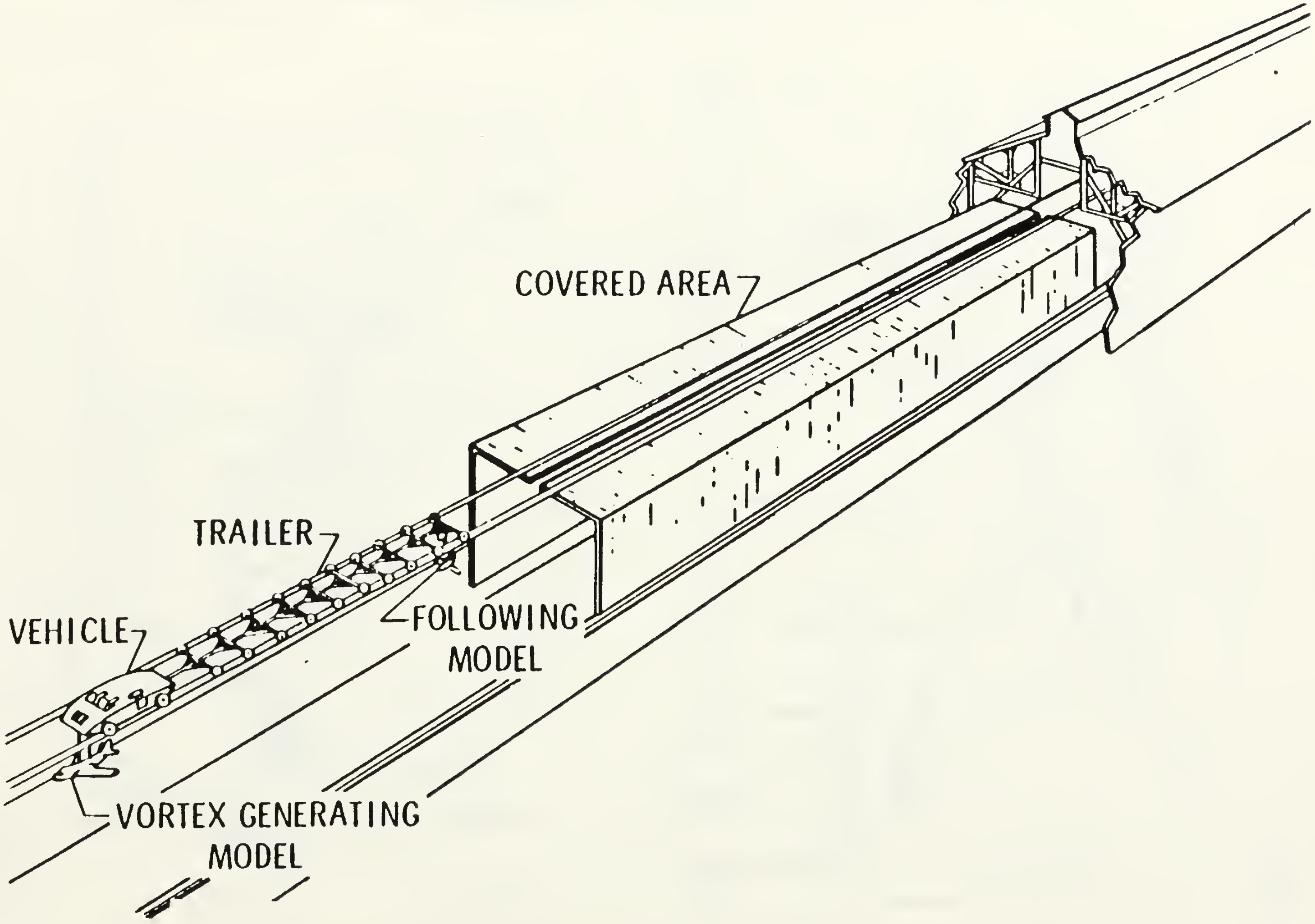
COVERED AREA
TRAILER
VEHICLE
FOLLOWING MODEL
VORTEX GENERATING MODEL

Figure 6 Arrangement of the Langley Vortex Research Facility [Ref. 28].

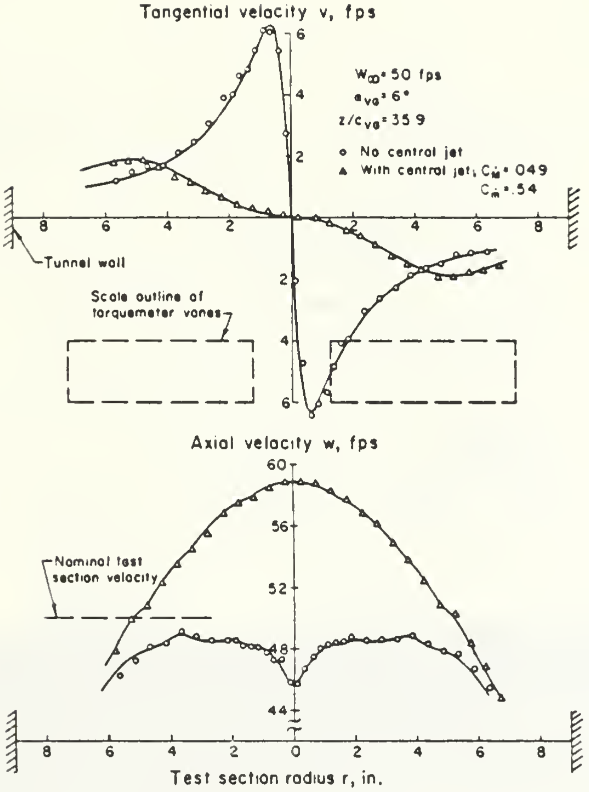

Figure 7 Effects of Central Jet on the Measured Tangential and Axial Mean Velocity Profiles [Ref. 25].

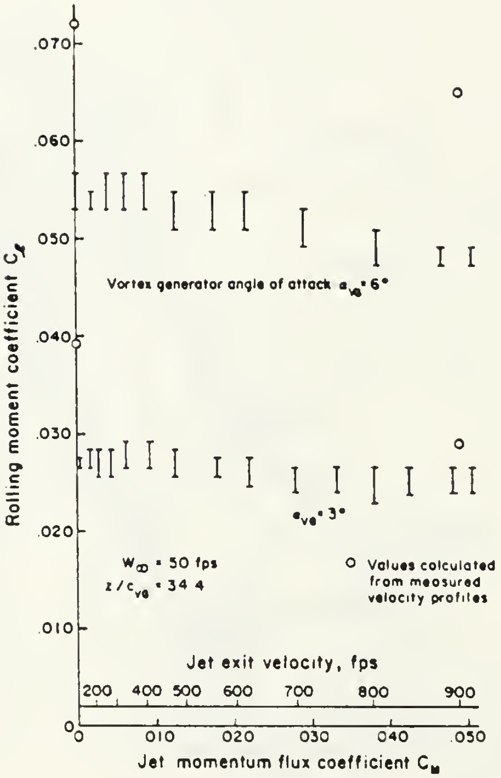

Figure 8 Effects of Central Jet on the Rolling Moment Coefficient [Ref. 25].

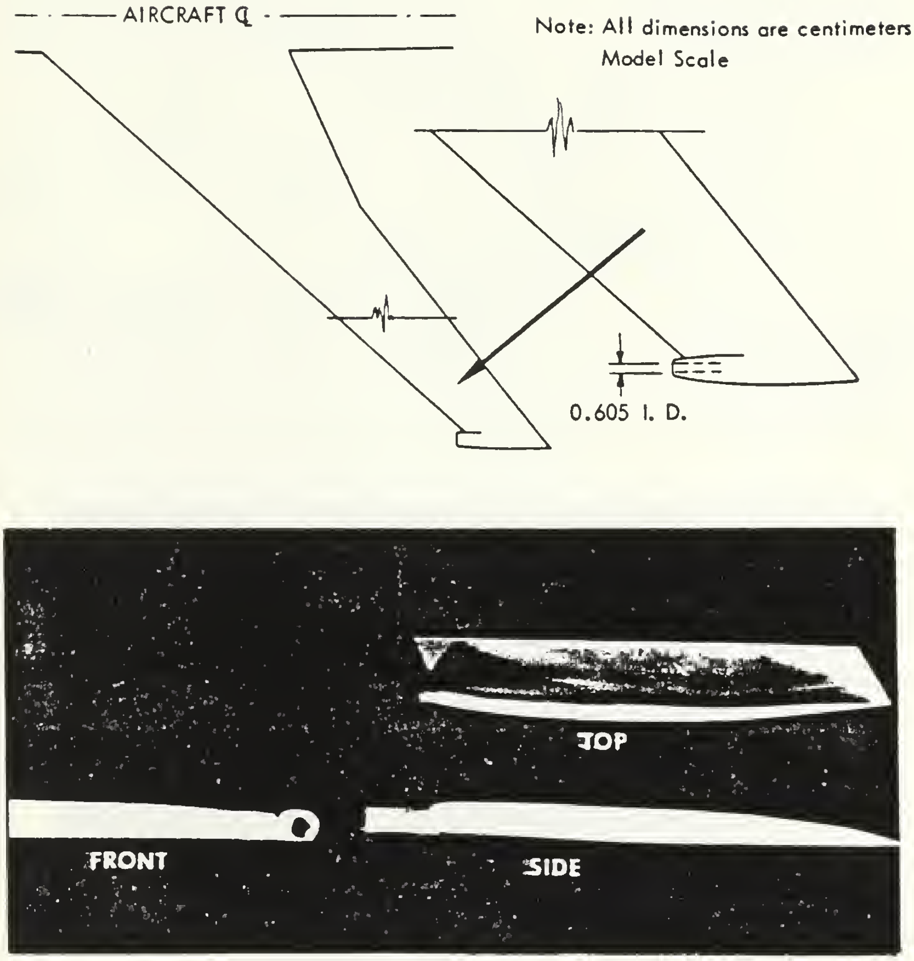
AIRCRAFT ℄
Note: All dimensions are centimeters
Model Scale
0.605 I. D.
TOP
FRONT
SIDE

Figure 9 Sketch and Close-Up Views of a Forward Blowing Jet [Ref. 27].

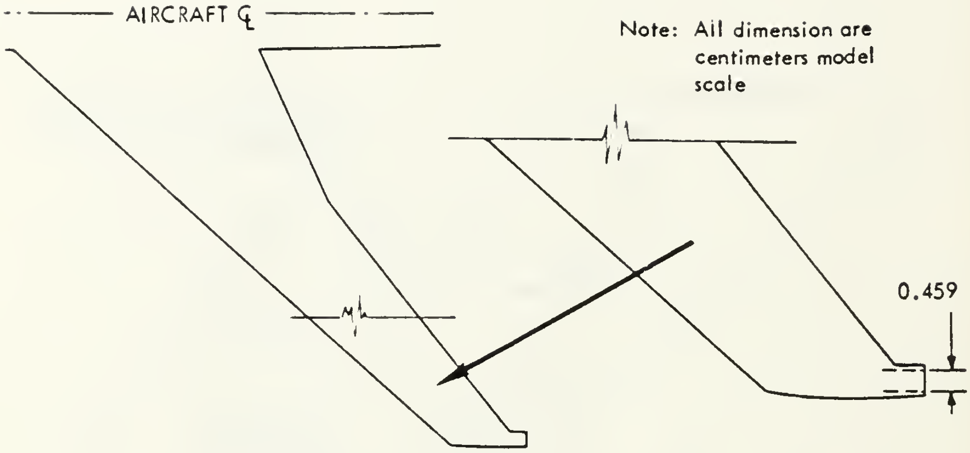
AIRCRAFT ℄
Note: All dimension are centimeters model scale
0.459

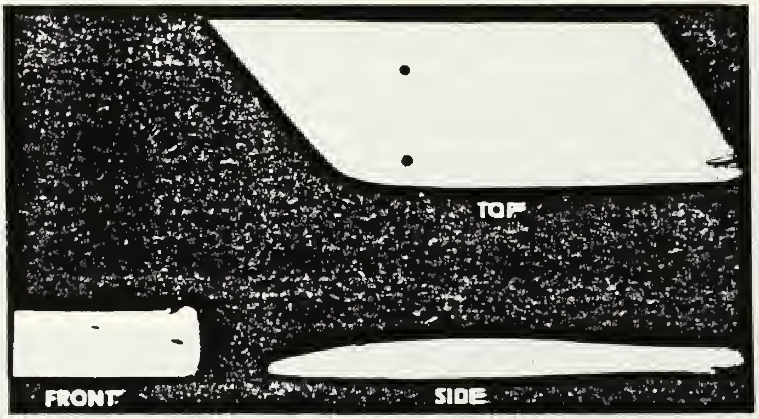
TOP
FRONT
SIDE

Figure 10 Sketch and Close-Up Views of a Rearward Blowing Jet [Ref. 27].

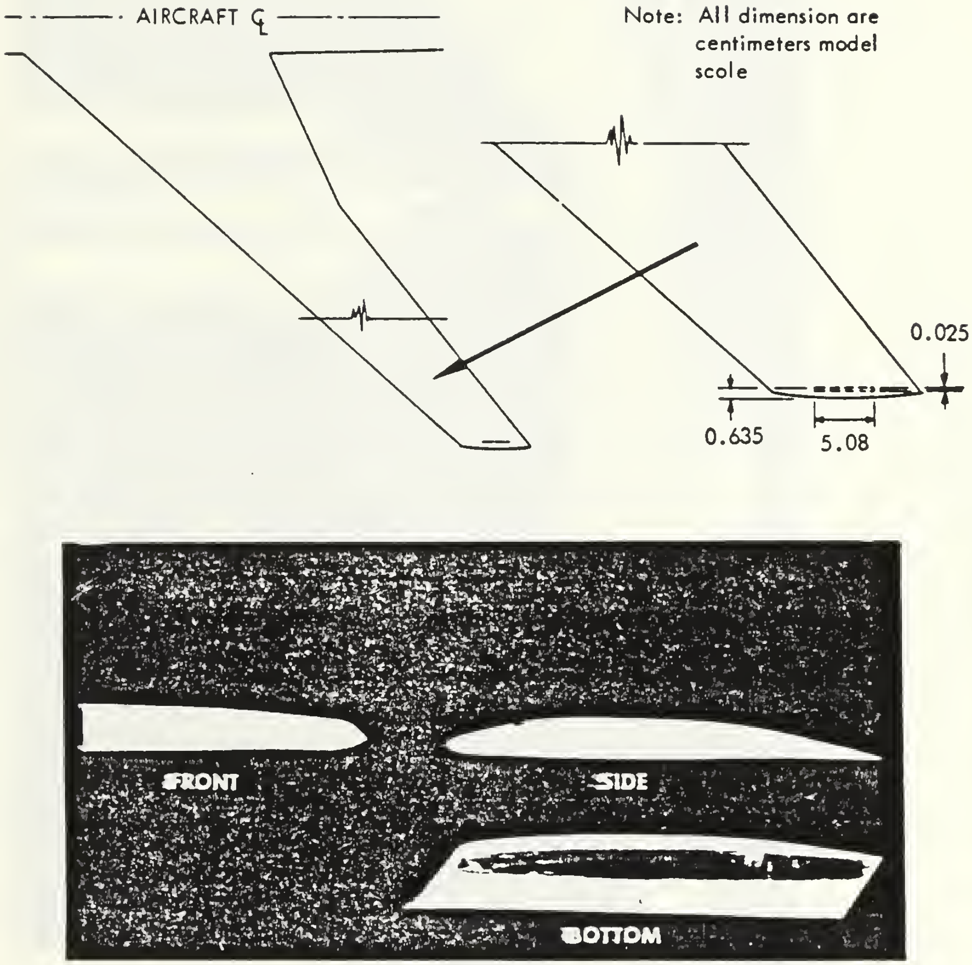
AIRCRAFT ℄
Note: All dimension are centimeters model scale
0.025
0.635
5.08
FRONT
SIDE
BOTTOM

Figure 11 Sketch and Close-Up Views of a Downward Blowing Jet [Ref. 27].

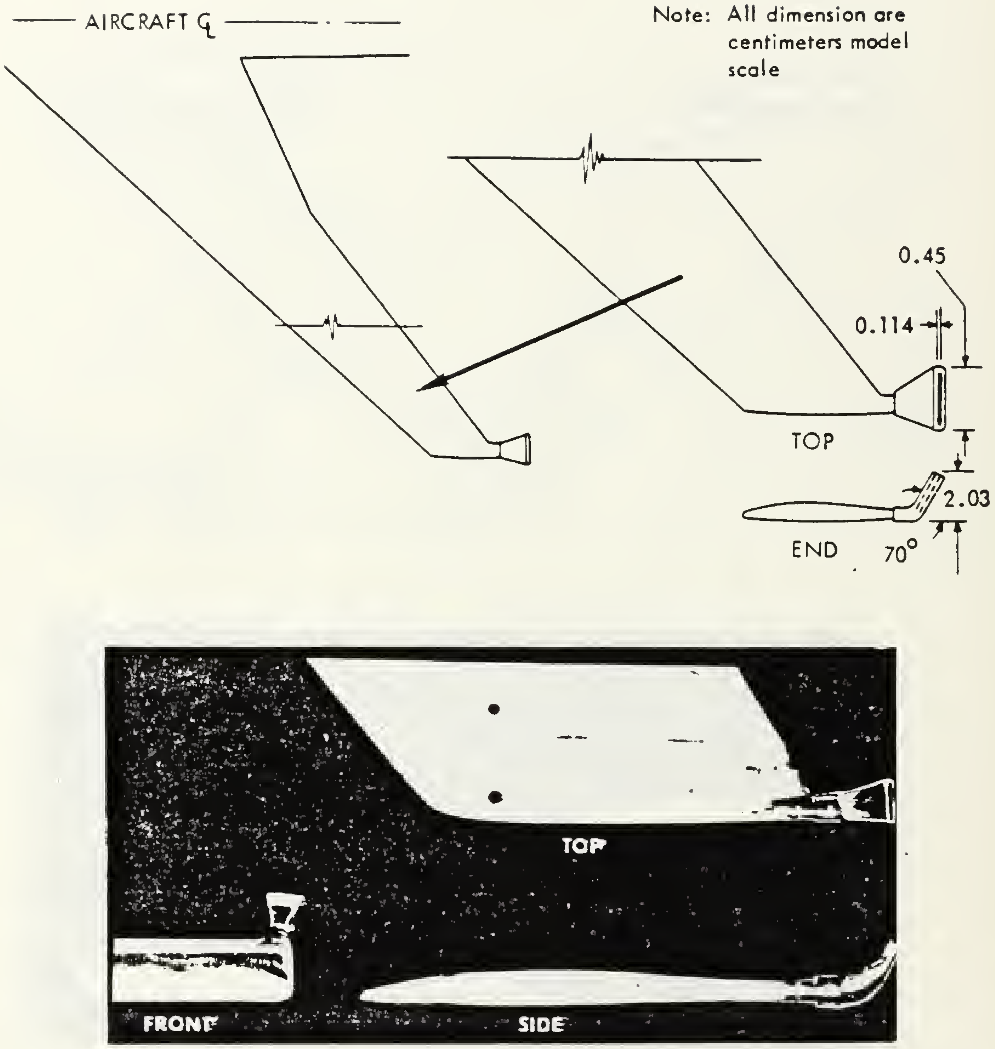
AIRCRAFT ℄
Note: All dimension are centimeters model scale
0.45
0.114
TOP
2.03
END
70°
TOP
FRONT
SIDE

Figure 12 Sketch and Close-Up Views of a Deflected Jet [Ref. 27].

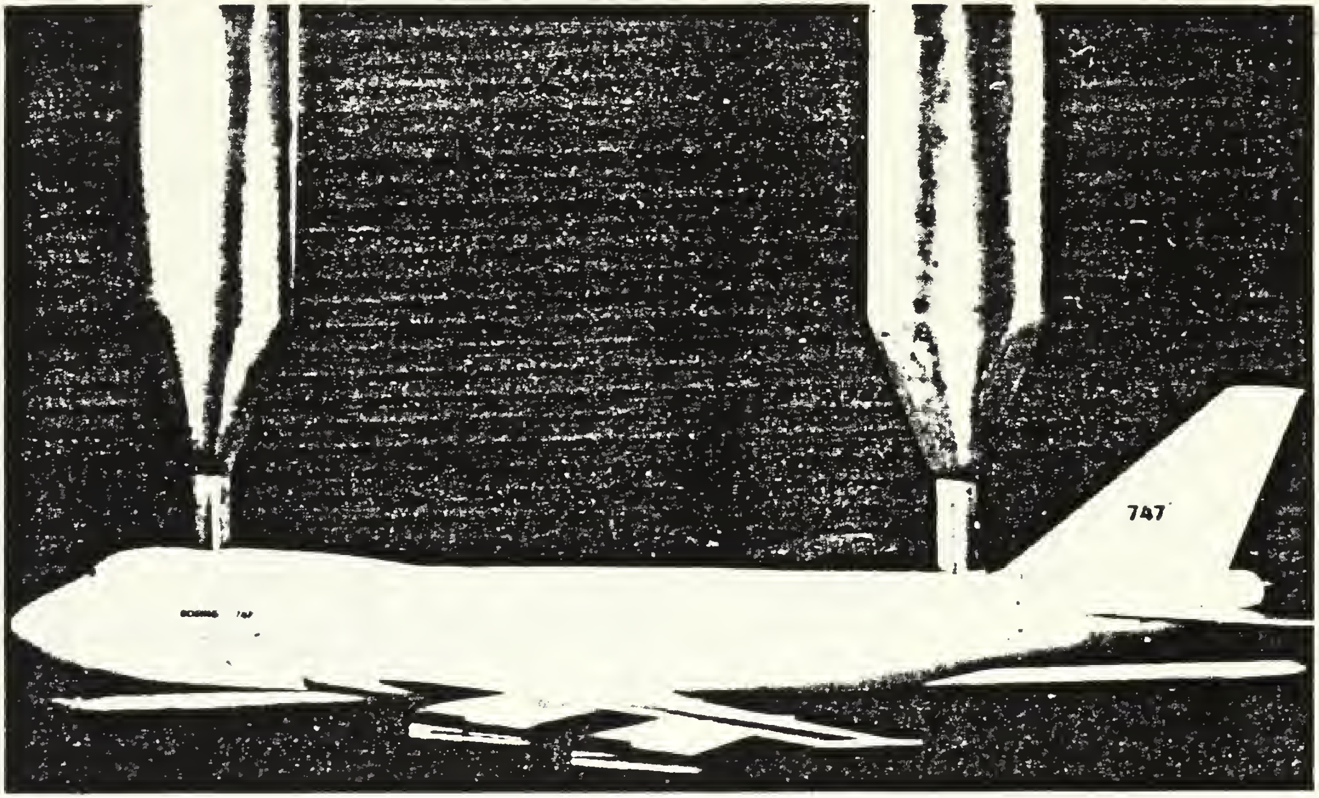

Figure 13 Basic Model of a Boeing 747 Aircraft [Ref. 27].

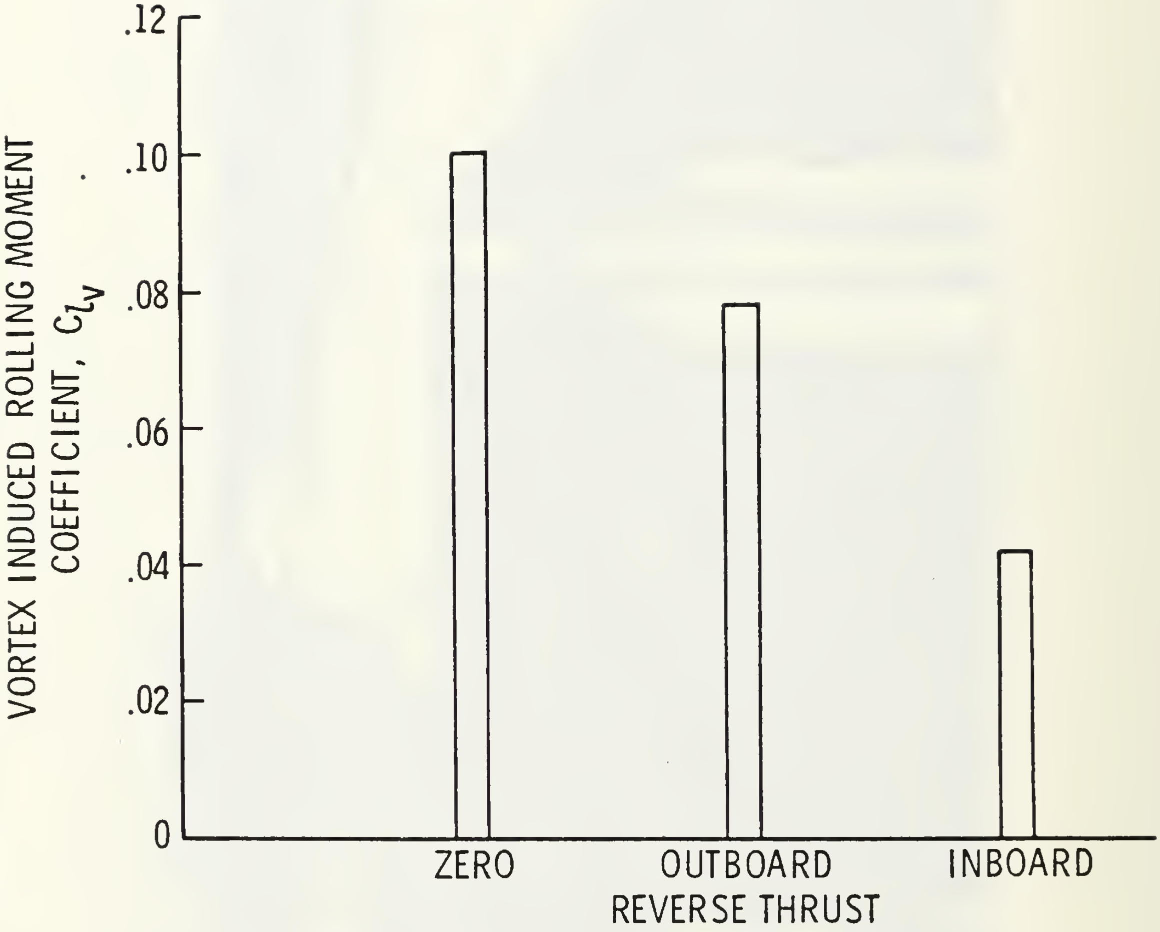

Figure 14 Effect of Engine Reverse Thrust on the Vortex Induced Rolling Moment Coefficient on a Learjet Probe Model [Ref. 28].

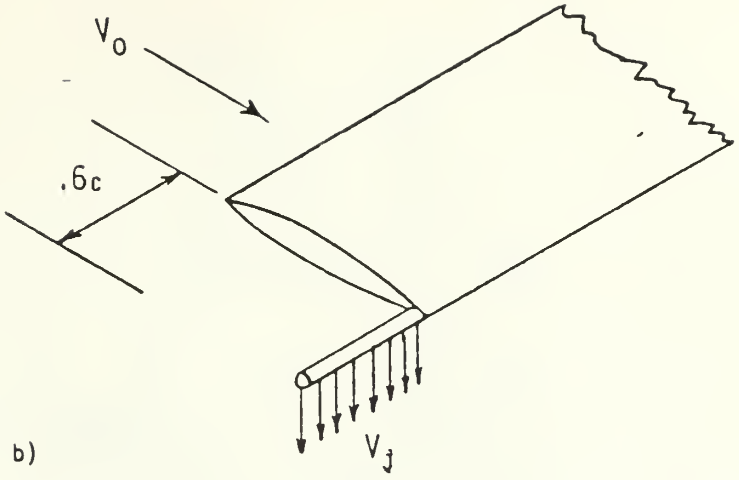

Figure 15 Sketch of a Spanwise Extended Blowing Tube [Ref. 30].

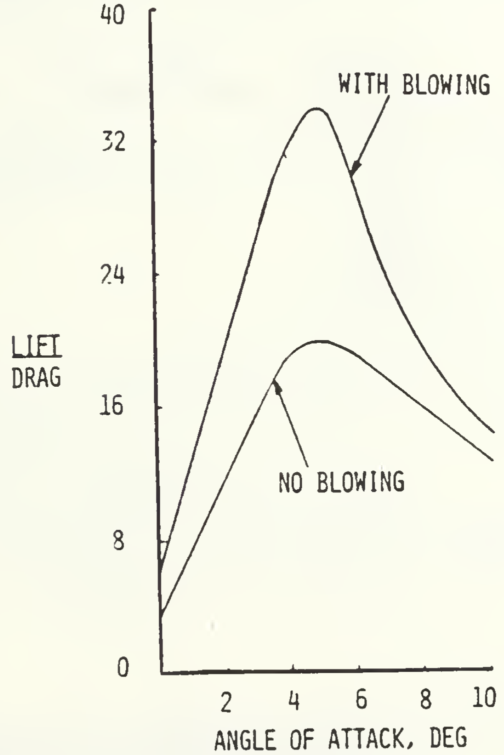

Figure 16 Effect on Lift-to-Drag Ratio from Spanwise Extended Tube Blowing [Ref. 30].

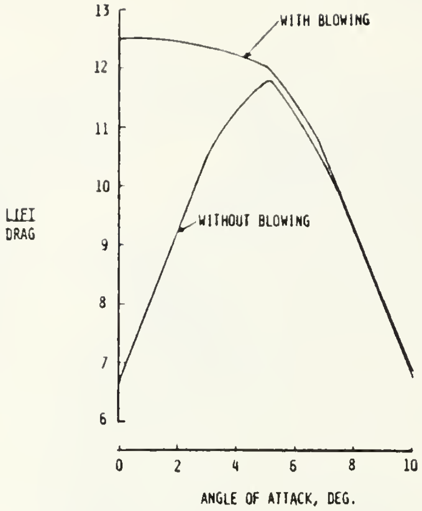

Figure 17 Effect on Lift-to-Drag Ratio from Spanwise Extended Tube Blowing at Transport Model Wingtip [Ref. 30].

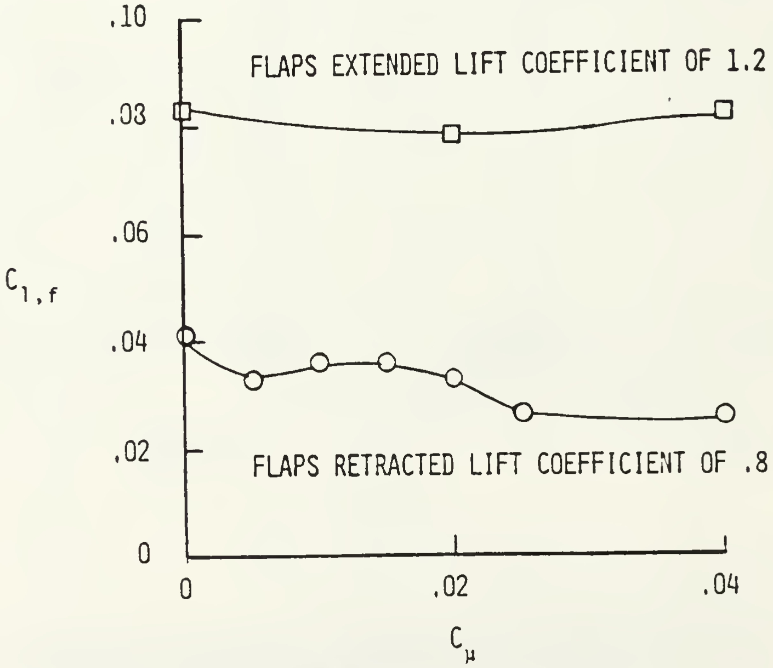

Figure 18 Rolling Moments Measured by a Small-Wing Model at 7.5 Spans Downstream a Transport Model with a Blowing Tube [Ref. 30].

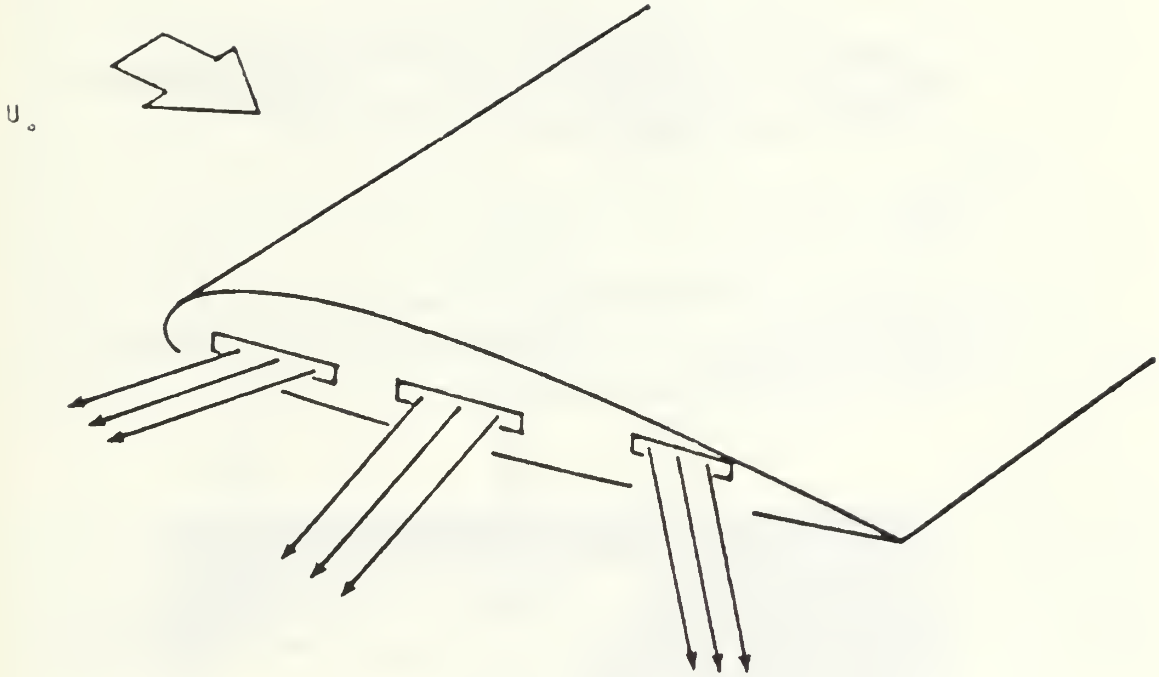

Figure 19 Sketch of Individually Controlled Discrete Wingtip Jets [Ref. 31].

(a) Cut-off View of Wing Model

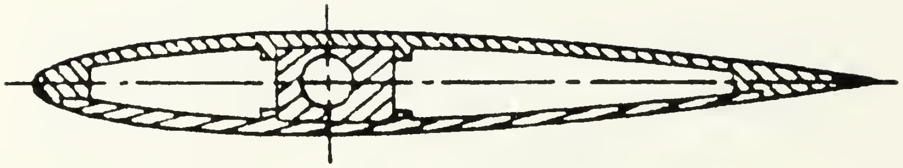

(b) Tip I

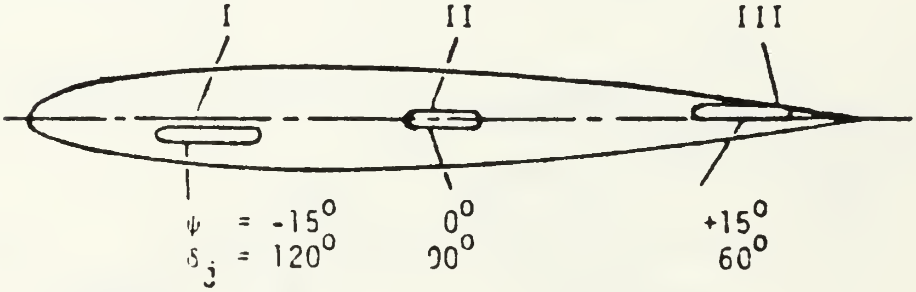
I
II
III
ψ = -15°
δj = 120°
0°
90°
+15°
60°

(c) Tip II

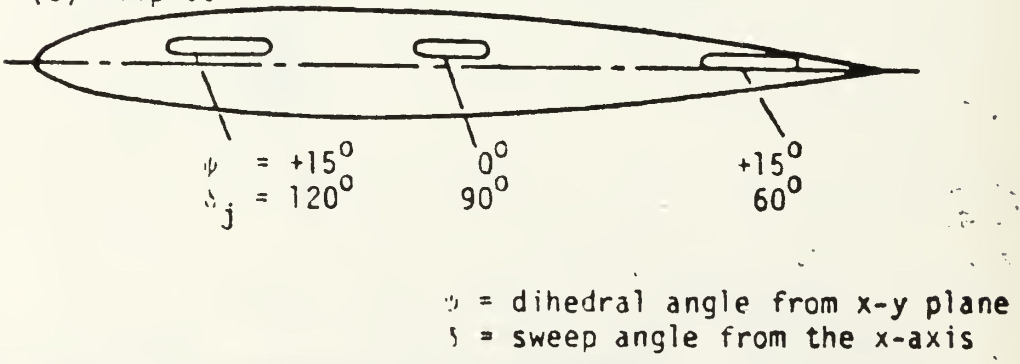
ψ = +15°
δj = 120°
0°
90°
+15°
60°
ψ = dihedral angle from x-y plane
δ = sweep angle from the x-axis

Figure 20 Two Typical Wingtip Jet Configurations [Ref. 31].

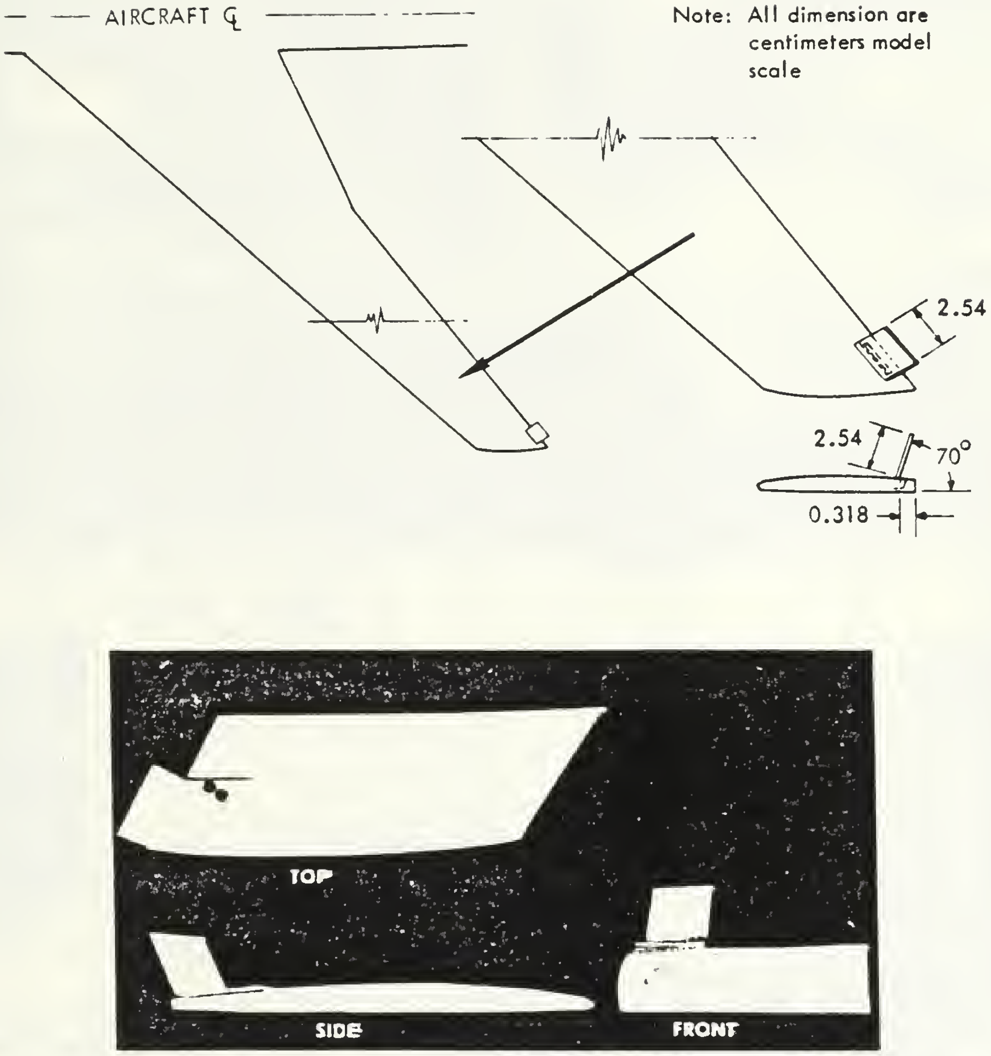
AIRCRAFT ℄
Note: All dimension are centimeters model scale
2.54
2.54
70°
0.318
TOP
SIDE
FRONT

Figure 21 Sketch and Close-Up Views of a Blown Flap [Ref. 27].

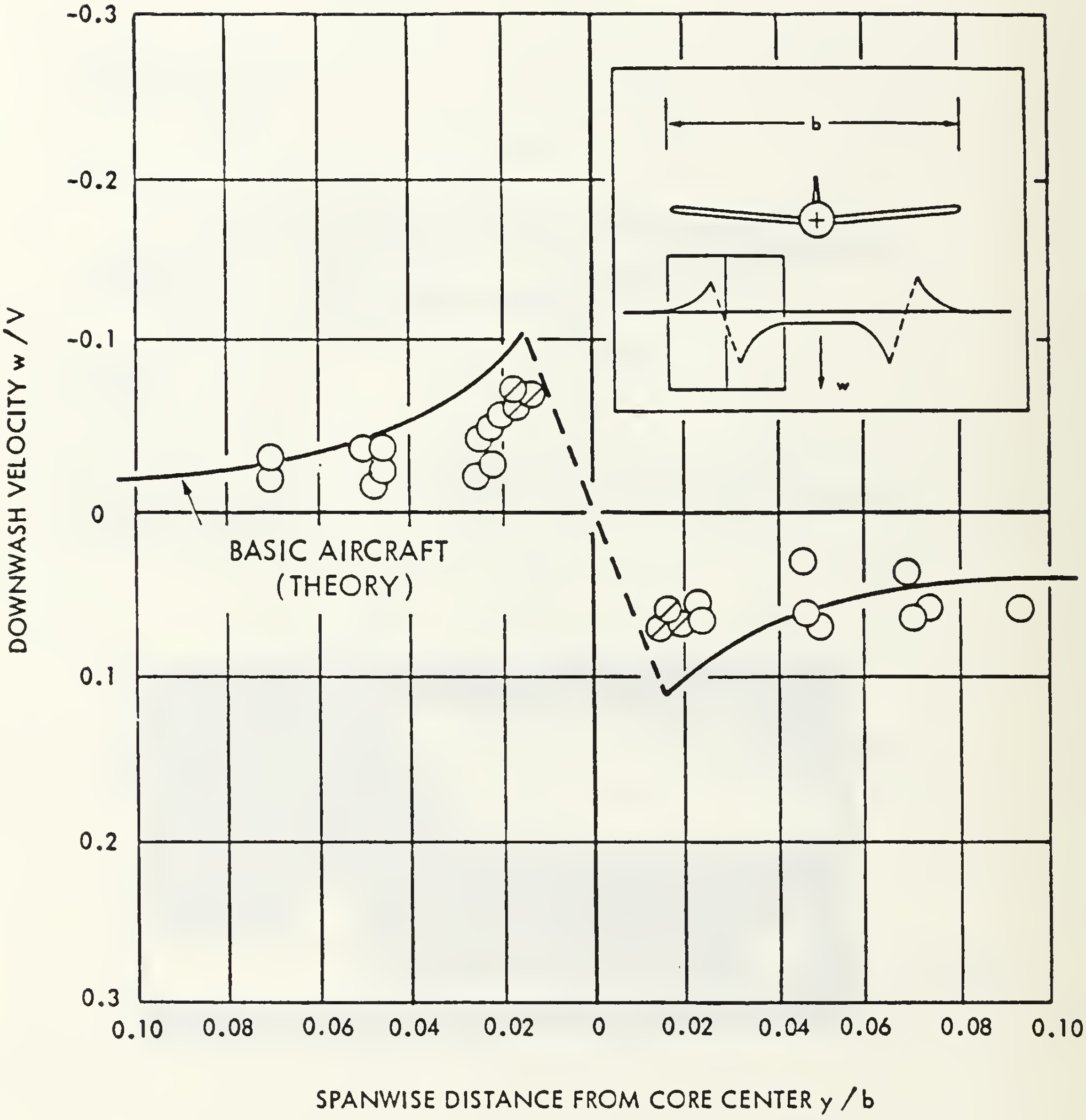

Figure 22 Effect of a Blown Flap on the Vortex Velocity Distribution [Ref. 27].

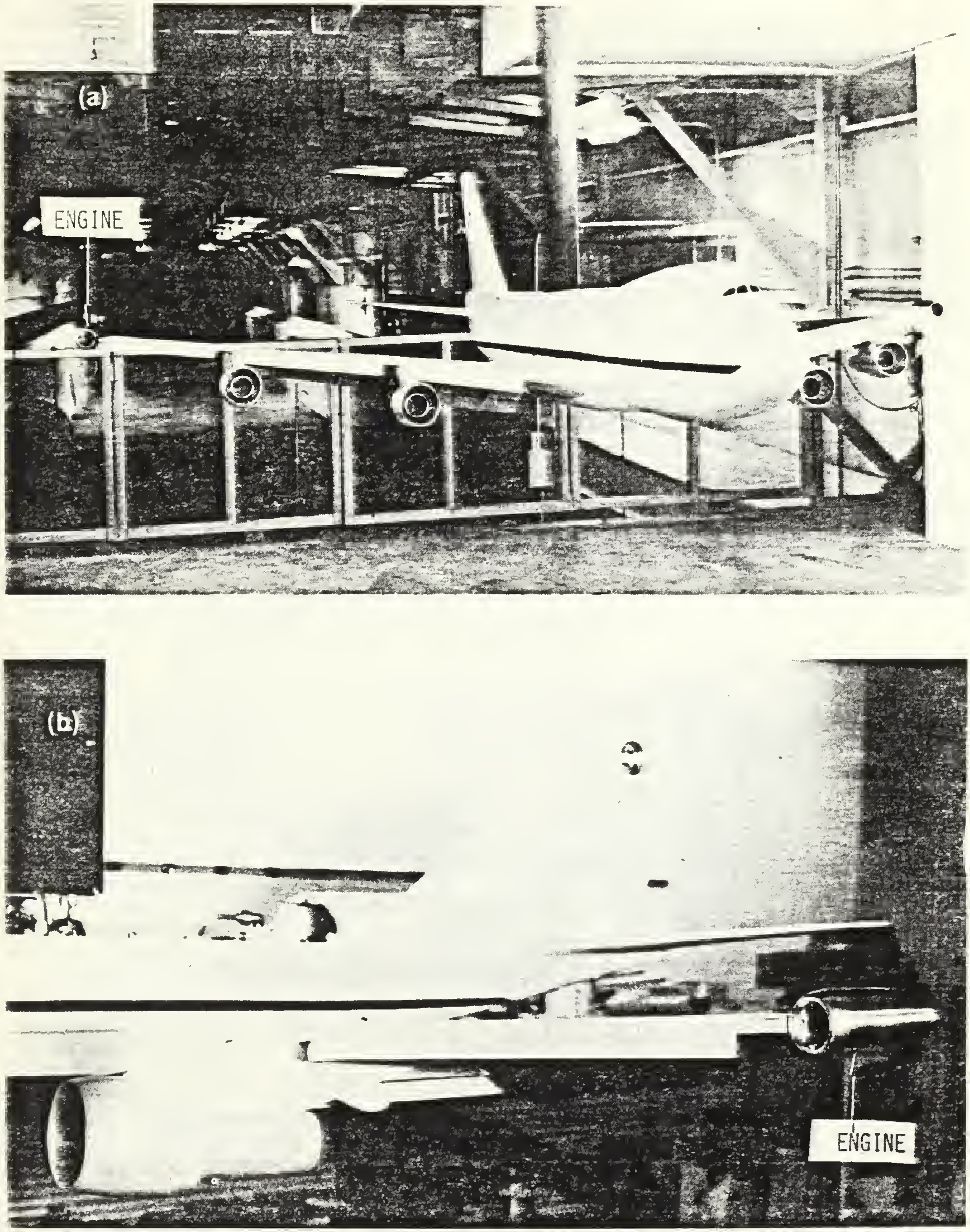
(a)
ENGINE
(b)
ENGINE

Figure 23 Wingtip-Mounted Engines on a Transport Model: Front and Side Views [Ref. 30].

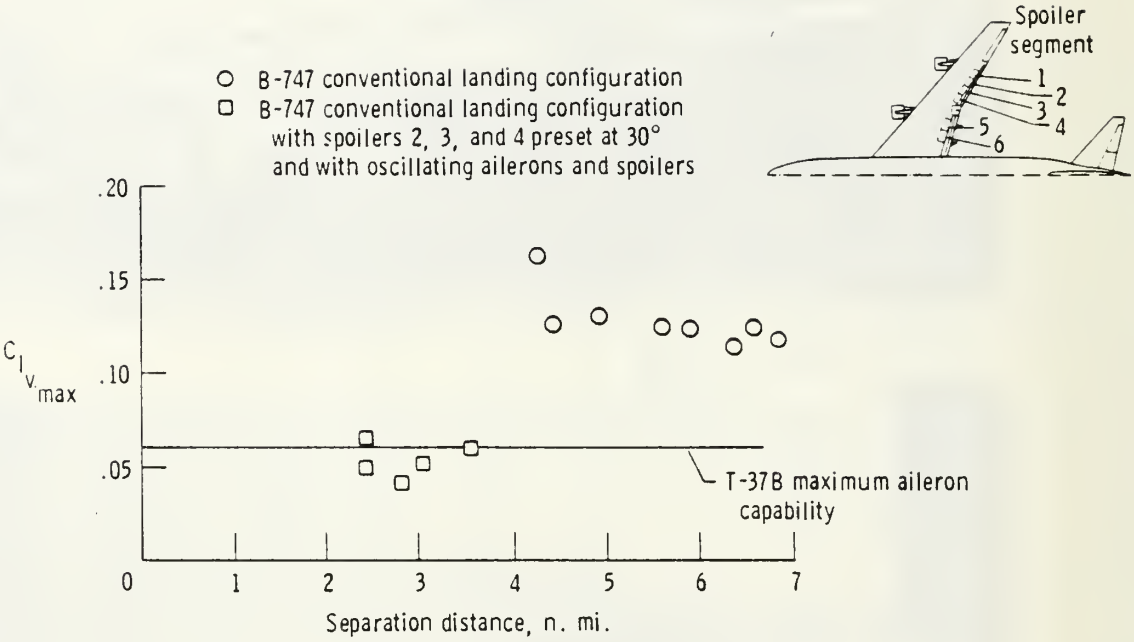

Figure 24 B-747 Wake Vortex Disturbance on a T-37B Probe Aircraft--Oscillating Ailerons and Spoilers [Ref. 34].

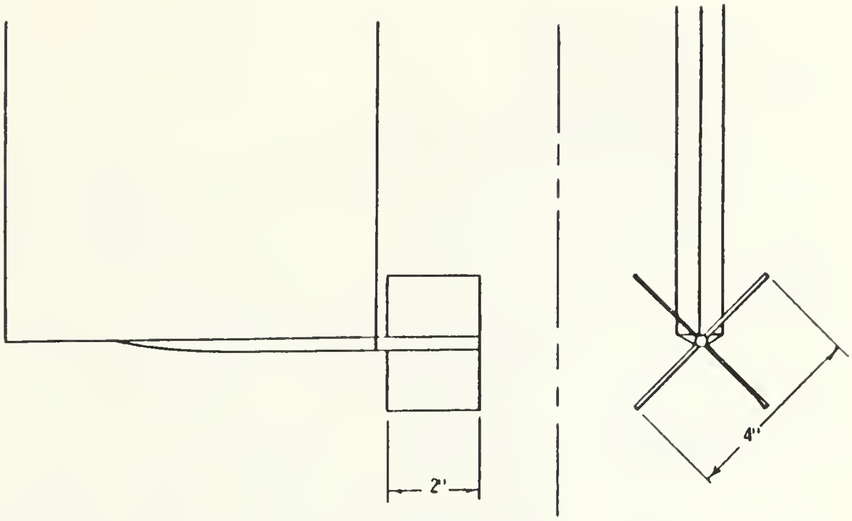

Figure 25 Sketch of Fixed Crossed Blades (Four Inch) [Ref. 35].

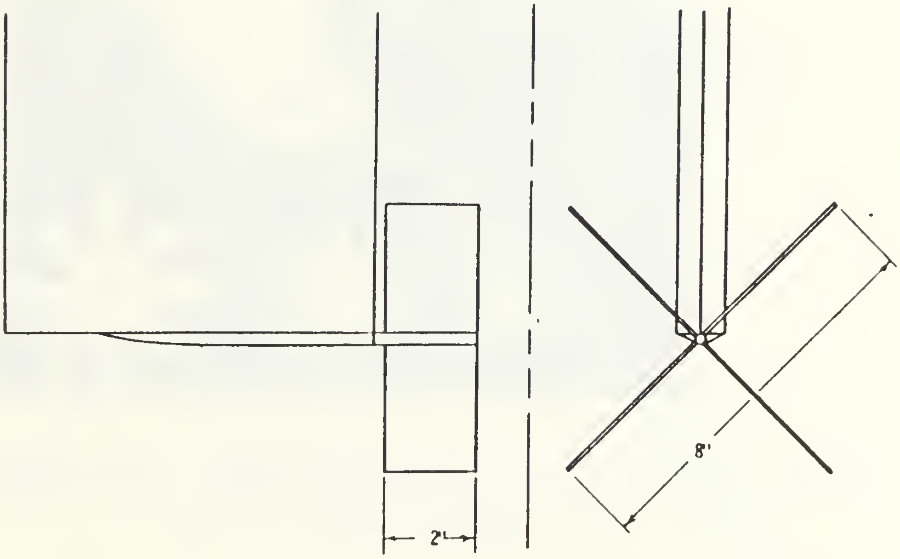

Figure 25a Sketch of Fixed Crossed Blades (Eight Inch) [Ref. 35].

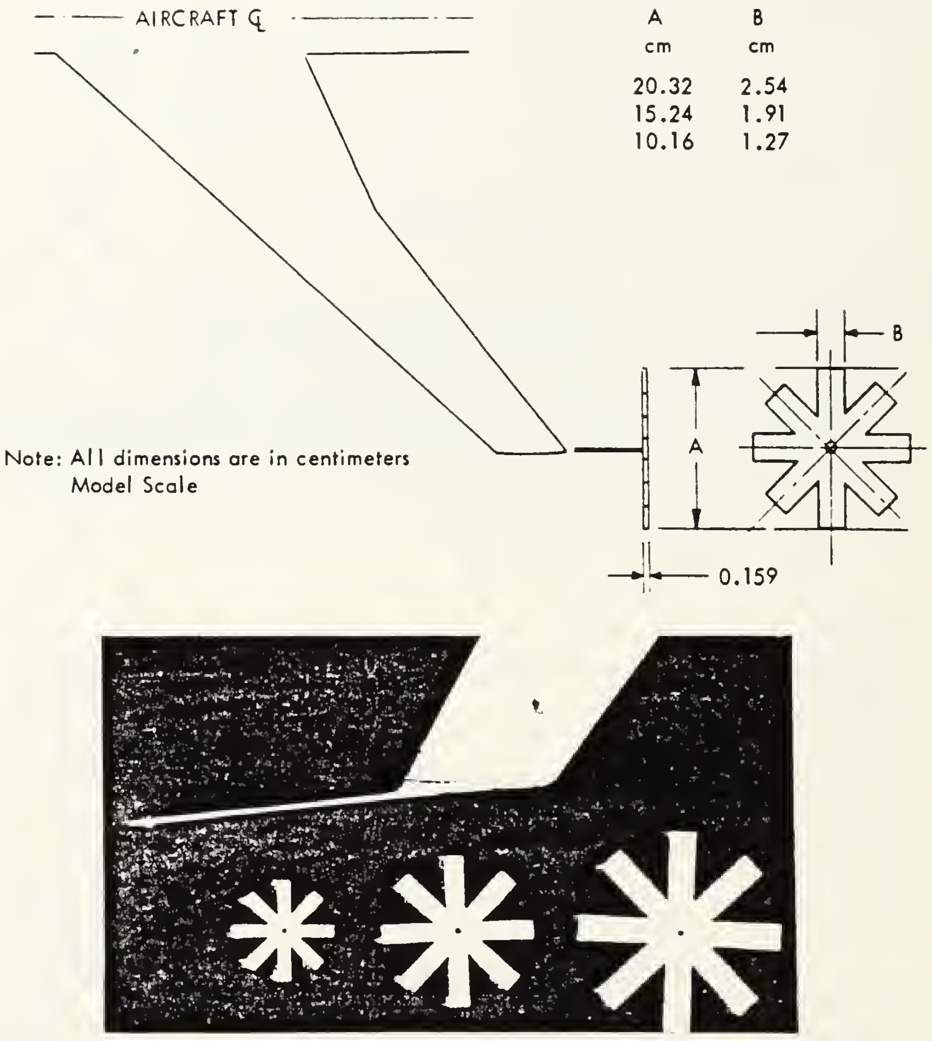
AIRCRAFT ℄
A
cm
20.32
15.24
10.16
B
cm
2.54
1.91
1.27
B
A
0.159
Note: All dimensions are in centimeters
Model Scale

Figure 26 Sketch and Close-Up Views of Wingtip Mounted Splines [Ref. 27].

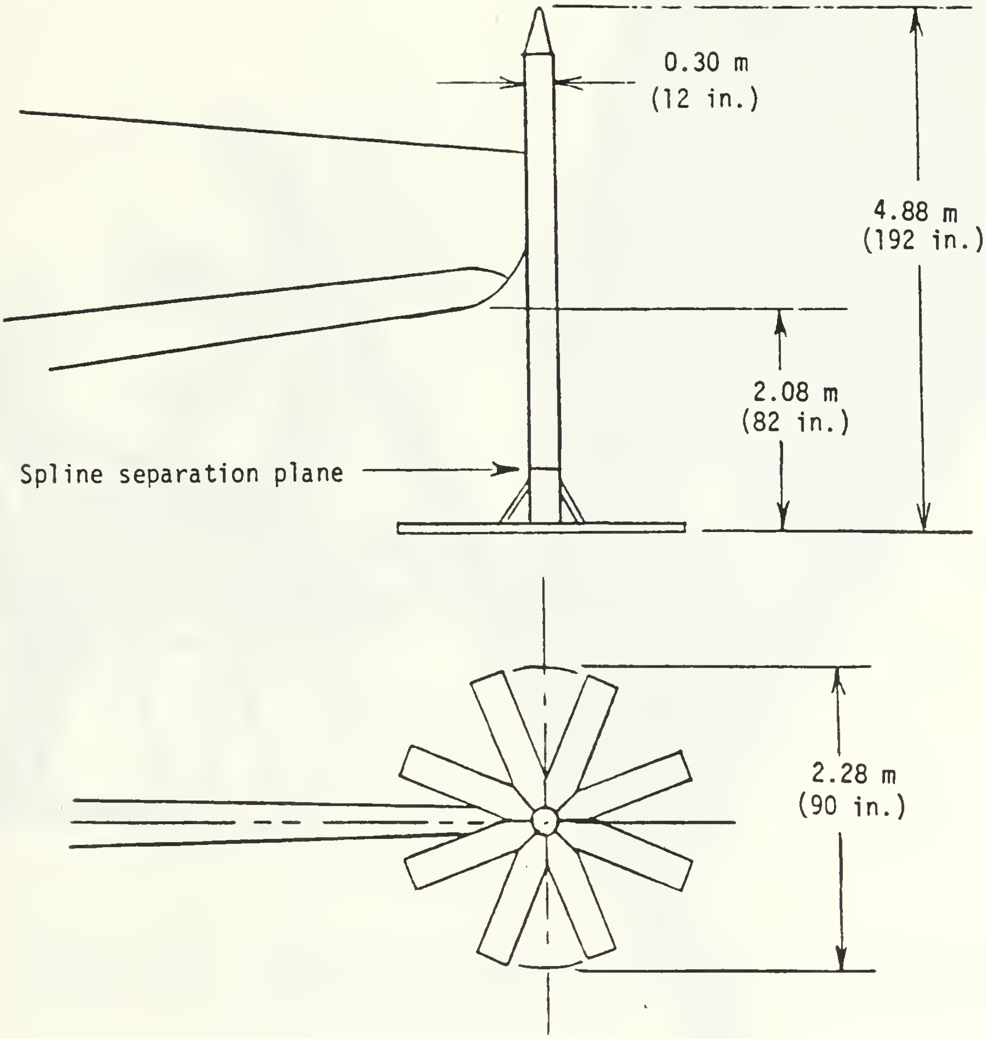
0.30 m
(12 in.)
4.88 m
(192 in.)
2.08 m
(82 in.)
Spline separation plane
2.28 m
(90 in.)

Figure 27 Sketch of Spline Assembly at Wingtip [Ref. 38].

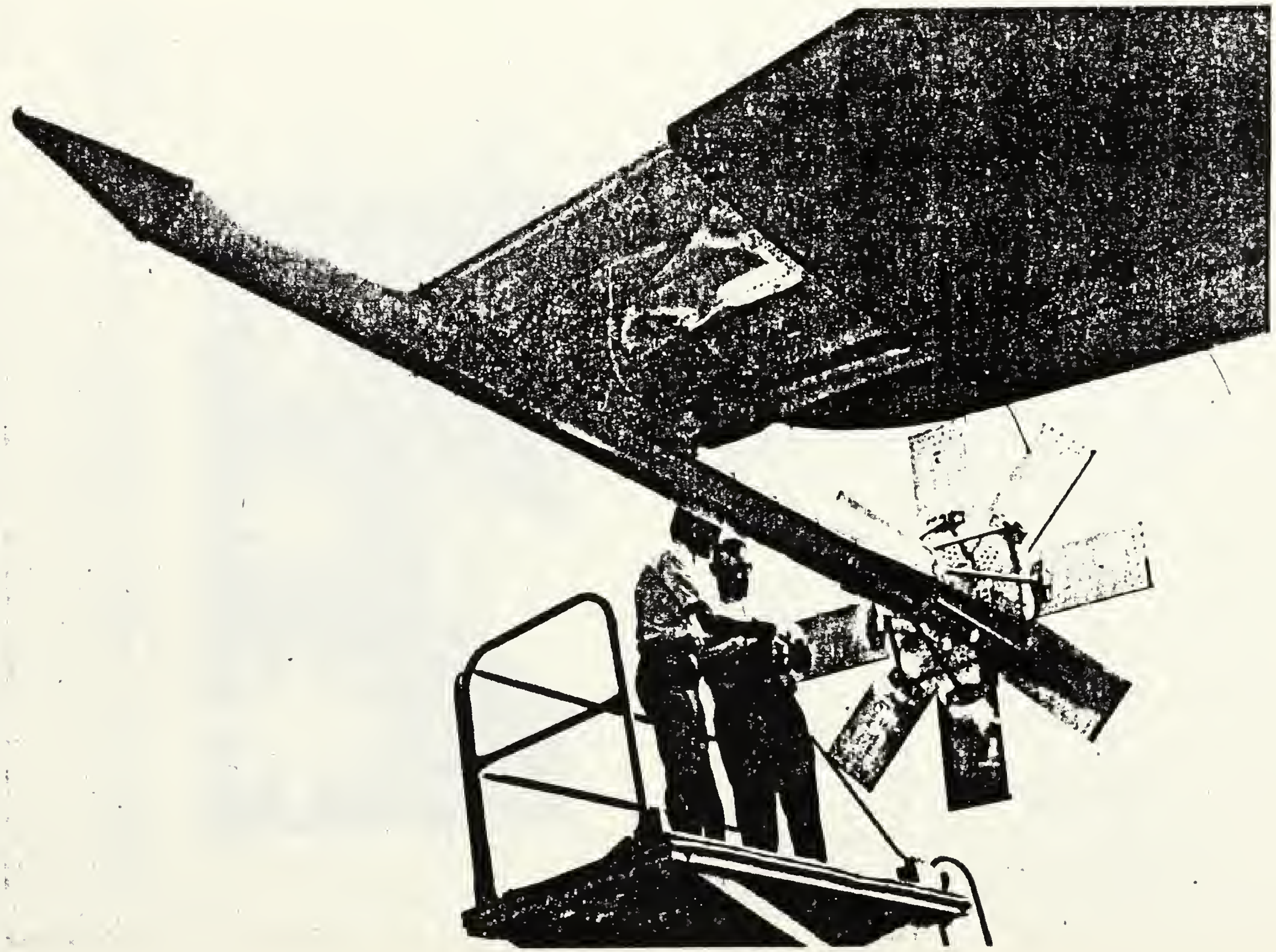

Figure 28 Photograph of the Spline Assembly on the Wingtip [Ref. 38].

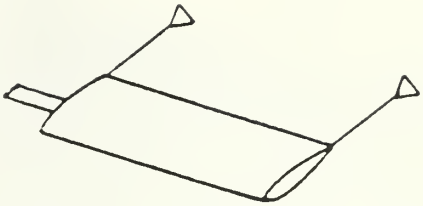

Cabled drogue
cones

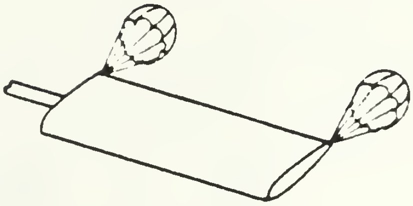

Cabled chutes

Figure 29 Sketch of Cabled Drogue Cone and Cabled Chute [Ref. 38].

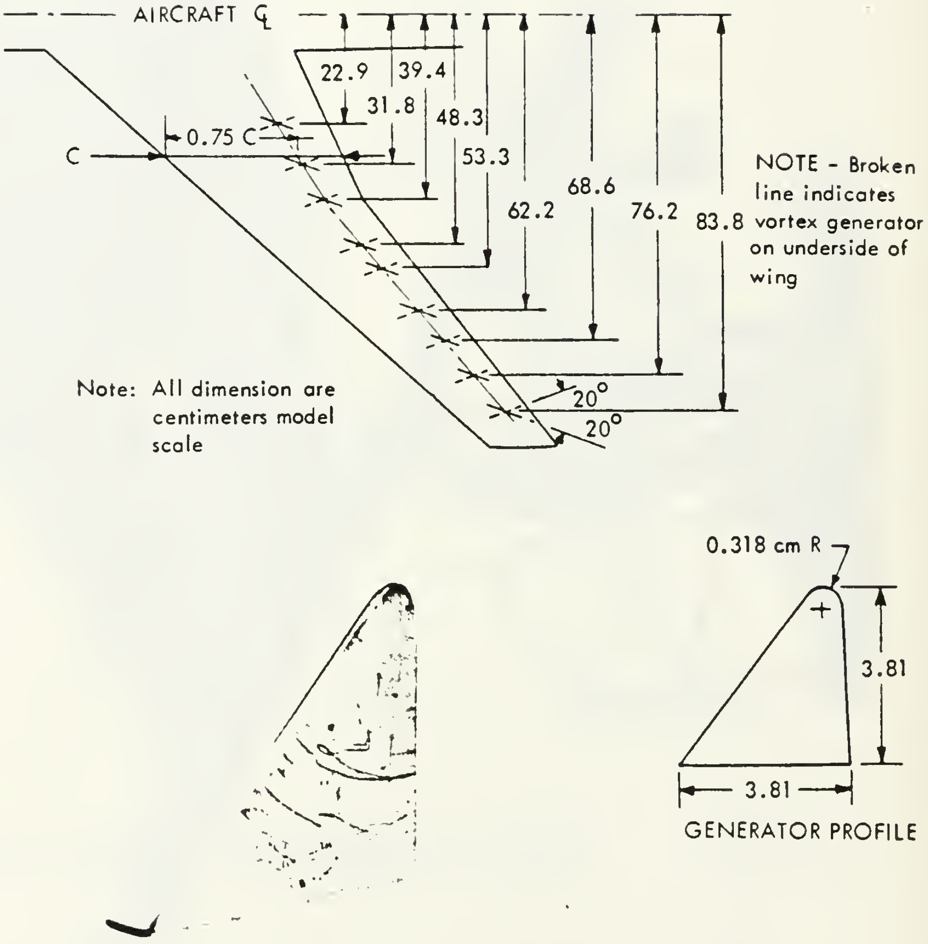
AIRCRAFT ℄
C
0.75 C
22.9
39.4
31.8
48.3
53.3
62.2
68.6
76.2
83.8
20°
20°
NOTE - Broken line indicates vortex generator on underside of wing
Note: All dimension are centimeters model scale
0.318 cm R
3.81
3.81
GENERATOR PROFILE

Figure 30 Sketch and Close-Up Views of a Vortex Generator [Ref. 27].

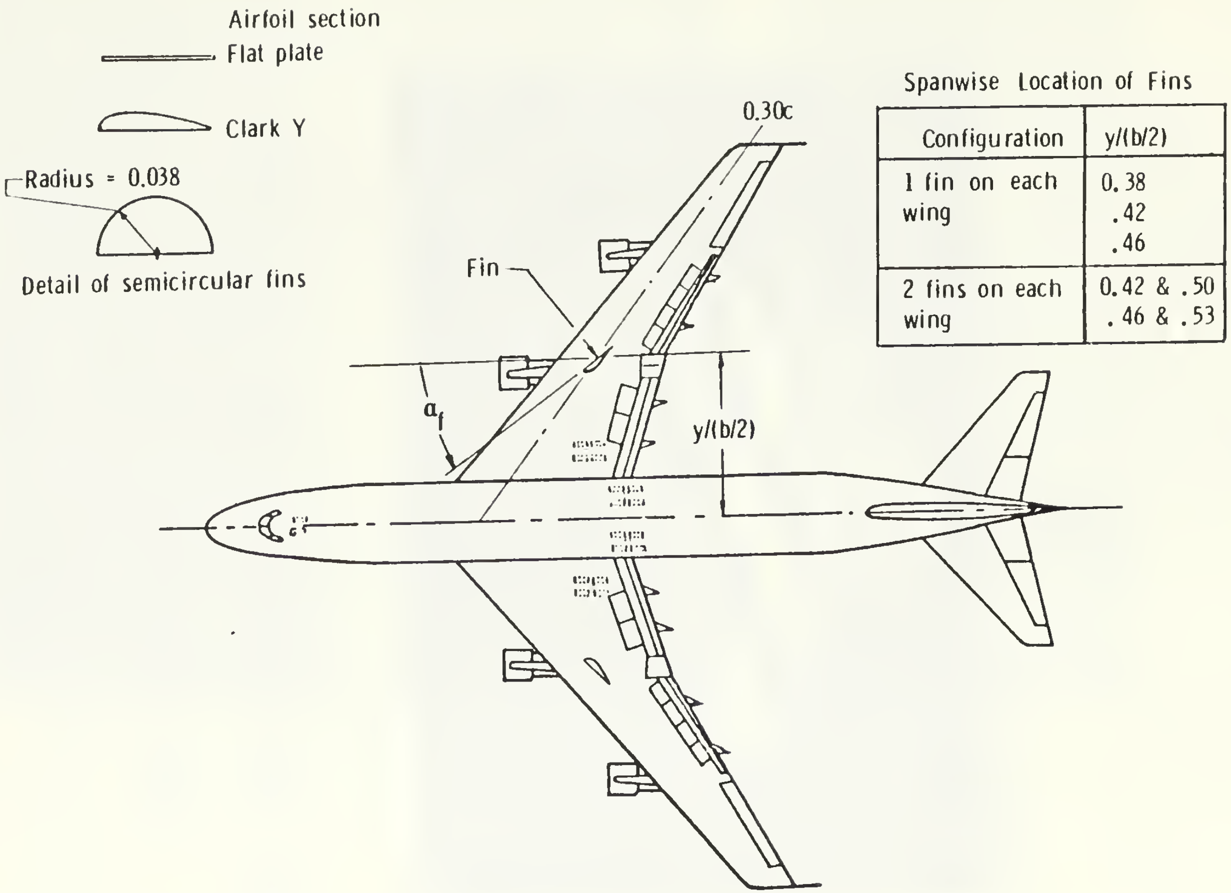

Airfoil section
Flat plate
Clark Y
Radius = 0.038
Detail of semicircular fins
Fin
0.30c
a_f
y/(b/2)

Spanwise Location of Fins

Configuration	y/(b/2)
1 fin on each wing	0.38 .42 .46
2 fins on each wing	0.42 & .50 .46 & .53

Figure 31 Sketch of Wingfins on a Transport Aircraft Model [Ref. 39].

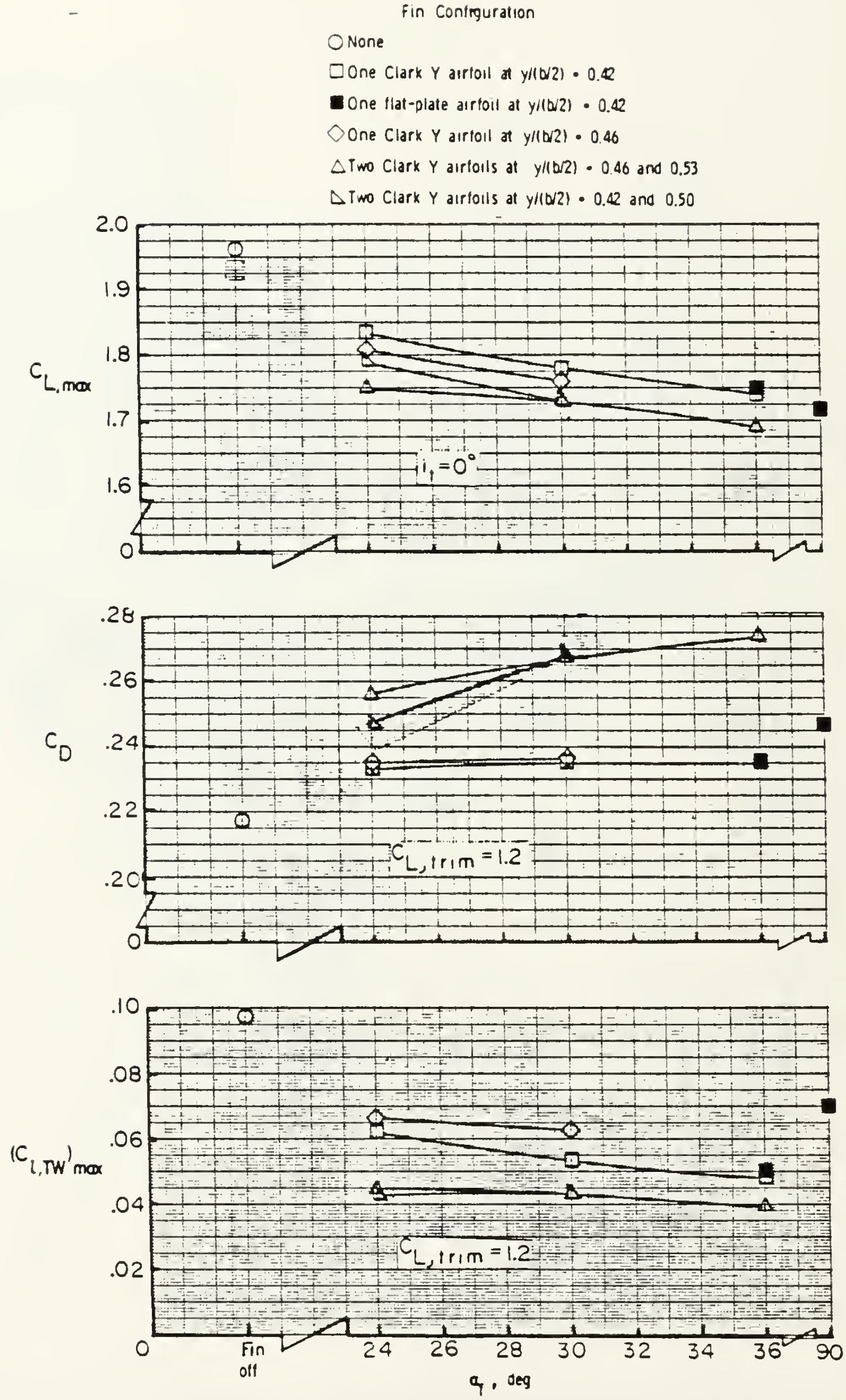

Figure 32 Summary of Reductions in Rolling Moment Coefficient for Various Wingfin Configurations (7.8 Spans Downstream) [Ref. 39].

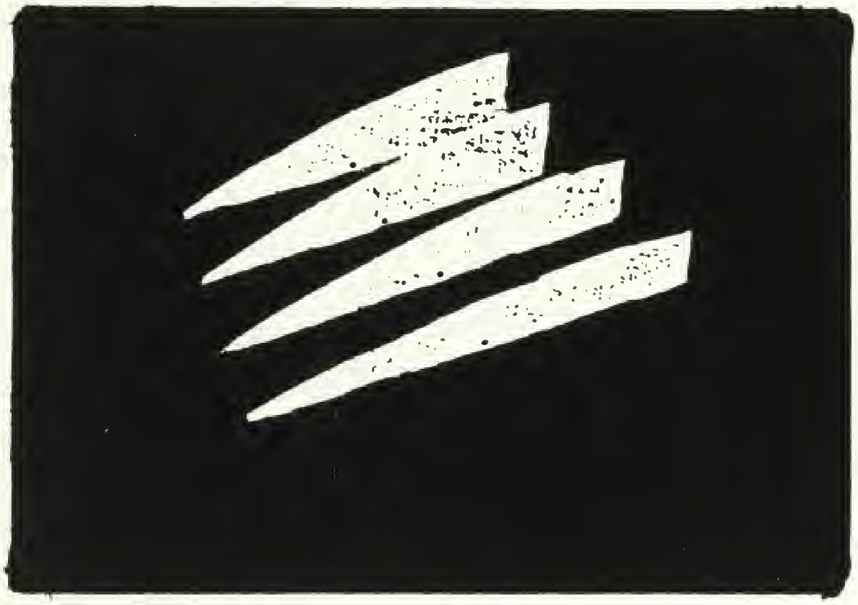

Figure 33 Parabolic Wingfins [Ref. 40].

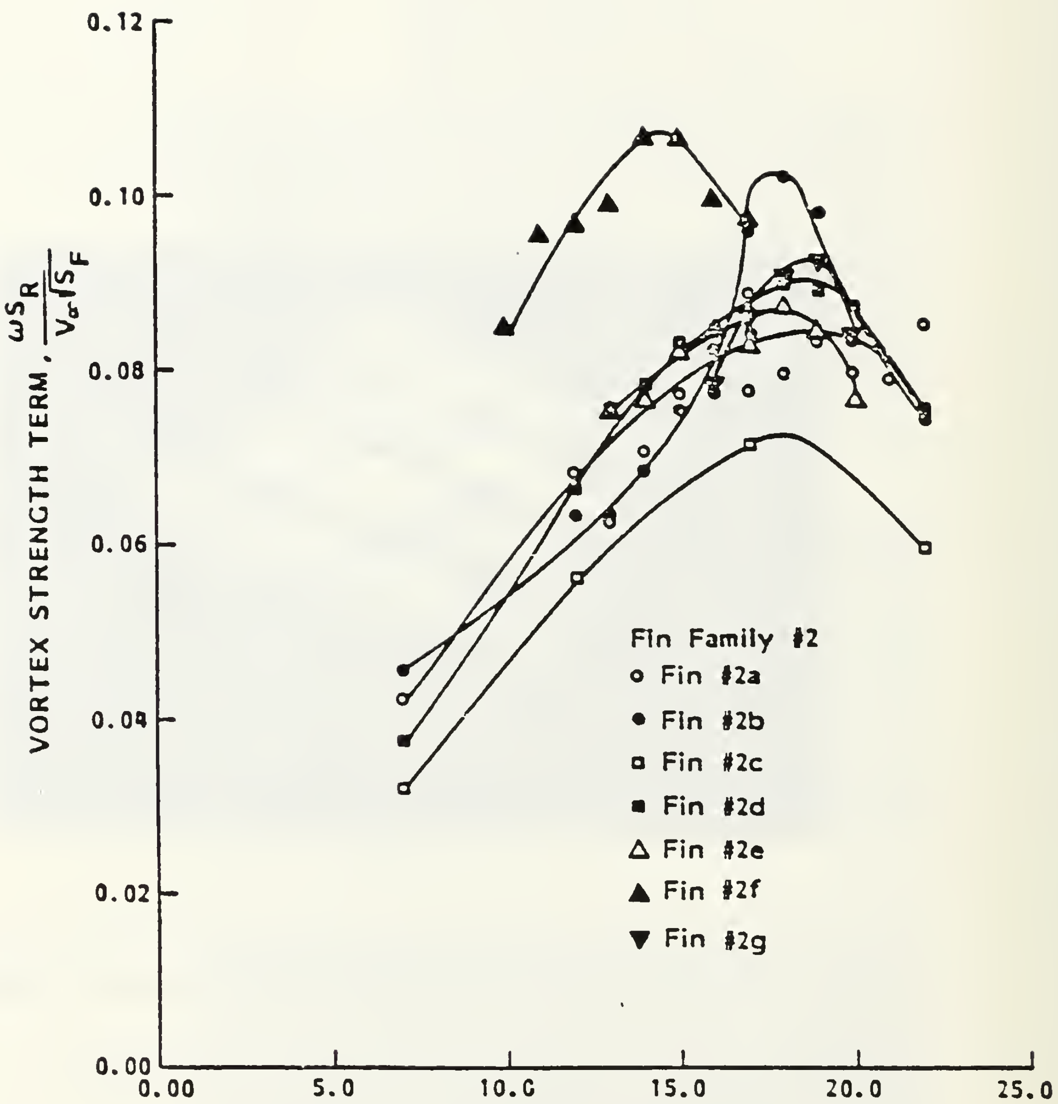

Figure 34 Vortex Strength Term vs. Fin Angle of Attack [Ref. 40].

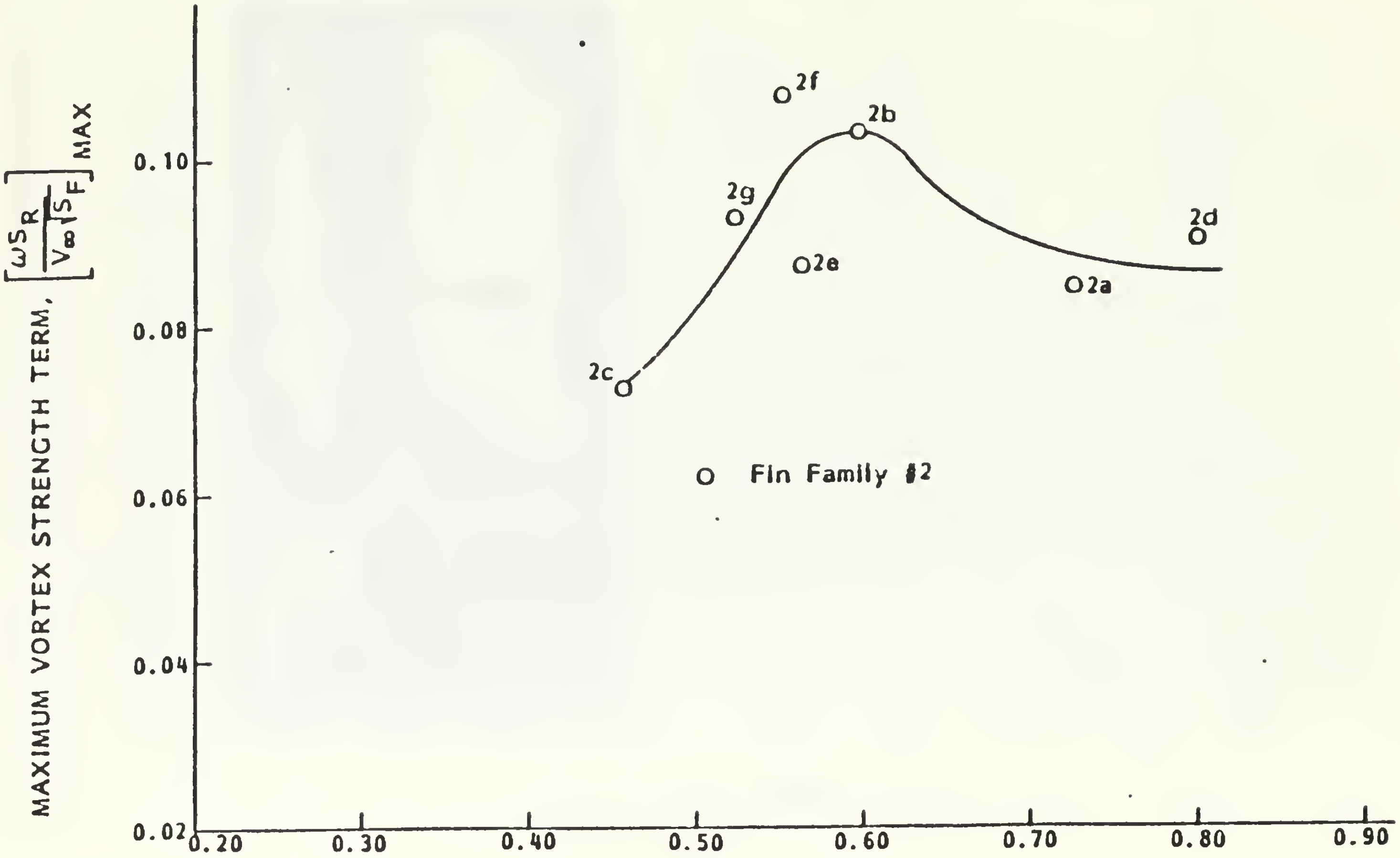

Figure 35 Maximum Vortex Strength Term vs. Fin Aspect Ratio [Ref. 40].

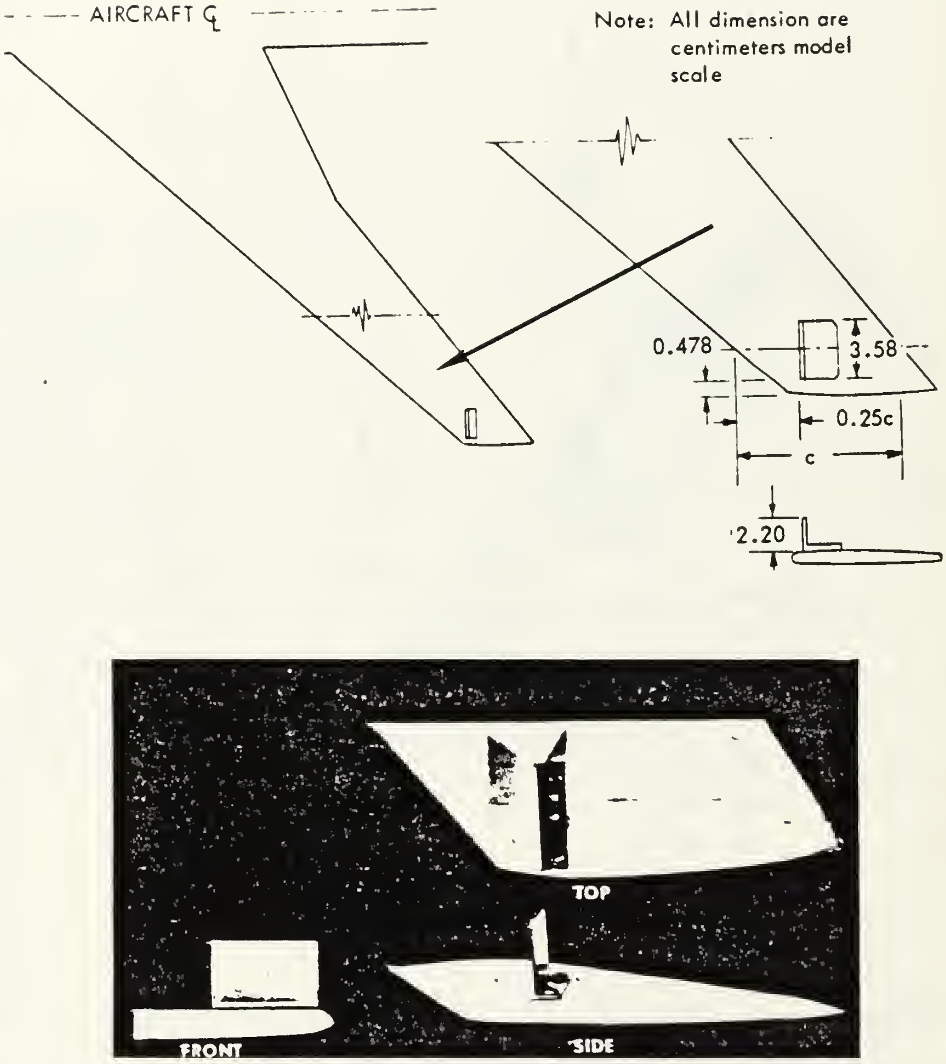
AIRCRAFT ℄
Note: All dimension are centimeters model scale
0.478
3.58
0.25c
c
2.20
TOP
FRONT
SIDE

Figure 36 Wingtip Mounted Spoiler [Ref. 27].

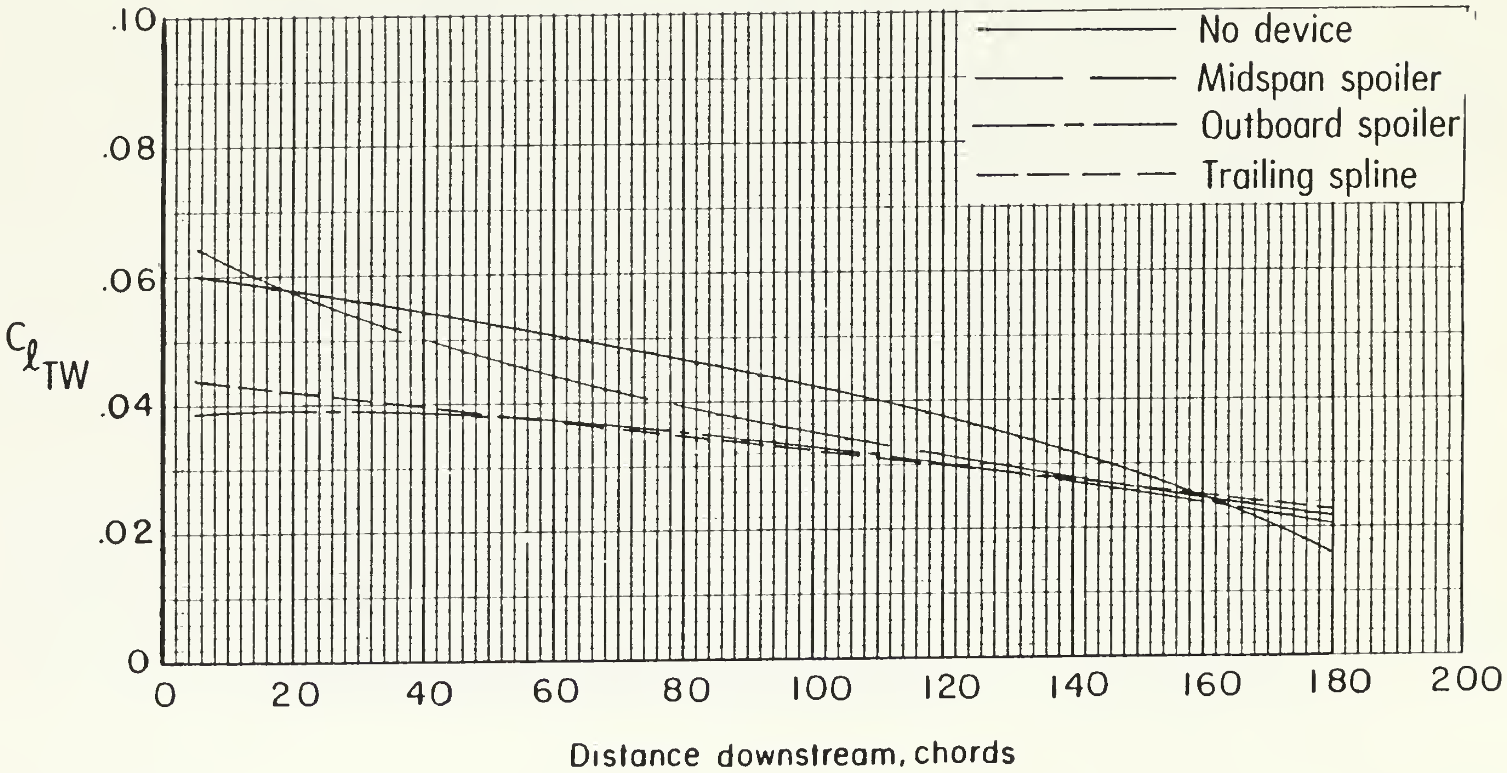

Figure 37 Variation of Rolling Moment Coefficient with Distance behind a Basic Model: No Device, Spoiler, Spline [Ref. 36].

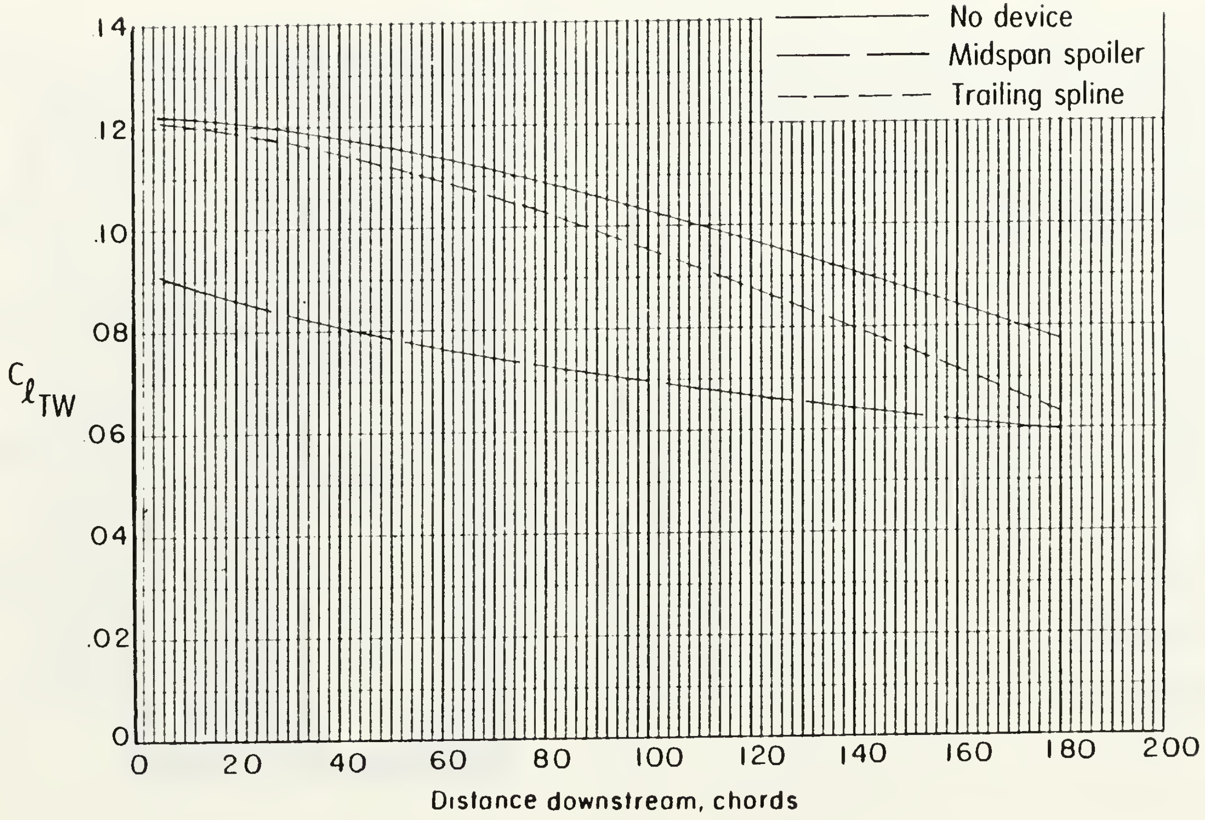

Figure 38 Variation of Rolling Moment Coefficient with Distance behind a Flapped Model: No Device, Spoiler, Spline [Ref. 36].

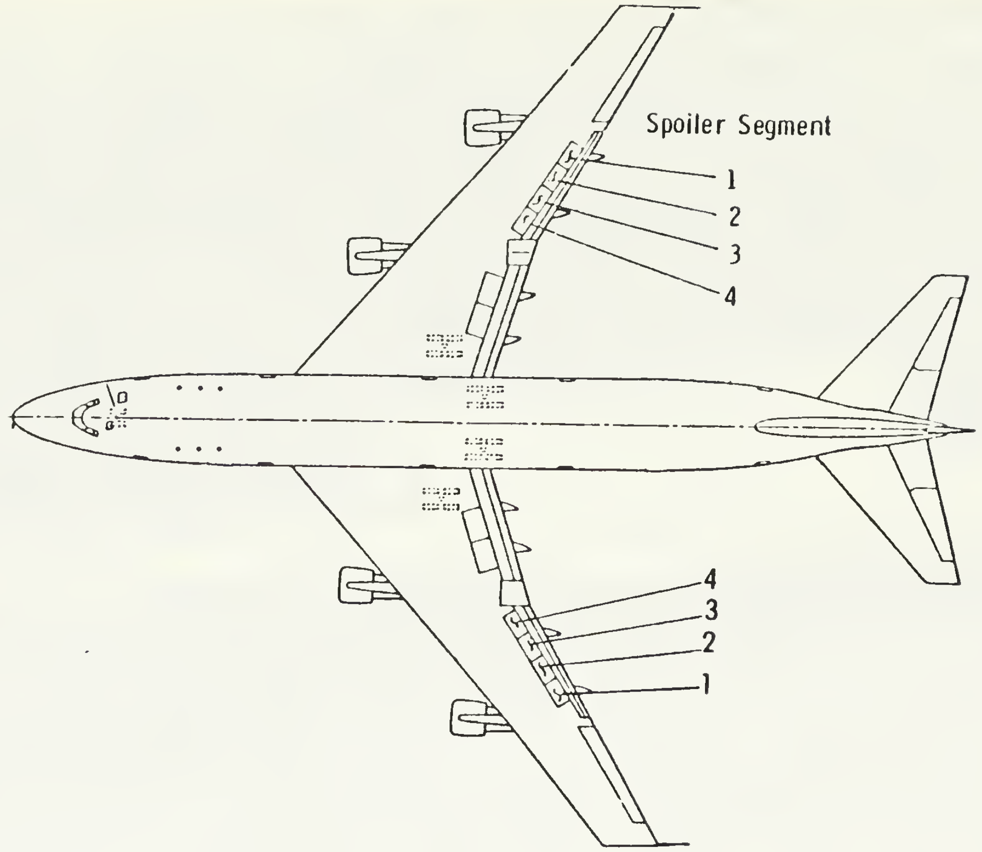
Spoiler Segment
1
2
3
4
4
3
2
1

Figure 39 Sketch of Flight Spoilers on a B-747 Aircraft Model [Ref. 42].

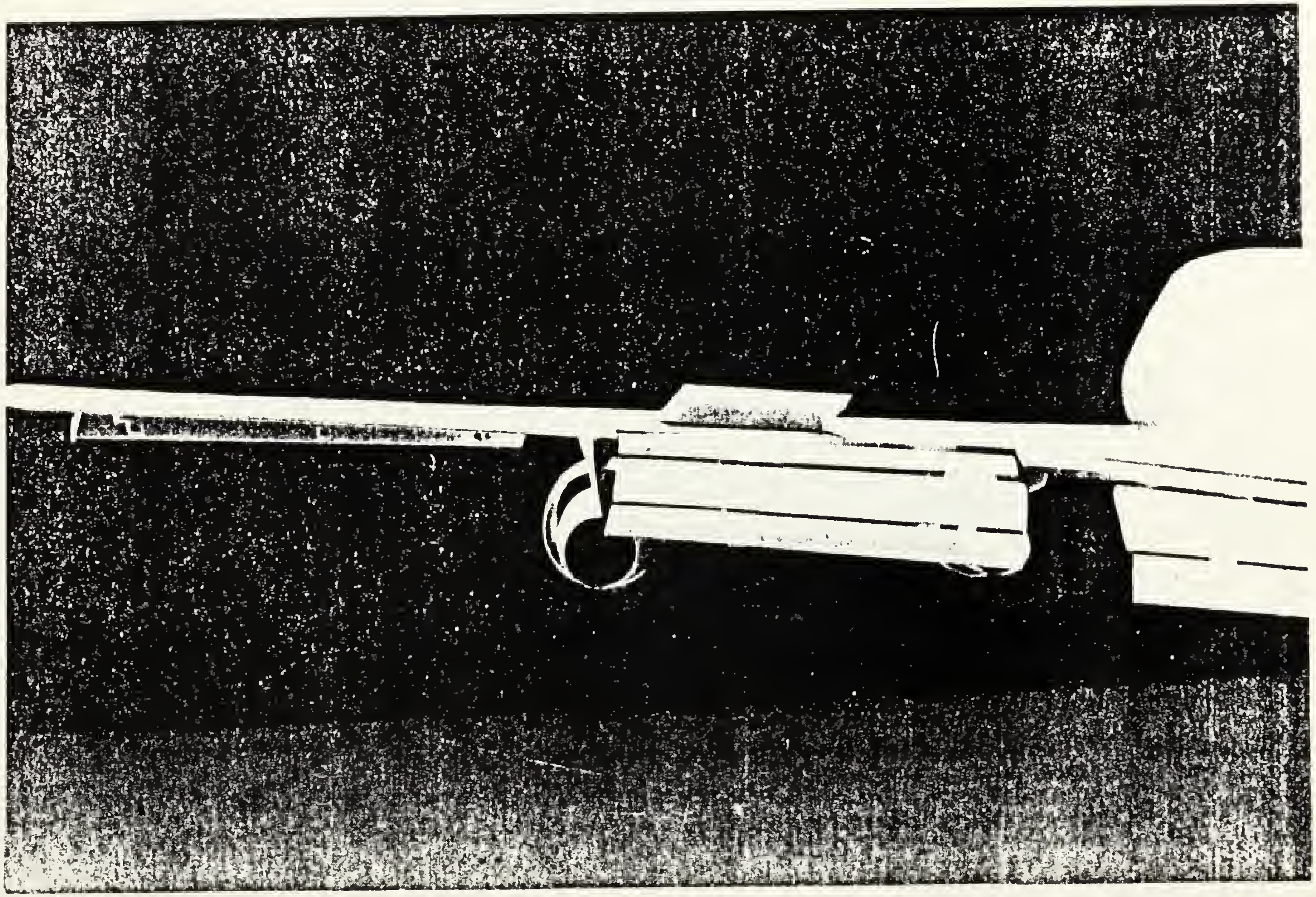

Figure 40 Photograph of Flight Spoilers on a B-747 Aircraft Model: Segments 1 and 2 Deflected 45 Degrees [Ref. 42].

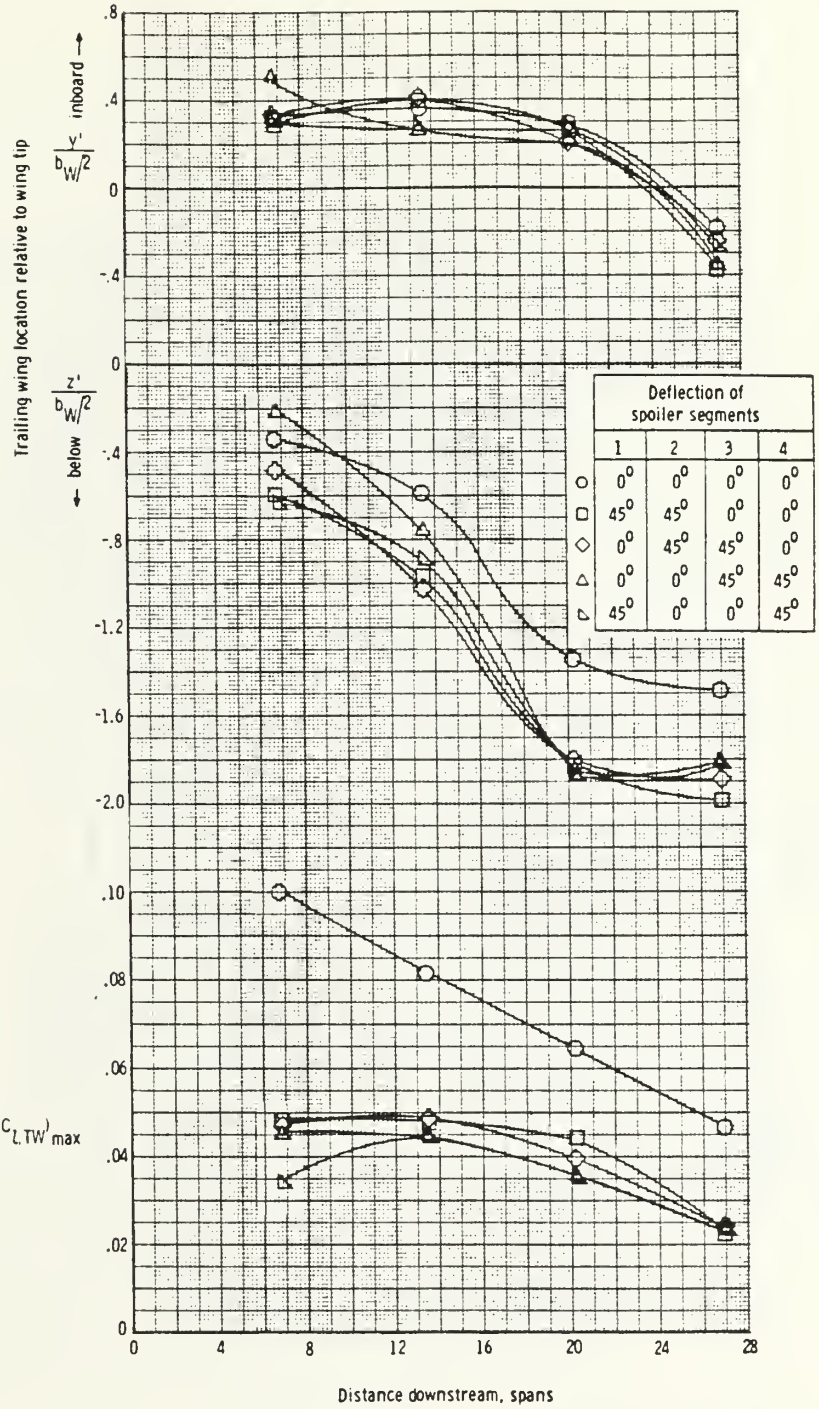

Figure 41 Variation of Rolling Moment Coefficient with Distance behind the B-747 Aircraft Model (Spoiler Deflection) [Ref. 42].

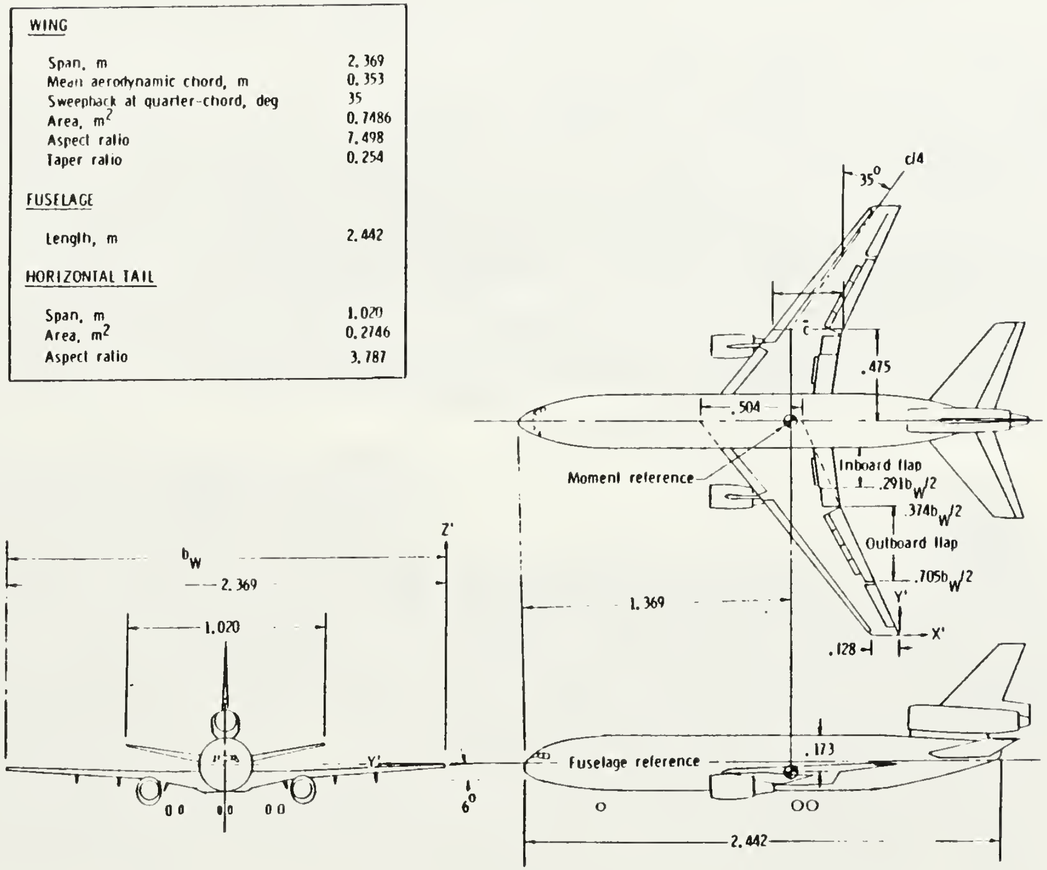

WING	
Span, m	2.369
Mean aerodynamic chord, m	0.353
Sweepback at quarter-chord, deg	35
Area, m^2	0.7486
Aspect ratio	7.498
Taper ratio	0.254
FUSELAGE	
Length, m	2.442
HORIZONTAL TAIL	
Span, m	1.020
Area, m^2	0.2746
Aspect ratio	3.787

35°
c/4
c̄
.475
.504
Moment reference
Inboard flap
.291b_W/2
.374b_W/2
Outboard flap
.705b_W/2
Y'
X'
.128
1.369
b_W
2.369
1.020
Z'
Y'
6°
Fuselage reference
.173
2.442

Figure 42 Three View Sketch of DC-10 Model with Flaps Retracted [Ref. 44].

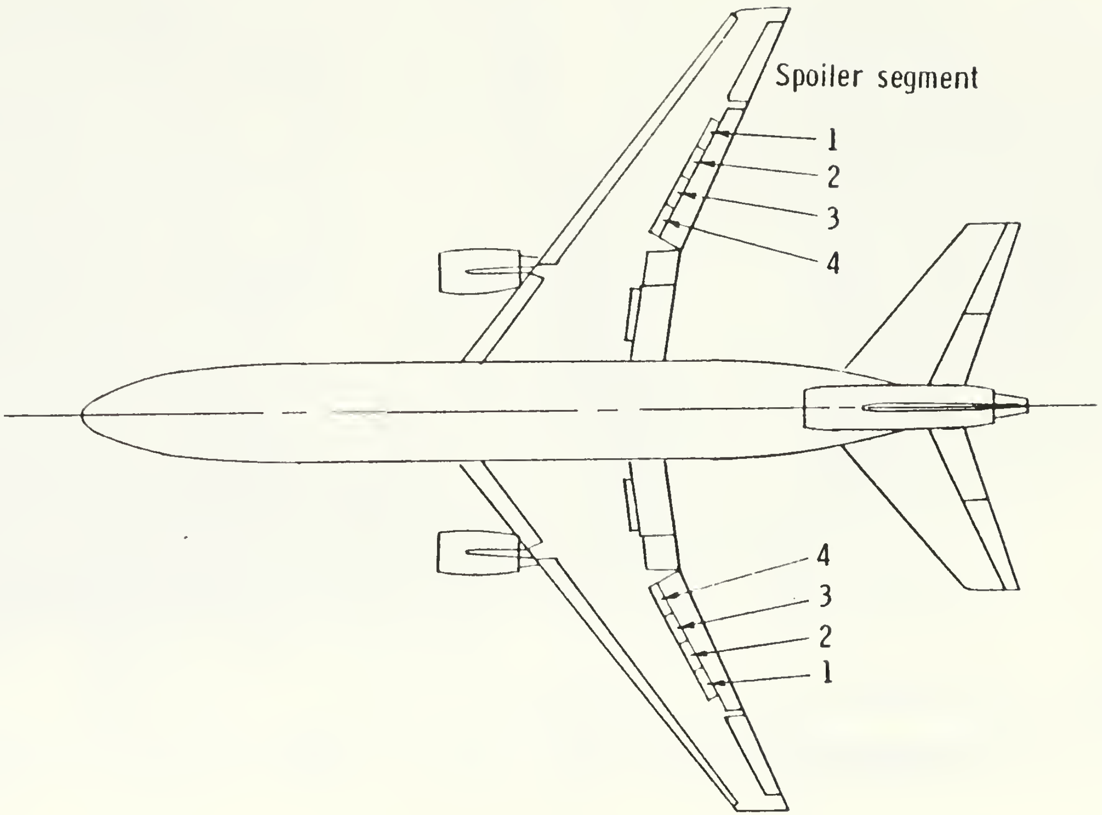
Spoiler segment
1
2
3
4
4
3
2
1

Figure 43 Sketch of Flight Spoilers on a DC-10 Model [Ref. 44].

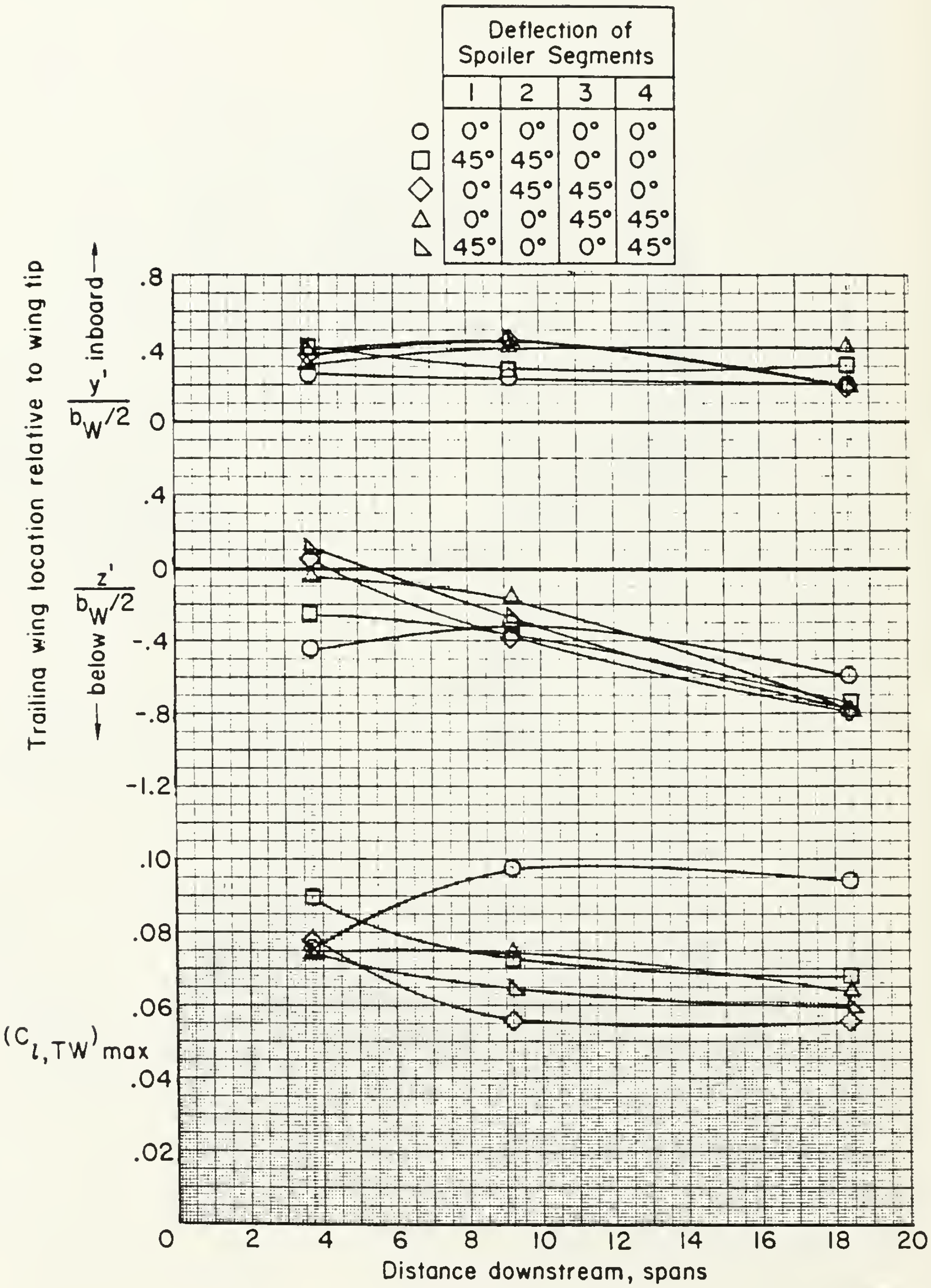

Figure 44 Variation of Rolling Moment Coefficient with Distance behind the DC-10 Aircraft Model (Spoiler Deflection) [Ref. 44].

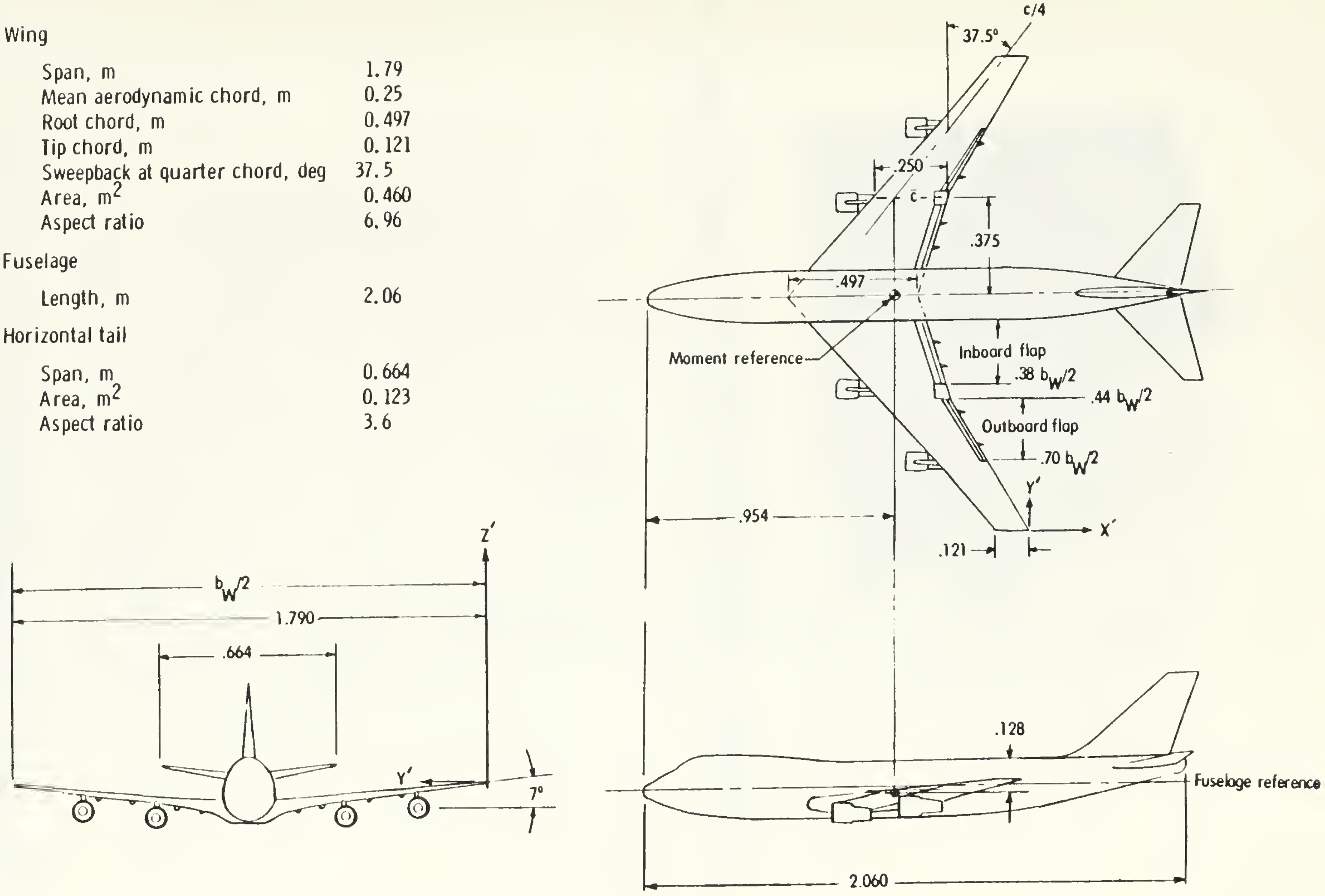
c/4
37.5°
.250
c̄
.375
.497
Moment reference
Inboard flap
.38 $b_W/2$
.44 $b_W/2$
Outboard flap
.70 $b_W/2$
Y′
X′
.954
.121
Z′
$b_W/2$
1.790
.664
Y′
7°
.128
Fuselage reference
2.060

Wing	
Span, m	1.79
Mean aerodynamic chord, m	0.25
Root chord, m	0.497
Tip chord, m	0.121
Sweepback at quarter chord, deg	37.5
Area, m^2	0.460
Aspect ratio	6.96
Fuselage	
Length, m	2.06
Horizontal tail	
Span, m	0.664
Area, m^2	0.123
Aspect ratio	3.6

Figure 45 Three View Sketch of B-747 Model with Flaps Retracted [Ref. 37].

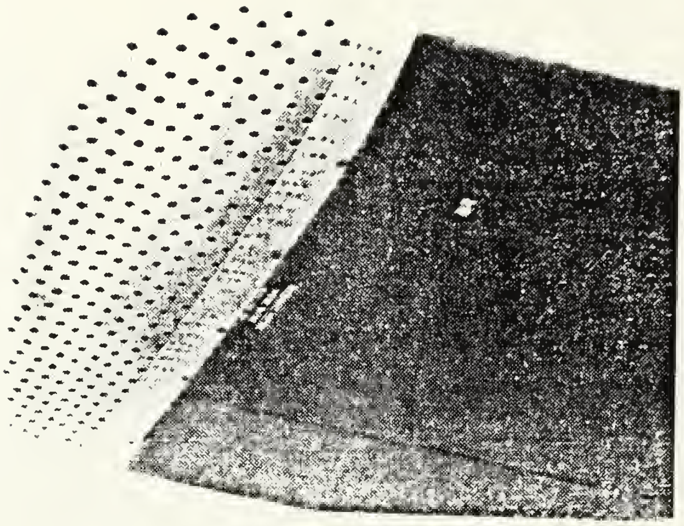

Figure 46 Photograph of a Porous Wingtip [Ref. 49].

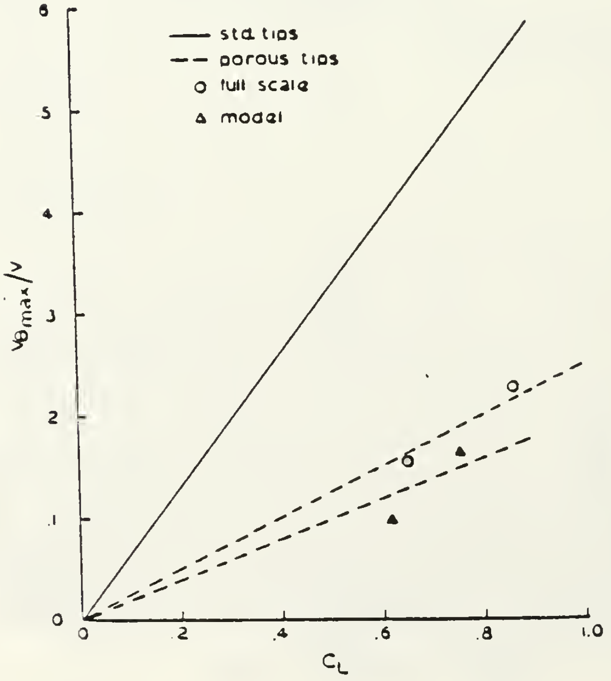

Figure 47 Nondimensional Maximum Tangential Velocity vs. Lift Coefficient [Ref. 49].

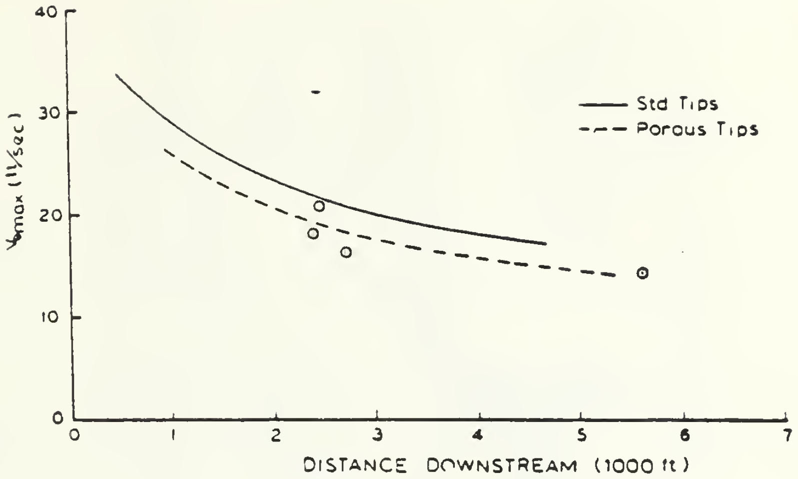

Figure 48 Maximum Tangential Velocity vs. Downstream Distance [Ref. 49].

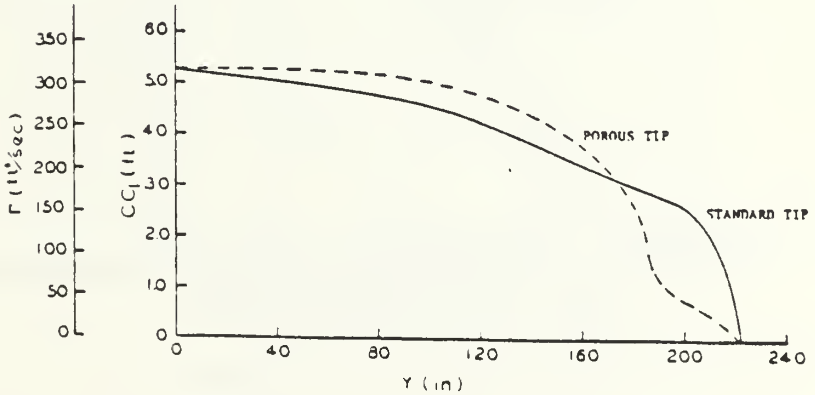

Figure 49 Lift Distribution on O-1A Wing with and without Porous Tip [Ref. 49].

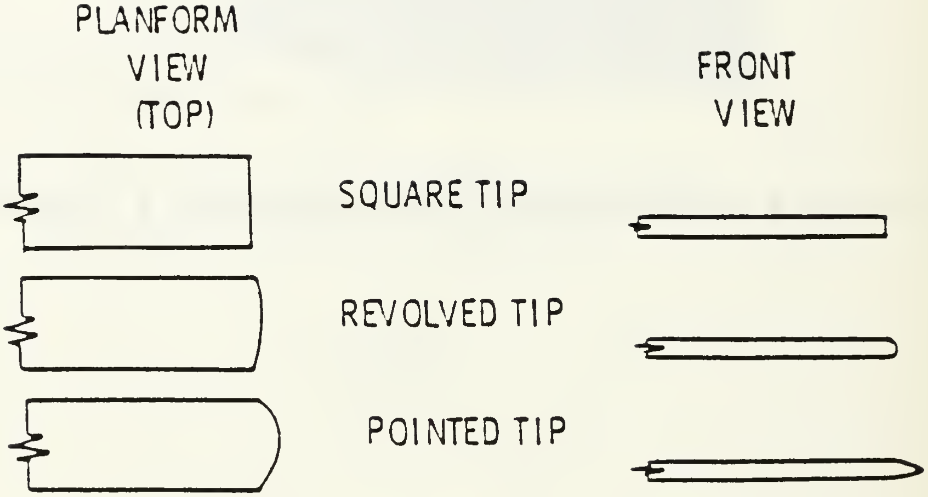
PLANFORM VIEW (TOP)
FRONT VIEW
SQUARE TIP
REVOLVED TIP
POINTED TIP

Figure 50 Wingtip Edge Shape Configurations [Ref. 50].

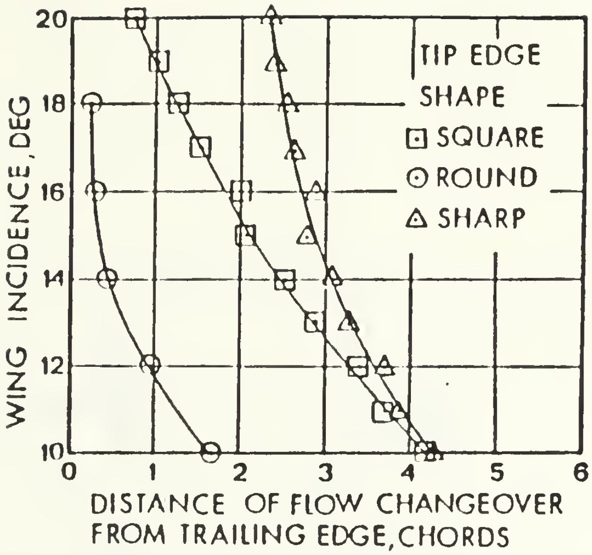

a) REYNOLDS NUMBER = 3.4×10^4

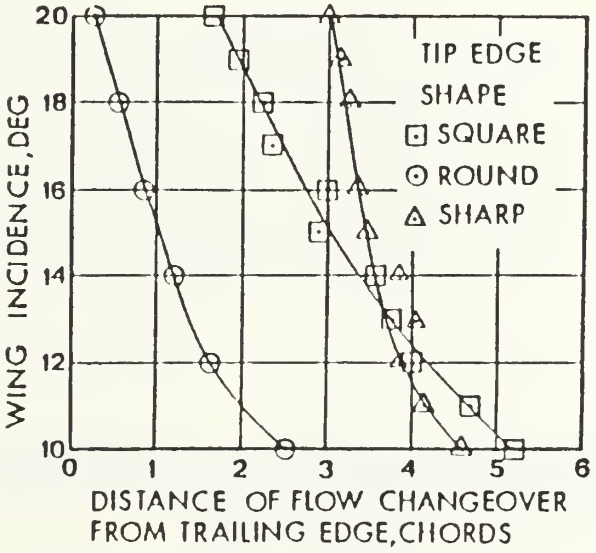

b) REYNOLDS NUMBER = 6.8×10^4

Figure 51 Changeover Position from Axial Velocity Excess to Axial Velocity Deficit behind NACA 6412 Wing Section [Ref. 20].

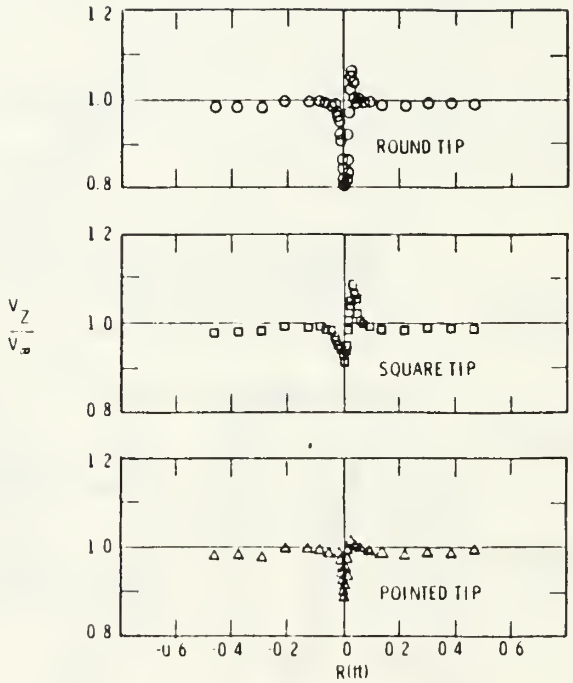

Figure 52 Comparison of Axial Velocity Profile for Various Wingtip Edge Shapes (20 Chordlengths Downstream) [Ref. 50].

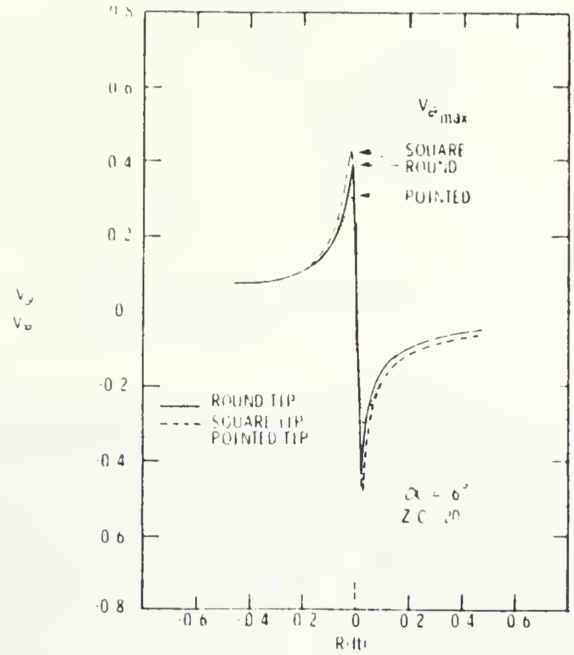

Figure 53. Comparison of Tangential Velocity Profile for Various Wingtip Edge Shapes (20 Chordlengths Downstream) [Ref. 50].

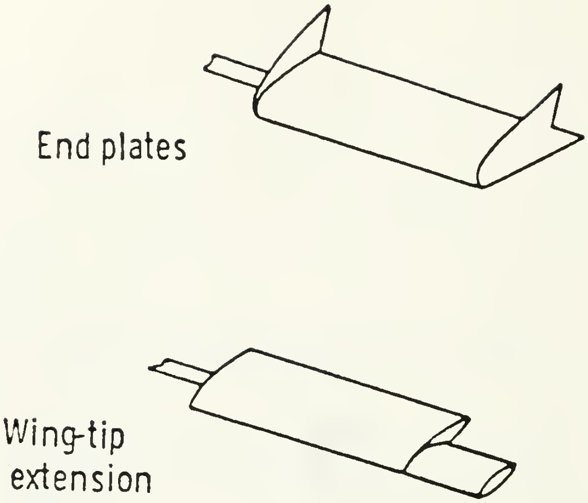
End plates
Wing-tip extension

Figure 54 Sketch of End Plate and Wingtip Extension [Ref. 38].

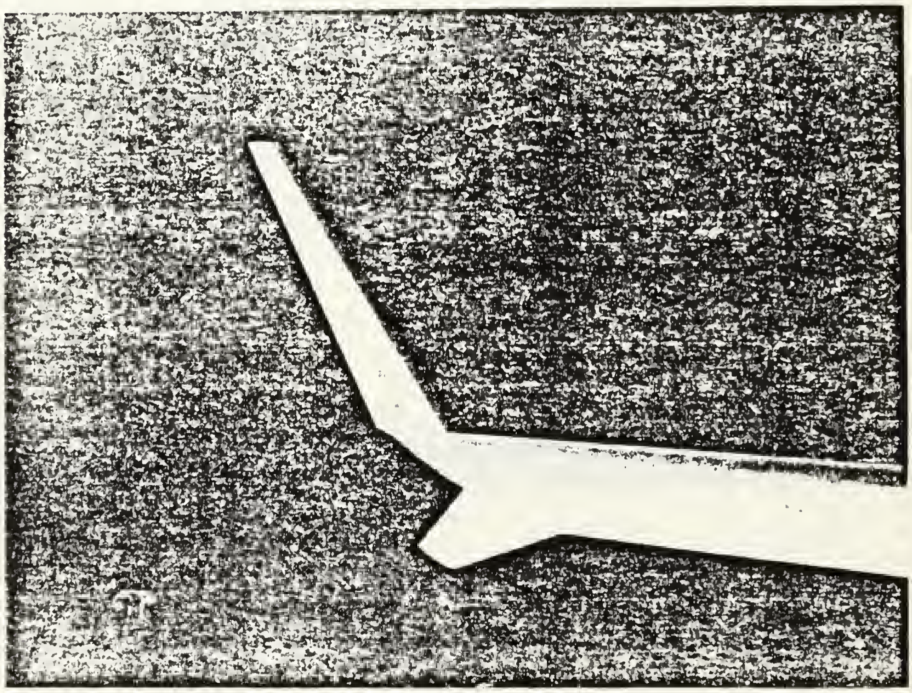

Figure 55 Photograph of Whitcomb Winglet [Ref. 53].

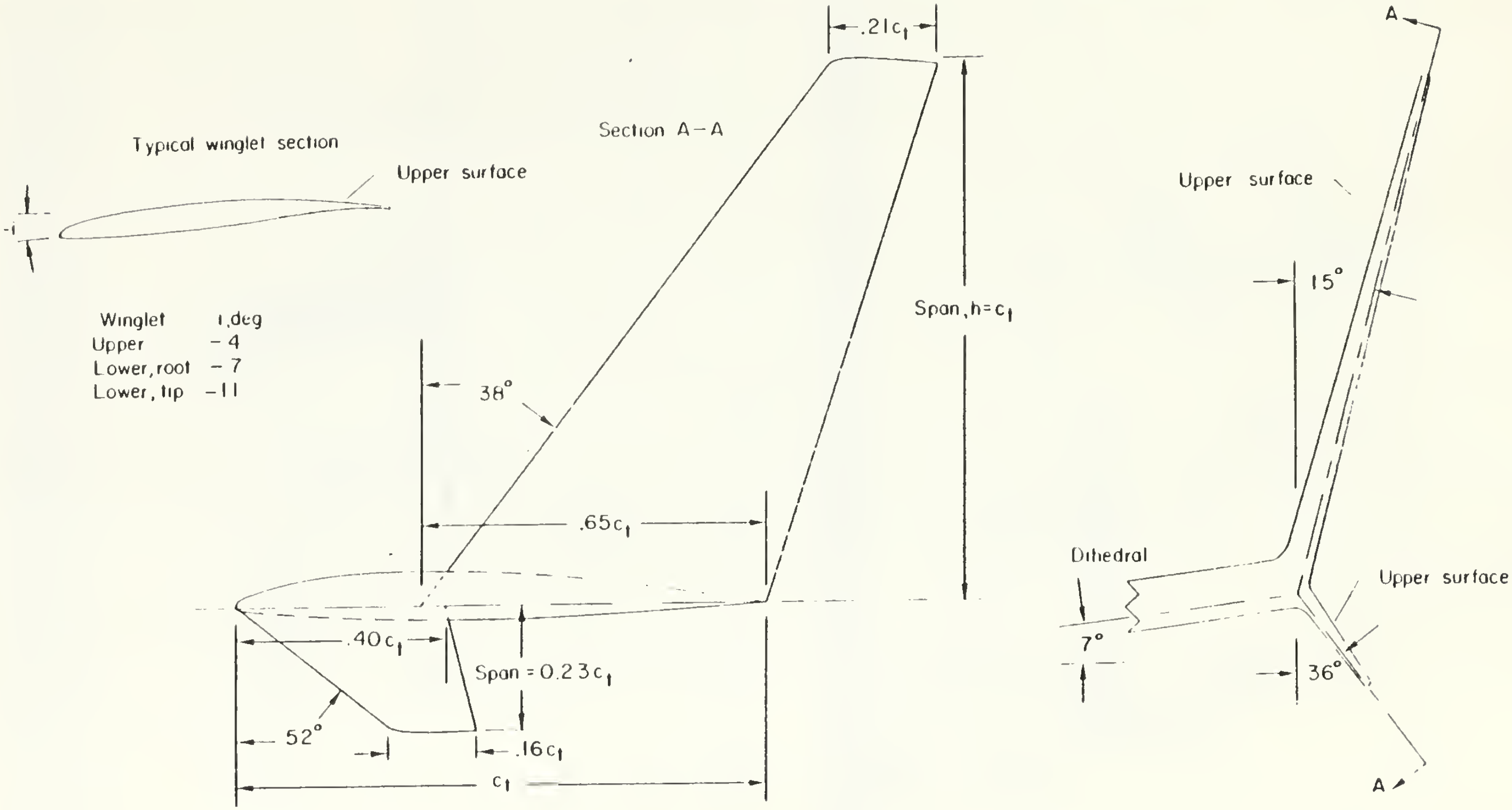
Typical winglet section
Upper surface
-i
Winglet i,deg
Upper -4
Lower, root -7
Lower, tip -11
Section A–A
.21c$_t$
Span, h=c$_t$
38°
.65c$_t$
.40c$_t$
Span = 0.23c$_t$
52°
.16c$_t$
c$_t$
A
Upper surface
15°
Dihedral
7°
Upper surface
36°
A

Figure 56 Geometric Drawing of the Whitcomb Winglet [Ref. 53].

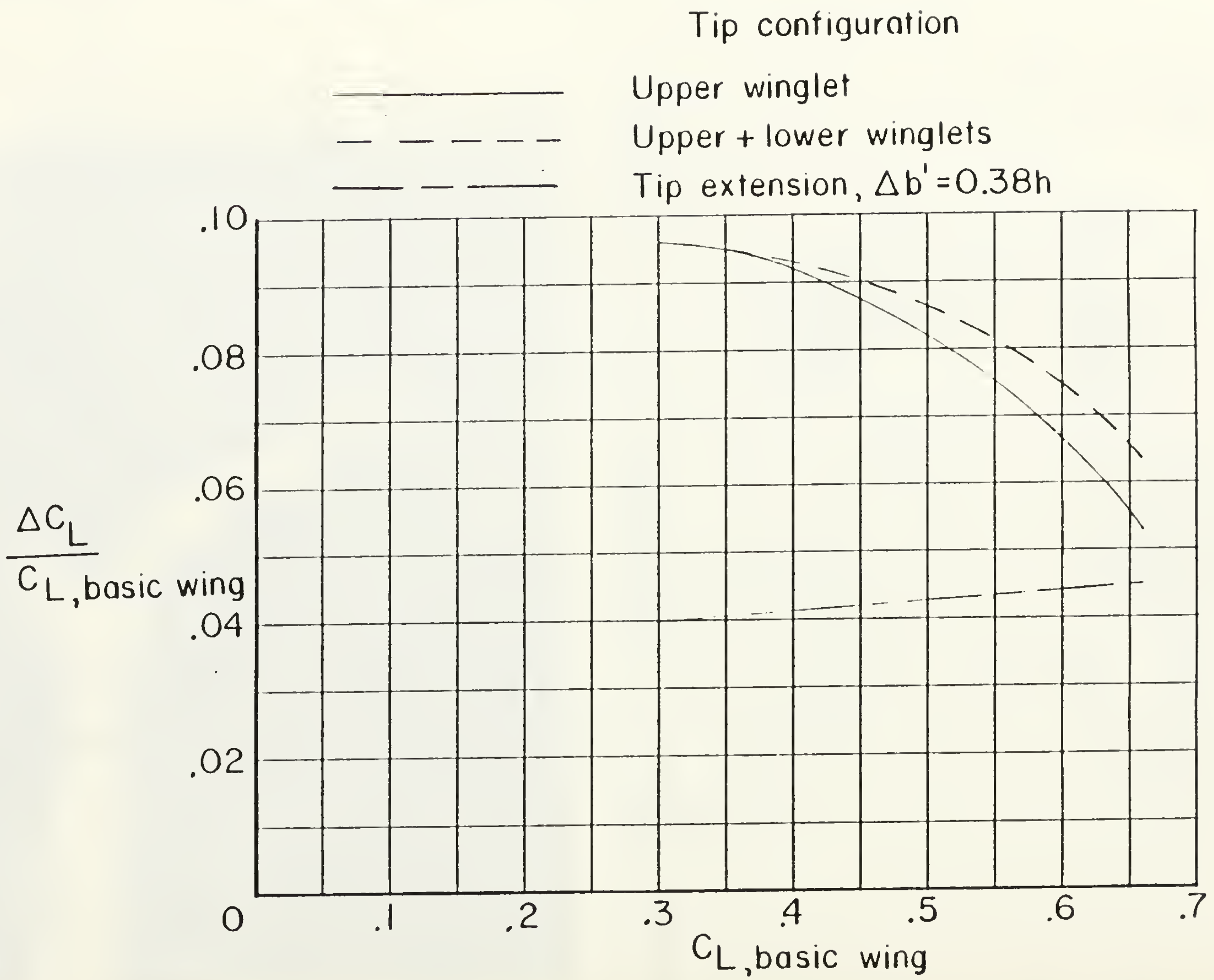

Figure 57 Incremental Lift Coefficient Variation for Constant Drag Coefficient (M=0.78) [Ref. 53].

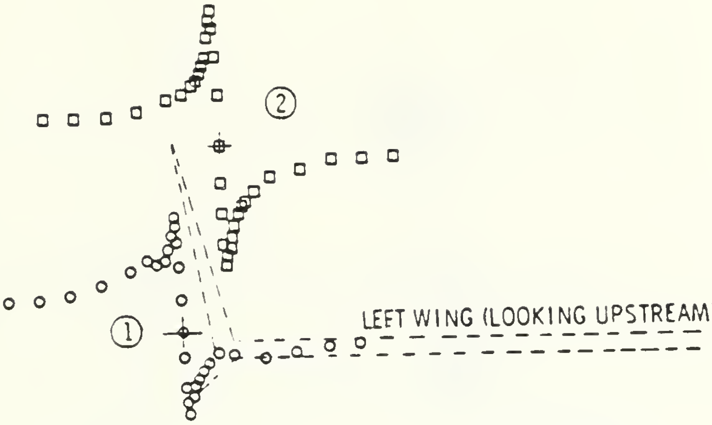

Figure 58 Tangential Velocity Profile Downstream Whitcomb Winglet (5 Chordlengths) [Ref. 50].

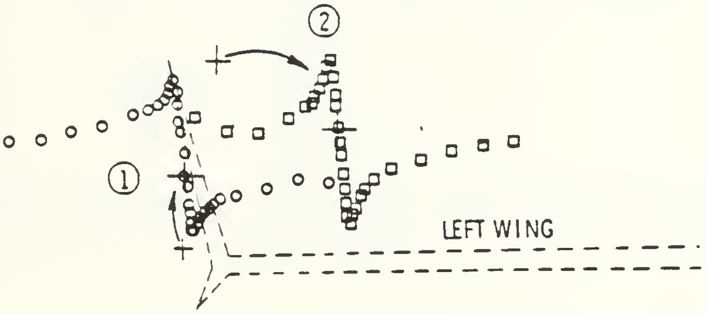

Figure 58a Tangential Velocity Profile Downstream Whitcomb Winglet (20 Chordlengths) [Ref. 50].

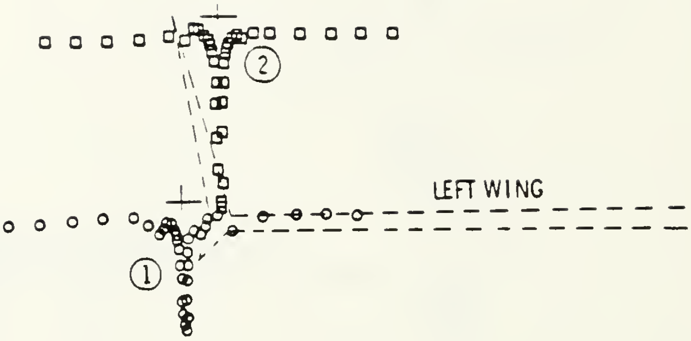

Figure 59 Axial Velocity Profile Downstream Whitcomb Winglet (5 Chordlengths) [Ref. 50].

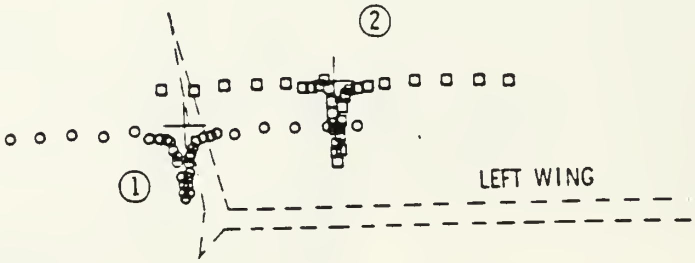

Figure 59a Axial Velocity Profile Downstream Whitcomb Winglet (20 Chordlengths) [Ref. 50].

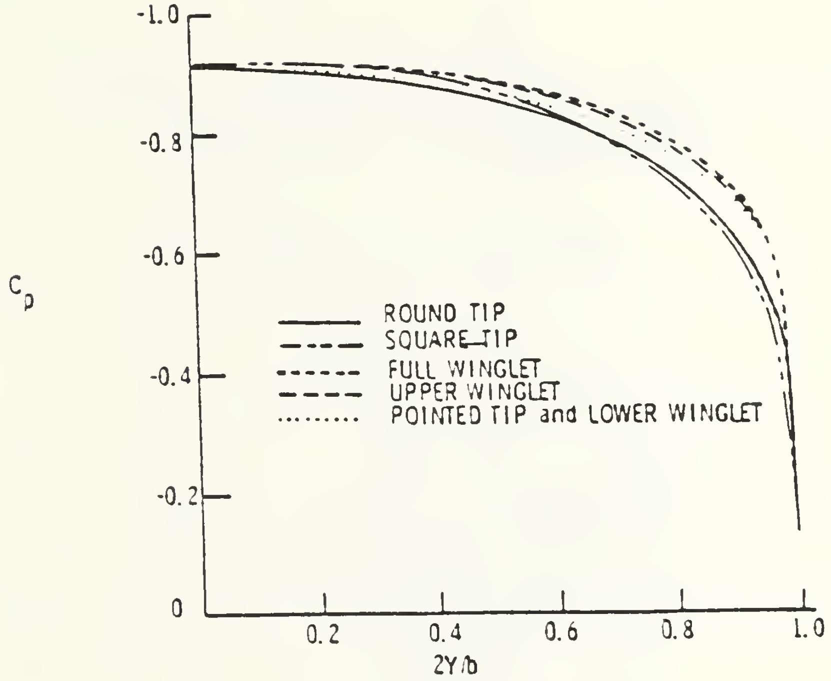

Figure 60 Spanwise Pressure Distribution for Various Wingtip Edge Shapes and Whitcomb Winglet [Ref. 50].

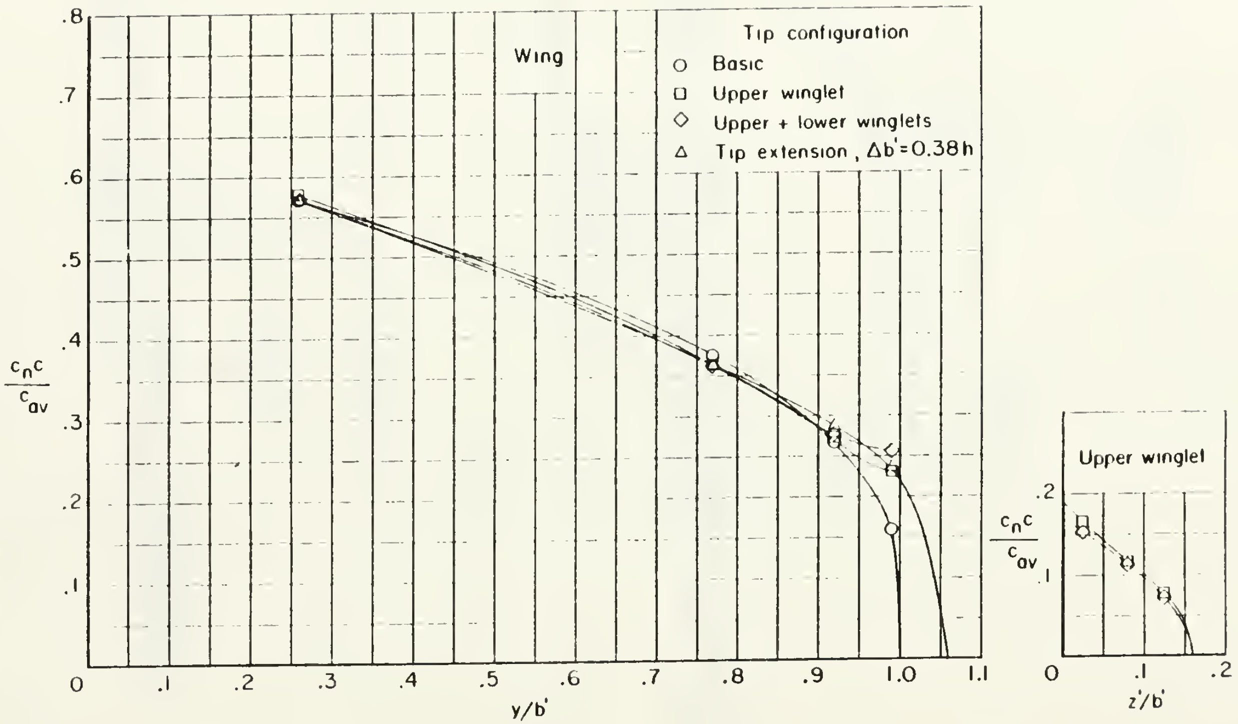

Figure 61 Spanwise Load Distribution of Whitcomb Winglet (M=0.78) [Ref. 53].

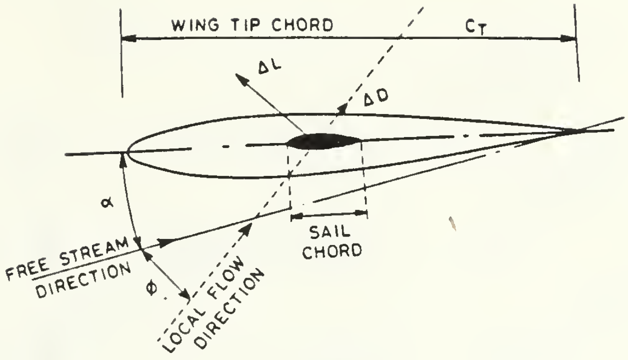
WING TIP CHORD
C_T
ΔL
ΔD
α
SAIL CHORD
FREE STREAM DIRECTION
φ
LOCAL FLOW DIRECTION

Figure 62 Forces on an Auxiliary Surface Mounted on the Tip of a Wing [Ref. 55].

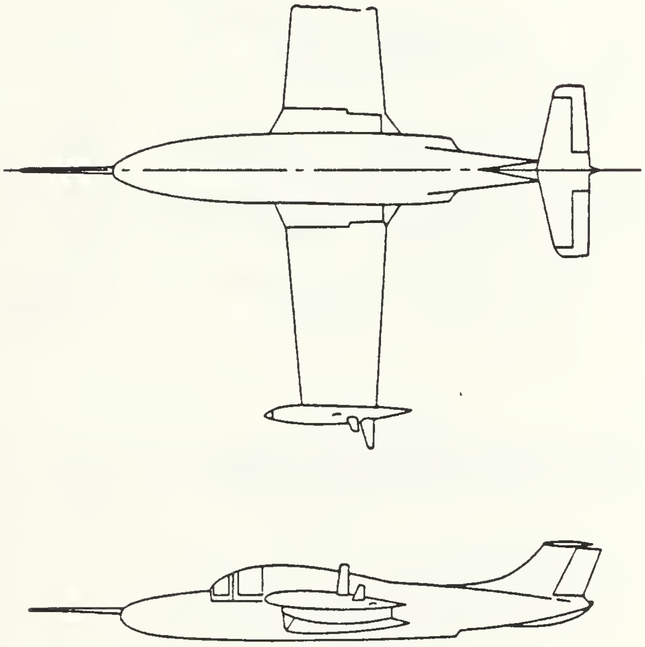

Figure 63 View of Paris Aircraft Fitted with Wingtip Sails [Ref. 55].

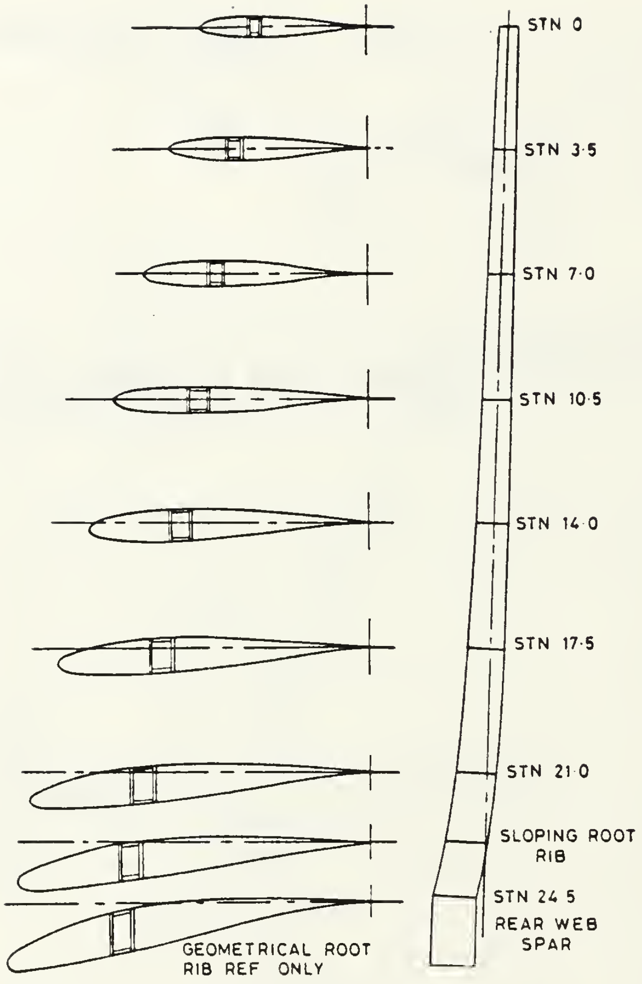
STN 0
STN 3·5
STN 7·0
STN 10·5
STN 14·0
STN 17·5
STN 21·0
SLOPING ROOT RIB
STN 24 5
REAR WEB SPAR
GEOMETRICAL ROOT RIB REF ONLY

Figure 64 Wingtip Sail Geometry [Ref. 55].

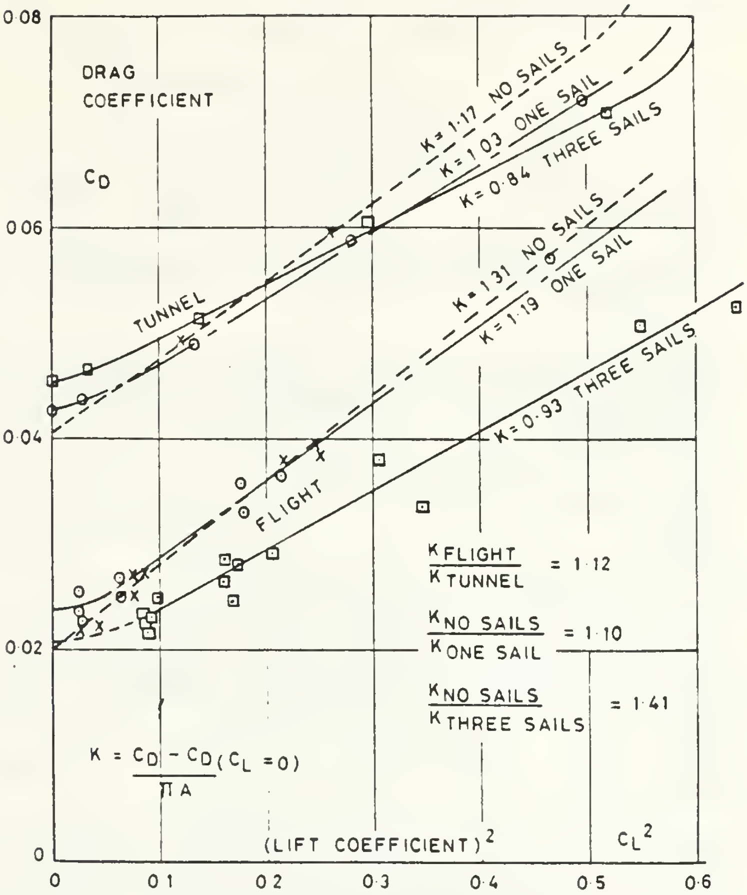

Figure 65 Effect of Wingtip Sails on Lift-Induced Drag [Ref. 55].

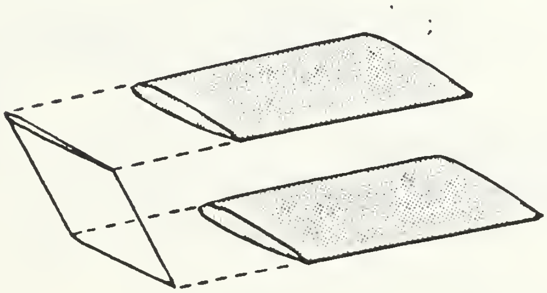

Figure 66 Sketch of Biplane Winglet [Ref. 58].

LIST OF REFERENCES

1. Lee, G.H., "Trailing Vortex Wakes," *Aeronautical Journal*, pp. 377-388, September 1975.

2. Bertin, John J. and Smith Michael L., *Aerodynamics for Engineers*, Prentice-Hall, pp. 163-170, 1979.

3. Westwater, E. L., "The Rolling Up of a Surface of Discontinuity," *Aeronautical Research Reports and Memoranda*, no. 1962, pp. 116-131, 1936.

4. Kaden, H., "Aufwicklung Einer Unstabilen Unstetiekeitsflache," *Ingenieur-Archiv 2*, pp. 140-168, 1931.

5. Spreiter, J.R. and Sacks, A.H., "The Rolling Up of a Trailing Vortex Sheet and its Effect on the Downwash behind Wings," *Journal of Aeronautical Science*, vol. 18, no. 1, pp.21-32, Jan. 1951.

6. Betz, A., *Behavior of Vortex Systems*, NACA TM 713, June 1933.

7. Donaldson, C. duP., *A Brief Review of the Aircraft Trailing Vortex Problem*, ARAP Report 155, Aeronautical Research Associates of Princeton, Princeton, N.J., May 1971.

8. Donaldson, C. duP., Snedeker, R.S., and Sullivan, R.D., "Calculation of Aircraft Wake Velocity Profiles and Comparison with Experimental Measurements," *Journal of Aircraft*, vol. 11, no. 9, pp. 547-555, September 1974.

9. Rossow, V., "On Inviscid Rolled-Up Structure of Lift-Generated Vortices," *Journal of Aircraft*, vol. 10, no. 11, pp. 647-650, November 1973.

10. Moore, D.W. and Saffman, P.G., *Axial Flow in Laminar Trailing Vortices*, Proceedings of Royal Society A333, pp. 491-508, 1973.

11. Lamb, H., *Hydrodynamics*, Sixth Edition, p. 592, Dover, 1945.

12. Dosanjh, D.S., Grasparek, E.P., and Eskinazi, S., "The Decay of a Viscous Trailing Vortex," *Aeronautical Quarterly*, vol. 13, no. 167, pp. 167-188, 1962.

13. Squires, H.B., "On the Growth of a Turbulent Vortex in Flow," Aeronautical Research Council CP666, 1954.

14. Govindaraju, S.P. and Saffman, P.G., "Flow in a Turbulent Trailing Vortex," The Physics of Fluids, vol. 14, no. 10, pp.2074-2080., October 1971.

15. Hoffmann, E.R. and Joubert, P.N., "Turbulent Line Vortices," Journal of Fluid Mechanics, vol. 16, no.3, pp.395-411, July 1963.

16. Batchelor, G.K., "Axial Flow in Trailing Line Vortices," Journal of Fluid Mechanics, vol. 20, no. 2, pp.645-648, December 1964.

17. Brown, Clinton E., "Aerodynamics of Wake Vortices," AIAA Journal, vol. 11, no. 4, pp.531-536, April 1973.

18. Chigier, N.A. and Corsiglia, V.R., "Wind Tunnel Studies of Wing Wake Turbulence," Journal of Aircraft, vol. 9, no. 12, pp. 820-825, December 1972.

19. Panton, R.L., Oberkampf, W.L., and Soskic, N., "Flight Measurements of a Wingtip Vortex," Journal of Aircraft, vol. 17, pp. 250-259, April 1980.

20. Thompson, D.H., "Experimental Study of Axial Flow in Wingtip Vortices," Journal of Aircraft, vol. 12, no. 11, pp. 910-911, November 1975.

21. Ciffone, D.L. and Orloff, K.L., "Application of Laser Velocimetry to Aircraft Wake-Vortex Measurements," Wake Vortex Minimization, NASA SP-409, pp. 157-192, 1977.

22. Staufenbiel, Rolf W., "Structure of Lift-Generated Rolled-Up Vortices," Journal of Aircraft, vol. 21, no. 10, pp. 737-744, October 1984.

23. Stickle, J.W. and Kelly, M.W., "Ground Based Facilities for Evaluating Vortex Minimization Concepts," Wake Vortex Minimization, NASA SP-409, pp. 129-155, 1977.

24. Rinehart, S.A., Balcerak, J.C., and White, R.P. Jr., An Experimental Study of Tip Vortex Modifications by Mass Flow Injection, Rochester Applied Science Associates, Inc., RASA Report 71-01, January 1971.

25. Snedeker, R.S., "The Effects of Air Injection on the Torque Produced by a Trailing Vortex," Journal of Aircraft, vol. 9, no. 9, pp.682-684, September 1972.

26. Poppleton, E.D., "Effect of Air Injection into the Core of a Trailing Vortex," *Journal of Aircraft*, vol. 8, no. 8, pp. 672-673, August 1971.

27. Kirkman, K.L., Brown, C.E., and Goodman, A., *Evaluation of the Effectiveness of Various Devices for Attenuation of Trailing Vortices Based on Model Tests in a Large Towing Basin*, NASA CR-2202, December 1973.

28. Patterson, J.C. Jr. and Jordan, F.L. Jr., "Thrust-Augmented Vortex Attenuation," *Wake Vortex Minimization*, NASA SP-409, pp. 251-270, 1977.

29. Yuan, S.W. and Bloom, A.M., *Experimental Investigation of Wingtip Vortex Abatement*, Ninth Conference of the International Council of Aeronautical Science, Haifa, Israel, August 25-30, 1974.

30. Dunham, R.E. Jr., "Unsuccessful Concepts for Aircraft Wake Vortex Minimization," *Wake Vortex Minimization*, NASA SP-409, pp. 221-249, 1977.

31. Wu, James and Vakili, A. *Aerodynamic Improvements by Discrete Wing Tip Jets*, Air Force Wright Aeronautical Laboratory, AFWAL-TR-84-3009, March 1984.

32. Patterson, James C. Jr., "Vortex Attenuation Obtained in the Langley Vortex Research Facility," *Journal of Aircraft*, vol. 12, no. 9, pp. 745-749, September 1975.

33. DeMeis, R., "New Tricks for Cutting Drag," *Aerospace America*, pp. 75-77, January 1985.

34. Barber, M.R. and Tymczyszyn, J.J., "Wake Vortex Attenuation Flight Tests," *A Status Report: 1980 Aircraft Safety and Operating Problems*, NASA CP-2170, Part II, pp. 387-408, 1981.

35. Uzel, J.N. and Marchman, J.F. III, *The Effect of Wing-Tip Modifications on Aircraft Wake Turbulence*, VPI-E-72-8, July 1972.

36. Croom, Delwin R., *Low-Speed Wind-Tunnel Investigation of Forward-Located Spoilers and Trailing Splines as Trailing-Vortex Hazard Alleviation Devices on an Aspect-Ratio 8 Wing Model*, NASA TM X-3166, February 1975.

37. Croom, D.R. and Dunham, R.E. Jr., *Low-Speed Wind-Tunnel Investigation of Span Load Alteration, Forward Located Spoilers, and Splines as Trailing-Vortex-Hazard Alleviation Devices on a Transport Aircraft Model*, NASA TN D-8133, December 1975.

38. Hastings, E.C. Jr., and others, Development and Flight Tests of Vortex-Attenuating Splines, NASA TN D-8083, December 1975.

39. Croom, D.R. and Holbrook, G.T., Low-Speed Wind-Tunnel Investigation of Wing Fins as Trailing-Vortex-Alleviation Devices on a Transport Airplane Model, NASA TP-1453, June 1979.

40. Iversen, J. and Moghadam, M., Experimental Investigation of Vortices Shed by Various Wing Fin Configurations, NASA CP-163874, January 1981.

41. Corsiglia, V.R., Jacobsen, R.A., and Chigier, N., "An Experimental Investigation of Trailing Vortices Behind a Wing with a Vortex Dissipator," Aircraft Wake Turbulence and its Detection, Plenum Press, pp.229-242, 1971.

42. Croom, D.R. Low-Speed Wind-Tunnel Investigation of Various Segments of Flight Spoilers as Trailing-Vortex-Alleviation Devices on a Transport Aircraft Model, NASA TN D-8162, March 1976.

43. Croom, D.R., Low-Speed Wind-Tunnel Parametric Investigation of Flight Spoilers as Trailing-Vortex-Alleviation Devices on a Transport Aircraft Model, NASA TP-1419, April 1979.

44. Croom, D.R., Vogler, R.D., and Thelander, J.A., Low-Speed Wind-Tunnel Investigation of Flight Spoilers as Trailing-Vortex-Alleviation Devices on an Extended-Range Wide-Body Tri-Jet Airplane Model, NASA TN D-8373, December 1976.

45. Barber, M.R., and others, "Vortex Attenuation Flight Experiments," Wake Vortex Minimization, NASA SP-409, pp. 369-403, 1977.

46. Corsiglia, V.R. and Dunham, R.E. Jr., "Aircraft Wake-Vortex Minimization by use of Flaps," Wake Vortex Minimization, NASA SP-409, pp. 305-338, 1977.

47. FAA/NASA Proceedings Workshop on Wake Vortex Alleviation and Avoidance, FAA-RD-79-105, September 1979.

48. Morris, D.J. and Holbrook, G.T., "Basic Research in Wake Vortex Alleviation using a Variable Twist Wing," A Status Report, 1980 Aircraft Safety and Operating Problems, NASA CP-2170, Part II, pp. 409-424, 1981.

49. Smith, Hubert C., "Method for Reducing the Tangential Velocities in Aircraft Trailing Vortices," Journal of Aircraft, vol. 17, no. 12, pp. 861-866, December 1980.

50. Faery, H.F. Jr. and Marchman, J.F. III, "Effect of Whitcomb Winglets and other Wingtip Modifications on Wake Vortices," Proceedings of the Aircraft Wake Vortices Conference, March 15-17, FAA-RD-77-68, pp. 207-215, June 1977.

51. El-Ramly, Z. and Rainbird, W.J., "Effects of Wing-Mounted Devices on the Trailing Vortex System in the Near Field," Proceedings of the Aircraft Wake Vortices Conference, March 15-17, FAA-RD-77-68, pp. 194-206, June 1977.

52. Clements, Harry R., "Canted Adjustable End Plates for the Control of Drag," Aeronautical Engineering Review, vol. 14, no. 7, pp. 40-44, July 1955.

53. Whitcomb, R.T., A Design Approach and Selected Wind-Tunnel Results at High Subsonic Speeds for Wing-Tip Mounted Winglets, NASA TN D-8260, July 1976.

54. Flechner, S.G., Jacobs, P.F., and Whitcomb, R.T., A High-Speed Wind Tunnel Investigation of Winglets on a Representative Second-Generation Jet Transport Wing, NASA TN D-8264, July 1976.

55. Spillman, J.J., "The Use of Wing Tip Sails to Reduce Vortex Drag," Aeronautical Journal, pp. 387-395, September 1978.

56. Spillman, J.J., Ratcliffe, H.Y., and McVitie, A.M., "Flight Experiments to Evaluate the Effect of Wingtip Sails on Fuel Consumption and Handling Characteristics," Aeronautical Journal pp. 279-281, July 1979.

57. Spillman, J.J. and McVitie, A.M., "Wingtip Sails which give Lower Drag at all Normal Flight Speeds," Aeronautical Journal, pp. 362-369, October 1984.

58. Gall, P.D. and Smith, H.C., Study of Winglets Applied to Biplanes, AIAA Paper 85-0279, January 1985.

INITIAL DISTRIBUTION LIST

		No. Copies
1.	Defense Technical Information Center Cameron Station Alexandria, Virginia 22304-6145	2
2.	Superintendent Attn: Library, Code 0142 Naval Postgraduate School Monterey, California 93943-5100	2
3.	Professor T. Sarpkaya, Code 69S1 Mechanical Engineering Naval Postgraduate School Monterey, California 93943-5100	10
4.	Department of Mechanical Engineering, Code 69 Naval Postgraduate School Monterey, California 93943-5100	2
5.	Department Chairman, Code 67Pl Department of Aeronautics Naval Postgraduate School Monterey, California 93943-5100	1
6.	Lieutenant Kenneth G. Heffernan, USN USS Saratoga (CV-60) Miami, Florida 34078-2740	2

3 APR 90 35841
214323

Thesis
H42143
c.1

Heffernan
Trailing vortex attenuation devices.

32140
22 AUG 88
3 APR 90 35782 per → 35841

23
at-

214323

Thesis
H42143
c.1

Heffernan
Trailing vortex attenuation devices.

thesH42143
Trailing vortex attenuation devices.
3 2768 000 64868 7
DUDLEY KNOX LIBRARY